Responses of Superoxide Dismutases to Oxidative Stress in *Arabidopsis thaliana*

by

Hatice Neval Erturk

Dissertation submitted to the Faculty of the

Virginia Polytechnic Institute and State University

in partial fulfillment of the requirements for the degree of

DOCTOR OF PHILOSOPHY

in

Biology

APPROVED:

Dr. Ruth G. Alscher, Co-chairman	Dr. Bruce J. Turner, Co-chairman
Dr. David R. Bevan	Dr. John L. Hess
Dr. George H. Lacy	Dr. Brenda W. Shirley

January, 1999
Blacksburg, Virginia

RESPONSES OF SUPEROXIDE DISMUTASES TO OXIDATIVE STRESS IN *ARABIDOPSIS THALIANA*

by

Hatice Neval Erturk

Ruth Grene Alscher, Chair (PPWS)

Department of Biology

ABSTRACT

Superoxide dismutases (SODs) catalyze the dismutation of superoxide radicals to oxygen and hydrogen peroxide. Mn SOD is localized in mitochondria, Cu-Zn SOD is in the cytosol and chloroplast, and Fe SOD is in chloroplasts. The effects of a chloroplast-localized oxidative stress, caused by methyl viologen or 3-(3, 4-dichlorphenyl)-1-1'dimethylurea (DCMU) on SOD populations were investigated. A cloned *Arabidopsis thaliana* Fe SOD gene was expressed in *Escherichia coli* and was purified from transformed cells. This protein was used to raise antibodies against *A. thaliana* Fe SOD which in turn were used to quantify the effects of oxidative stress on Fe SOD protein. Effects of oxidative stress on enzyme activity were measured in native gels. Fe SOD responded to oxidative stress with an increase in activity, but not in antibody reactive protein. Two novel forms of Fe SOD activity, with faster migration rates in activity gels, were detected. Mn SOD, a mitochondrial enzyme, responded to the stress with an increase in activity. In contrast, the activity or amount of Cu-Zn SOD protein did not respond to this oxidative stress.

In light of these results, we propose that SODs respond to oxidative stress at the enzyme and gene levels. Mitochondrial Mn SOD responded to a chloroplast-localized stress with an increase in activity, suggesting either that the site of action for methyl

viologen is not exclusively in the chloroplast or that there are other signals among the compartments of the cell. Fe SOD, but not Cu-Zn SOD responded to stress, suggesting that Fe SOD may be the stress responsive enzyme in this organelle.

Evolutionary relationships among different isoforms were investigated based on the known primary, secondary, and tertiary structures of these isoforms. The three dimensional structure of *A. thaliana* Fe SOD was modeled by using structures of crystallized *E. coli* and *Pseudomonas ovalis* Fe SODs as templates. Comparison of prokaryotic Fe SOD with eukaryotic isoforms showed that Fe and Mn SODs are structurally homologous, whereas Cu Zn SOD is not.

This dissertation is dedicated to my Father.

Acknowledgments

I would like to thank Dr. Ruth Alscher for giving me the opportunity to work under her guidance for the last three and a half years. Thanks for the encouragement, for being there for me whenever I needed guidance, for your willingness to answer my questions--even at 4:00 am in the morning--and for keeping me focused. You have been an excellent mentor and also a great friend. Your friendship as well as your guidance have been an honor to me.

I would like to thank Dr. David Bevan, Dr. John Hess, Dr. George Lacy, Dr. Brenda Shirley, and Dr. Bruce Turner for serving on my advisory committee. Dr. Bevan patiently spent long hours in front of the computer training me to model the three-dimensional structure of *A. thaliana* Fe SOD. The obstacles I faced during immunoblotting of SODs would not have been surmounted without the help and insights I received from Dr. Hess. Dr. Lacy spent long hours perfecting my dissertation and encouraging me to finish it. Dr. Shirley made valuable contributions to the molecular biology aspect of my project. Dr. Turner served as my co-adviser and has been a big encouragement to me during the course of my studies.

The cDNA clone of the Fe SOD gene that was used to raise the antibodies against Fe SOD protein was provided by Dr. Mark Van Montogu, and the anti-sera against Cu-Zn and Mn SODs were provided by Dr. Robert Last and Dr. Daniel Kliebenstein. An air respirator was provided by the Health and Safety Department of Virginia Tech, and the funds for the air filters were provided by the Biology Department of Virginia Tech. I am grateful for their generous contribution.

I would like to thank Dr. Joe Cowles and Dr. Don McKeon for their support during the problems I encountered while I studied; the support and advice I received from them have been invaluable. Many thanks to Ms. Janet Donahue for the time and technical input she generously gave and to Mr. Joel Donahue for his tremendous help with the set up and use of his computer. The friendship, support, and encouragement I received from the Donohues have been priceless. I am thankful to Dr. Muriel Lederman (Biological Science Initiative) for allowing me use of the computers during the writing of my dissertation, and to Zeke Erskine for his technical input during my final presentation. Many thanks to Ms. Michelle Lawrence-Walker for generously spending her time proof-reading. Her talent in writing has been an invaluable contribution to my dissertation. Special thanks to my brother, Mr. Barbaros Erturk, for his help in photographing the plants that have been used in my research. Part of my studies at Virginia Tech was supported by Hacettepe University, College of Science, Ankara-Turkey, and the Grace Covenant Presbyterian Church Education Fund. I thank them for their support of me. Thanks to Ms. Verlyn Stromberg, Ms. Sue Meredith, and Ms. Moss Baldwin for being great friends, and for helping me with technical issues. Without them my plants would have been quite thirsty and the Plant Molecular Biology building without laughter.

Many thanks to my friends in Blacksburg. As an international student away from home, I have found love, support, encouragement, and another home here over the years. Without them I could not have completed this important task. Last, but not least, many thanks go to my mother. Her love and support have upheld me over the long years of my

education. She is a great mother. *Sevgili anneme calismalarim boyunca bana gosterdigi buyuk destek ve yillar boyunca bana verdigi sonsuz sevgi icin minneterim.*

TABLE OF CONTENTS

CHAPTER I. INTRODUCTION

1. Formation of Toxic Oxygen Species in Plant Cells 2
    1.1. Chloroplasts 3
    1.2. Peroxisomes 8
    1.3. Mitochondria 11
    1.4. Apoplast 12
2. Defense Against Reactive Oxygen Species 12
3. Superoxide Dismutases (SODs) 17
    3.1. Copper-Zinc Superoxide Dismutase (Cu-Zn SOD) 22
    3.2. Manganese Superoxide Dismutase (Mn SOD) 29
    3.4. Iron Superoxide Dismutase (Fe SOD) 31
4. Oxidative Stress 34
    4.1. Abiotic Stress 35
        4.1.1. Ozone 35
        4.1.2. Salt 35
        4.1.3. Herbicides 36
        4.1.4. High Light Stress 36
        4.1.5. Sulfur Dioxide (SO_2) 37
    4.2. Biotic Stress 37
5. Role of SODs in Controlling Oxidative Stress in Plants 38
6. Dissertation Research Objectives 44

CHAPTER II. MATERIALS AND METHODS

1. Cloning of Mature *A. thaliana* Fe SOD Gene into Bacterial Expression Vector 47
2. Expression and Purification of Enzymatically Active Recombinant Fe SOD Enzyme from *E. coli* 56
3. Antibody Production 60

4. Plant Material 60
5. Determination of Optimum Surfactant Concentration 60
6. Stress Treatments 61
7. Effects of Light on SODs of Stress Treated Plants 64
8. DNA Gel Blot Analysis 64
9. Preparation of Plant Material for Denaturing and Non-Denaturing PAGE 65
10. Specificity of the Antibodies 66
11. Densitometric Scanning of the Non-Denaturing Gels and Western Blots 67
12. Comparison of Sequences 70
13. Modeling of the Three Dimensional Structure of *A. thaliana* Fe SOD Protein 70

CHAPTER III. RESULTS

1. Expression of *A. thaliana* Fe SOD protein in *E. coli* 75
2. Production of Anti-Fe SOD antibodies 75
3. Fe SOD gene copy number in the *A. thaliana* genome 82
4. Oxidative Stress treatments 85
    4.1. Effects on Fe SOD 90
    4.2. Effects on Mn SOD 93
    4.3. Effects on Cu-Zn 99
    4.4. Effects of Light on Oxidative Stress Responses 102
5. Comparison of SOD Sequences 105
6. Generation of the Three Dimensional Structure of *A. thaliana* Fe SOD Protein 114

CHAPTER IV. DISCUSSION

1. Analysis of SOD Genes in *A. thaliana* 134
2. Analysis of Multiple SOD Isoenzymes in *A. thaliana* 135
3. Effects of Oxidative Stress on SOD Populations 136

3.1. Effects of Oxidative Stress on Fe SOD Enzyme and Protein 136
3.2. Effects of Oxidative Stress on Mn SOD Enzyme and Protein 140
3.3. Effects of Oxidative Stress on Cu-Zn SOD Enzyme and Protein 145
3.4. Effect of Light on Oxidative Stress Responses 147
4. Comparison of the Fe, Mn and Cu-Zn SOD Sequences 148
5. Summary: Responses of *A. thaliana* Fe and Mn SODs to Oxidative Stress 152
CHAPTER V. BIBLIOGRAPHY 155
Curriculum vitae 167

LIST OF FIGURES

CHAPTER I. INTRODUCTION

Figure 1. Reactive Oxygen Species (ROS) Scavenging in Chloroplast 7

Figure 2. Model proposed for the function of the ascorbate-glutathione cycle in leaf peroxisomes. 10

Figure 3. Proposed scheme for supplying hydrogen peroxide (H_2O_2) to lignin biosynthesis. 14

Figure 4. Subcellular localization of SOD proteins. 19

Figure 5. The illustration of successive reduction and reoxidation reaction of Cu (II) at the active center of Cu-Zn SOD by O_2^- radical. 25

CHAPTER II. MATERIALS AND METHODS

Figure 6. Full length *A. thaliana* Fe SOD cDNA sequence. 49

Figure 7. Molecular cloning strategy of Fe SOD cDNA into shuttle vector PNoTA/T7. 51

Figure 8. Molecular cloning strategy of Fe SOD cDNA into pET-32c(+) vector. 58

Figure 9. Treatments of *A. thaliana* with the appropriate solvents. 63

Figure 10. Sensitivities of SOD enzymes to different inhibitors. 69

Figure 11: Alignment of amino acid sequences of *E. coli*, *P. ovalis*, and *A. thaliana*. 72

CHAPTER III. RESULTS

Figure 12. Thx-Fe SOD protein expression in *E.coli.*. 77

Figure 13. SDS-PAGE of purified Thx-Fe SOD fusion protein. 79

Figure 14. Enzyme activity of purified Thx-Fe SOD protein. 81

Figure 15. Protein blot of *A. thaliana* leaf extract probed with Fe SOD anti-sera raised in chickens. 84

Figure 16. DNA gel blot profile of wildtype *A. thaliana* genomic DNA. 87

Figure 17. Effects of surfactant treatment on *A. thaliana* seedlings. 89

Figure 18. Effects of methyl viologen and DCMU treatments on Fe SOD of *A. thaliana*. 92

Figure 19. Appearance of two novel Fe SOD activity bands. 95

Figure 20. Effects of methyl viologen and DCMU treatments on Mn SOD of *A. thaliana*. 98

Figure 21. Effects of methyl viologen and DCMU treatments on Cu-Zn SOD of *A. thaliana*. 101

Figure 22. Effects of light and methyl viologen on SOD activities on *A. thaliana*. 104

Figure 23: Comparison of amino acid sequences of known chloroplastic and cytosolic plant Cu-Zn SODs. 107

Figure 24. Phylogenetic tree of plant Cu-Zn SODs. 109

Figure 25. Comparison of amino acid sequences of twelve known plant and prokaryotic Fe and Mn SODs. 111

Figure 26. Phylogenetic tree of plant Fe and Mn SODs. 113

Figure 27. Comparison of amino acid sequences of plant Fe, Mn, chloroplastic Cu-Zn, and cytosolic Cu-Zn SODs. 116

F**igure 28.** Phylogenetic tree of plant Fe, Mn, cytosolic Cu-Zn, and chloroplastic Cu-Zn SODs. 118

Figure 29. Stereo image of modeled *A. thaliana* Fe SOD protein. 120

Figure 30. Comparison of the secondary structure of modeled *A. thaliana* Fe SOD to known bacterial Fe SODs. 123

Figure 31. Comparison of the secondary structure of modeled *A. thaliana* Fe SOD to known Mn SODs. 125

Figure 32. Comparison of the secondary structure of modeled *A. thaliana* Fe SOD to known Cu-Zn SODs. 127

Figure 33. Comparison of the three dimensional structures of modeled *A. thaliana* Fe SOD with the SODs with known three dimensional structures. 131

Chapter I

Introduction

1. Formation of Toxic Oxygen Species in Plant Cells

Oxygen, the most essential element for aerobic life is relatively stable. Because the electrons of oxygen (O_2) are directional with a parallel spin state, its divalent reduction is kinetically limited by the relatively slow electron spin inversion process. When O_2 is involved in a reaction, it has to be activated, permitting spin inversion of one electron at a time. This univalent pathway requires the generation of intermediates. The first reduced intermediate is the superoxide radical (O_2^-).

Superoxide radicals are formed through;

1. reduction of a non-reactive O_2 molecule in the triplet ground state ($^3O_2$) by excited pigments that have undergone charge separation (Elstner and Osswald, 1994)

2. univalent reduction of O_2 by a reductant with sufficiently negative electrochemical potentials to donate electrons to oxygen (E_0 $O_2/O_2^{-\cdot}$ = -0.33 V), and

3. univalent oxidation of H_2O_2, reverse dismutation (Fridovich, 1989).

O_2 activation may occur in different compartments of the cell (Elstner, 1991), including mitochondria, chloroplasts, microsomes, glyoxysomes, peroxisomes, apoplasts, and the cytosol. Because the measurement of O_2^- is technically difficult, evidence for increased O_2^- within the cell comes from changes in the concentrations of antioxidant molecules and changes in the specific activities of enzymes, such as superoxide dismutase, peroxidases, and enzymes of the Asada-Halliwell pathway (Quartacci and Navari-Izzo,

1992; Fridovich, 1986). A reliable method to measure the amount of intracellular superoxide levels is through measuring rapid inactivation of (4Fe-4S)-containing dehydratases, *e.g.,* aconitase. Superoxide oxidizes the clusters of these dehydratases resulting in loss of Fe (II). This is a reversible reaction and the balance between these opposing processes can be used as a measure of superoxide (Fridovich, 1986). All the compartments of the cell are possible sites for O_2^- formation, but chloroplasts, mitochondria and peroxisomes are thought to be the most important generators of reactive oxygen species (ROS) (Fridovich, 1986).

1.1. Chloroplast

Aside from chemosynthesis, photosynthesis is the only energy-producing mechanism on earth. Photosynthesis involves one oxidation and one reduction process. The overall oxidation reaction is the oxidation of water (H_2O) by the removal of electrons with the release of O_2. The overall reduction reaction is the reduction of CO_2 to form organic compounds, such as carbohydrates. In contrast to respiration where electrons are removed from carbon compounds, passed downhill to react with a strong electron acceptor (O_2), and then combined with H^+ to make H_2O, the photosynthetic mechanism drives the electrons--uphill, away from H_2O, to a weaker electron acceptor, CO_2. Photosynthesis involves three major electron transport complexes. These are Photosystem I (PS I), cytochrome b_6-f complex, and Photosystem II (PS II). Light is the source of the energy used in this process. In plants and photosynthetic protista, the light

harvesting apparatus is located in the thylakoid membranes of the chloroplasts. When light reaches the plant surface, photosynthetically available radiation (PAR) enters into the plants and is absorbed by photosynthetic pigments at the site of thylakoid membranes. This captured light excites the electrons (e^-) of the pigment molecule. Photosynthetic pigment molecules can stay in an excited state only for a short time, one nanosecond or less. This excitation energy can either be lost as heat energy or fluorescence as the electron moves back to its ground stage, or some of it can be moved to photosystem II (PS II) and from there electrons are transferred to PS I by the function of cytochrome b_6-f ($cytb_6$-f). Between these two electron transport chains, ATP is formed by a mechanism called photophosphorylation which is very similar to oxidative phosphorylation in mitochondria. PS I is located in the stromal thylakoids. Transfer of the electrons to ferredoxin (Fd) occurs at PS I. The final electron transport step is the reduction of $NADP^+$ to NADPH. After this step chemical energy harvested by the light reaction is used to reduce carbon dioxide to organic carbohydrate molecules and other processes. This reduction occurs in the stroma of the chloroplasts through reactions of the Calvin Cycle, also known the Photosynthetic Carbon Reduction (PCR) cycle. The enzyme activation that starts the PCR cycle takes place when electrons from reduced Fd move to a small protein called thioredoxin to reduce it. Triosephosphates are formed as the end product of the PCR cycle.

Photosynthesis is one of the crucial elements of oxidative life, but when there is

not enough ferredoxin available as the electron acceptor in the photosynthetic process, electrons from PS I react with molecular O_2 and reduce it univalently, and the reactive O_2 species (ROS) are formed as a result of this reduction reaction (Figure 1) (Asada et al. 1994; Fridovich, 1995 & 1986; Rubinstein and Luster, 1993). Similarly, when $NADP^+$ is not available in adequate amounts as a result of insufficient oxidation of NADPH during the Calvin Cycle, again, the electrons can be accepted by O_2 causing the formation of superoxide radicals. Formation of superoxide takes place on either side of the thylakoid membranes as well as in the aprotic interior of the thylakoid membranes (Asada and Takahashi, 1987; Takahashi and Asada, 1988). The photoreduction of O_2 in the chloroplasts was first demonstrated by Mehler (1951) as the formation of hydrogen peroxide (H_2O_2). Superoxide O_2 is dismutated to H_2O_2 at neutral pH. The change observed in the chloroplast pH is further evidence of O_2 formation in the chloroplast. O_2^- can act both as an reductant and as an oxidant. As a reductant it can give rise to more reactive O_2 species, such as singlet oxygen ($^1O_2$), superoxide (O_2), hydrogen peroxide (H_2O_2) and hydroxyl radicals (OH^-). O_2^- causes the oxidation of polyphenols, catecholamines, tocopherols, leucoflavins, ascorbate, and thiols (Fridovich, 1989). It also inactivates catalases (Kono and Fridovich, 1983), peroxidases (Okajima, 1972), dihydroxy acid dehydratase (Kuo et al. 1987), and thiol containing enzymes, such as thioredoxin-

Figure 1. Reactive Oxygen Species (ROS) Scavenging in Chloroplast Involving SOD: Proposed Thylakoid and Stromal Pathways. In thylakoid-associated scavenging, superoxide radicals are dismutated by superoxide dismutase (SOD) (either an Fe or Cu-Zn form) and the resultant H_2O_2 is scavenged by thylakoid-bound ascorbate peroxidase (tAPX). In stromal-associated scavenging, reactive oxygen species (ROS) that escape the thylakoid pathway are dismutated by Fe (or Cu-Zn) and stromal APX (sAPX). Monodehydroascorbate (MDA) radicals produced by APX are converted to ascorbate (AsA) through reactions with ferrodoxin (Fd) (thylakoid) or monodehydroascorbate reductase (MDHAR) (stromal). Reduction of dehydroascorbate (DHA) to AsA is catalyzed by dehydroascorbate reductase (DHAR) via the stromal ascorbate-glutathione pathway.

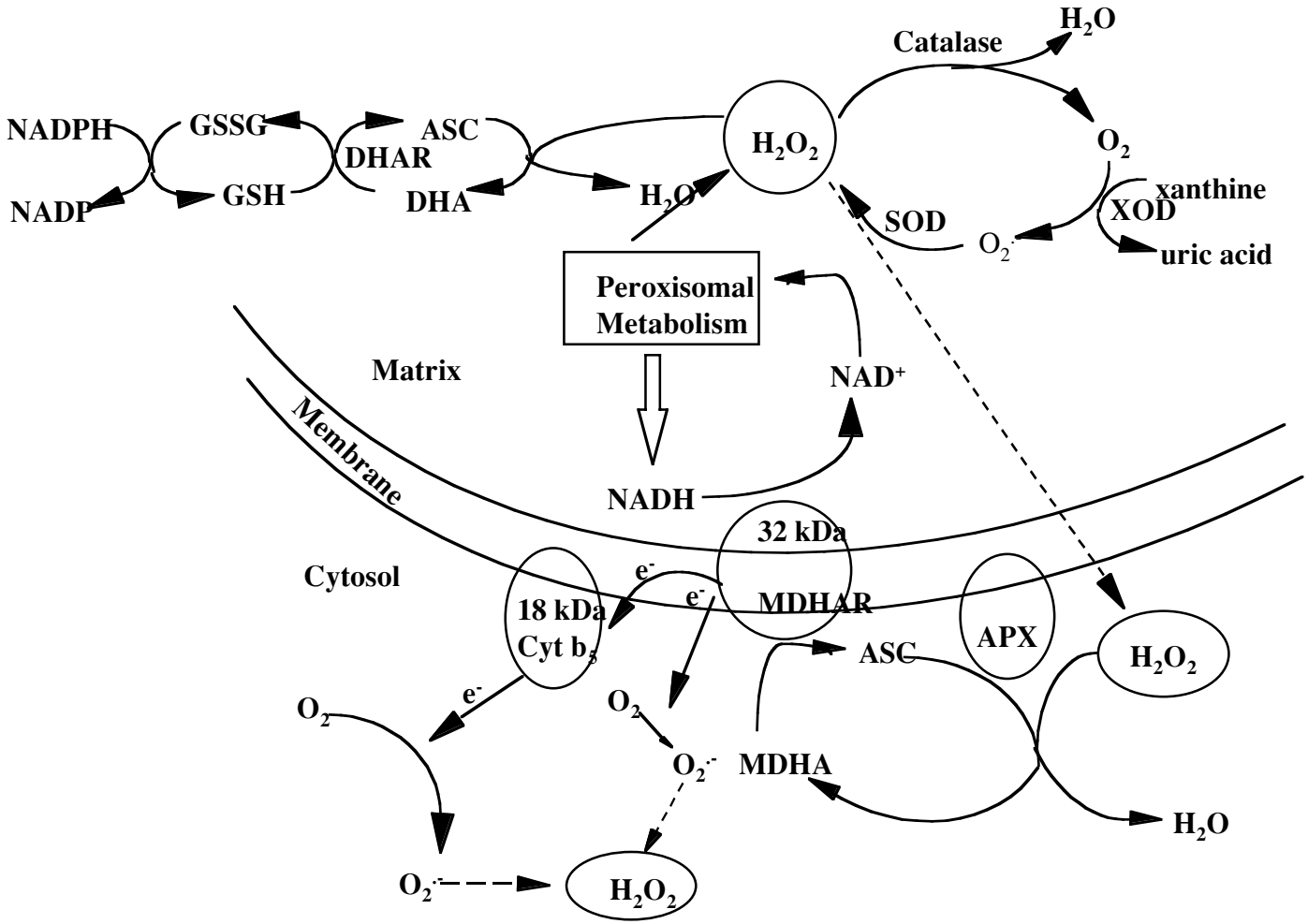
NADPH
GSSG
ASC
DHAR
NADP
GSH
DHA
H_2O
H_2O_2
Catalase
H_2O
O_2
xanthine
XOD
uric acid
SOD
$O_2^{\cdot-}$
Peroxisomal Metabolism
Matrix
NAD^+
Membrane
NADH
32 kDa
MDHAR
Cytosol
e^-
e^-
18 kDa
Cyt b_5
APX
ASC
H_2O_2
e^-
O_2
O_2
$O_2^{\cdot-}$
MDHA
H_2O
$O_2^{\cdot-}$
H_2O_2

modulated enzymes of the stroma (Tanaka et al, 1982).

1.2. Peroxisomes

Peroxisomes carry out several essential functions of the cell including peroxisomal oxidation and respiration, fatty acid β-oxidation, glyoxylate metabolism, and ether lipid synthesis. The basic enzymatic components of these organelles are flavin oxidases, which produce H_2O_2 (Huang et al. 1983; van den Bosch, 1992). Superoxide radicals are formed in peroxisomes as a result of the oxidative type of metabolism carried out in these organelles. Two sites have been identified for superoxide generation in peroxisomes. One of these is located in the matrix. In this system xanthine oxidase has been identified as the superoxide-generating system (Sandalio et al. 1987). The second superoxide generating system is located in the peroxisomal membranes. This is an NADH-dependent production of superoxide. A small electron transport chain composed of a flavoprotein NADH:ferricyanide reductase and cytochrome b_5 is where the superoxide radicals are generated (del Rio et al. 1998) (Figure 2). Lopez-Huertas et al. (1996) isolated peroxisomal membranes from pea (*Pisum sativum*) plants and examined for the presence of proteins involved in superoxide generation. They reported that at least three proteins are involved in formation of superoxide in peroxisomal membranes. Superoxide dismutases (E.C. 1.15.1.1; SODs) scavenging for O_2^- radicals in peroxisomes were also detected in peroxisomes. A peroxisomal manganase (Mn)-containing SOD was located immunochemically in *P. sativum* protoplasts (del Rio et al. 1983). del Rio (1983) and

Figure 2. Model proposed for the function of the ascorbate-glutathione cycle in leaf peroxisomes. In the peroxisomal membranes the trans-membrane protein MDHAR can oxidize NADH on the matrix side of the peroxisomal membrane and transfer the reducing equivalents as electrons to the acceptor monodehydroascorbate on the cytosolic side of the membrane. In this process, molecular O_2 could also act as an electron acceptor, with the concomitant formation of $O_2^{\cdot-}$. This radicals are removed by Mn SOD located in the peroxisomes. The end product of this reaction, H_2O_2, is removed by APX at the site of peroxisomal membranes.

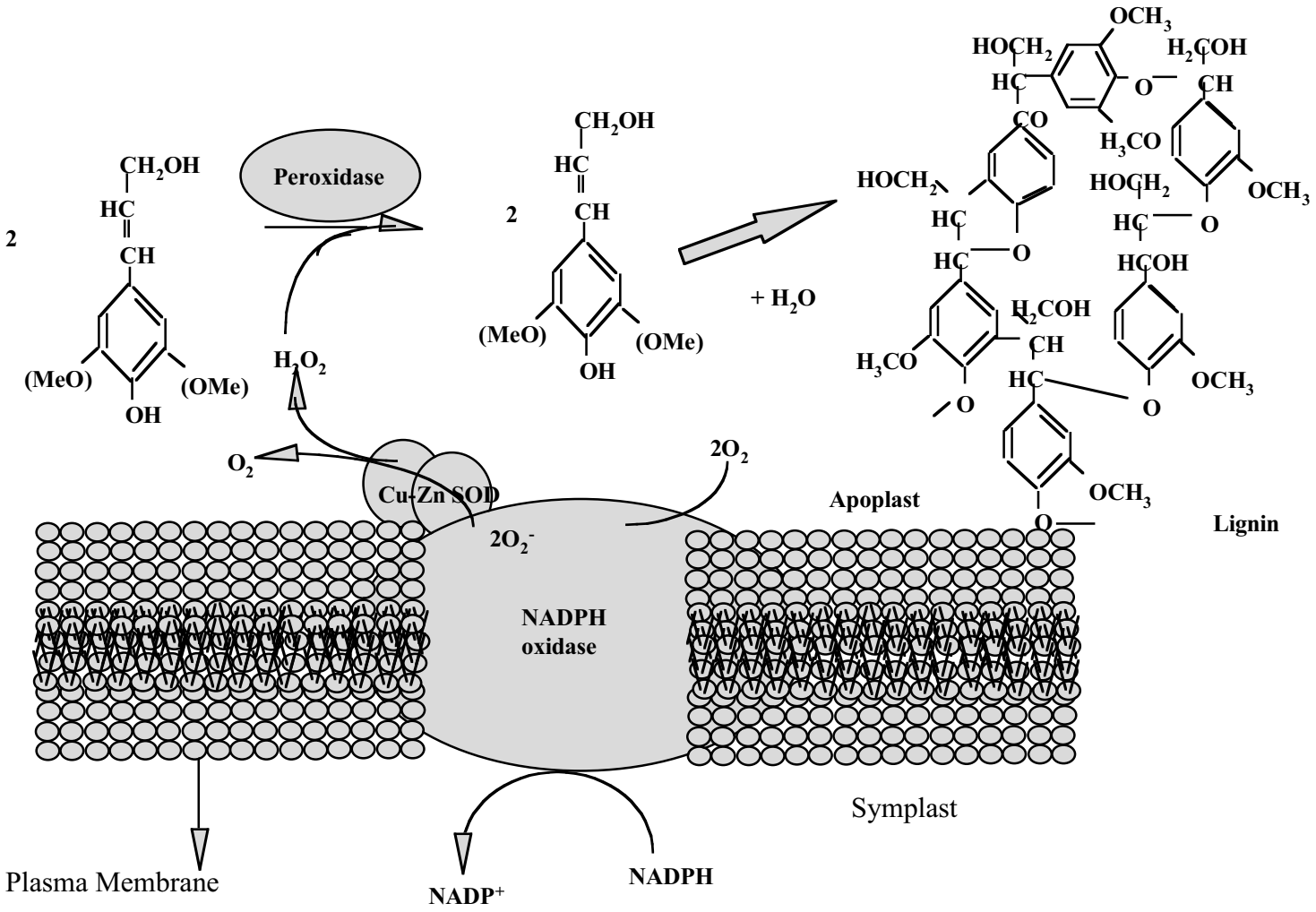
Peroxidase
2
(MeO)
(OMe)
OH
H_2O_2
O_2
$2O_2$
Cu-Zn SOD
$2O_2^-$
NADPH
oxidase
+ H_2O
Apoplast
Lignin
Symplast
Plasma Membrane
$NADP^+$
NADPH

Sandalio et al. (1987) both reported Mn SOD activity in purified peroxisomal membranes as well as in mitochondria in *P. sativum*, although they both concluded that the presence of Mn SOD in mitochondria was a result of contamination of the mitochondrial fraction with the peroxisomal membrane. However further investigation showed that there are two different Mn SODs located in the cell, one located in the peroxisome and one in mitochondria (del Rio et al. 1992). More recently a Cu/Zn-containing SOD was located in the matrix of the peroxisomes of watermelon (*Citrullus vulgaris*) cotyledons (Bueno et al. 1995). del Rio et al. (1998) suggested that senescence causes important variations in oxidative metabolism in peroxisomes. SOD enzyme populations in peroxisomes composed of different isozymes may change as a result of senescence.

1.3. Mitochondria

Similar to the chloroplast, mitochondria also have an electron transfer chain through which ATP is formed from ADP and P*i.* This process is called oxidative phosphorylation, and the last electron acceptor of this chain is O_2 which is reduced by cytochrome oxidase. In addition to this tetravalent reduction of O_2, formation of reactive (O_2) species has also been reported in mitochondria (Nohl et al. 1981). In animal mitochondria, formation of ROS may occur either between the rotenone and antimycin-sensitive electron carriers or at the cytochrome *b*-c_1 segments (Elstner, 1991). In plants, in addition to the mitochondrial electron chain, the alternate pathway of respiration is associated with the electron transport chain. Possible sites of (O_2) activation have been

found at the redox level of the NADH dehydrogenase(s) or ubiquinone-cytochrome *b* (Elstner, 1991).

1.4. Apoplast

A mechanism for superoxide generation and the involvement of copper-zinc (Cu-Zn) SOD in its conversion to H_2O_2 in apoplast was proposed by Ogawa et al (1997) using spinach hypocotyls. Because of its involvement in lignin biosynthesis, H_2O_2 is a necessary component of apoplasts in plant cells. Ogawa et al. (1997) suggested that H_2O_2 for lignin biosynthesis is produced by the removal of O_2^- anions by Cu-Zn SOD located in the plasma membrane. Superoxide radicals necessary for this reaction are proposed to produced by NAD(P)H oxidase also localized in the plasma membrane (shown in Figure 3; Ogawa et al. 1997). The authors also suggested that there is a synchronic regulation between the generation of superoxide anions and the expression of the Cu-Zn SOD enzyme. Studies carried out with the Cu-Zn SOD inhibitors showed that very little H_2O_2 is produced although there is continuous production of superoxide radicals in the absence of Cu-Zn SOD activity. Therefore, this study concluded that Cu-Zn SOD is crucial for lignin biosynthesis (Ogawa et al. 1997).

2. Defense Against Reactive Oxygen Species

O_2 molecules have a strong negative charge. This negative charge decreases the degree of damage caused by superoxide radical as an oxidant. When this charge is

Figure 3. Proposed scheme for supplying hydrogen peroxide (H_2O_2) to lignin biosynthesis. Superoxide radicals formed as a result of NAD(P)H oxide are converted to H_2O_2 as a result of Cu-Zn SOD activity present in the apoplast as a membrane bound enzyme. This H_2O_2 is used in lignin biosynthesis as phenyl alanine is converted to lignin.

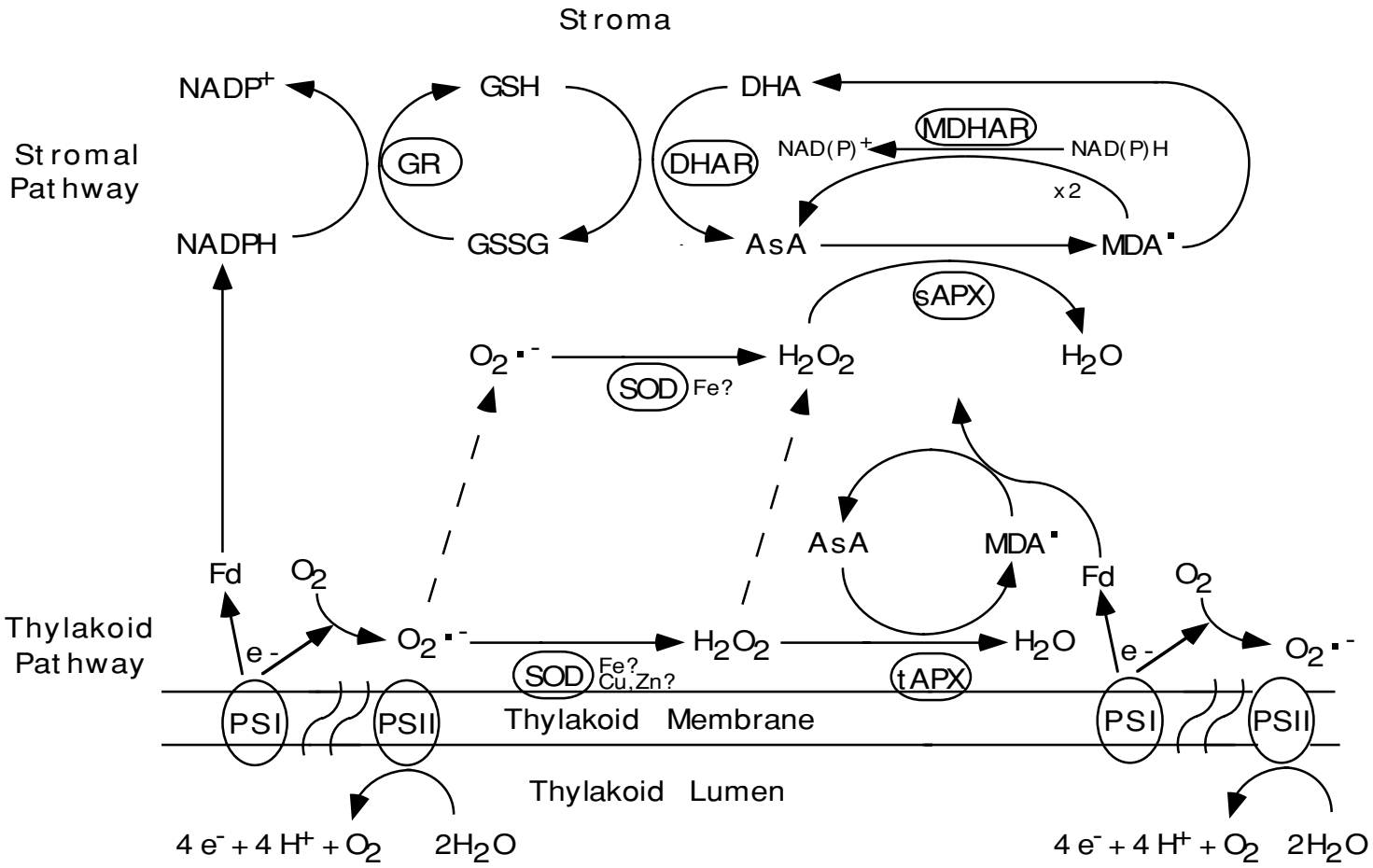
Stroma
NADP+
GSH
DHA
MDHAR
NAD(P)+
NAD(P)H
Stromal Pathway
GR
DHAR
x 2
NADPH
GSSG
AsA
MDA·
sAPX
O2·-
H2O2
H2O
SOD Fe?
Fd
O2
AsA
MDA·
Fd
O2
Thylakoid Pathway
e-
O2·-
H2O2
H2O
e-
O2·-
SOD Fe? Cu,Zn?
tAPX
PSI
PSII
Thylakoid Membrane
PSI
PSII
Thylakoid Lumen
4 e- + 4 H+ + O2
2H2O
4 e- + 4 H+ + O2
2H2O

neutralized via association with a proton or a metal cation, stronger oxidants, *i.e.* MeO_2^+(metal oxides), are formed (Fridovich, 1989). These radicals are more potent oxidants than superoxide itself. $HO_2^{\cdot}$ reacts with polyunsaturated fatty acids with a higher rate constant than that of superoxide. O_2 does not oxidize NAD(P)H, but MnO_2^+, a product of metal ion conversion of (O_2) and peroxoxanadyl, reacts with NAD(P)H, causing its oxidation, which may increase the formation of (O_2).

Dismutation of O_2^- gives rise to H_2O_2. The metal ion interaction of H_2O_2 by ferric and cupric complexes also causes the formation of HO^- and $HO^{\cdot}$. OH^- and $HO^{\cdot}$ indiscriminately react with the biomolecules of the cell at diffusion-limited rates causing denaturation of proteins, mutation of DNA, and lipid peroxidation, all of which cause serious physiological damage to the organism (Cadenas, 1989; Fridovich, 1989; Halliwell, 1987).

SODs are the first line of defense against oxidative stress. These enzymes catalyze the disproportionation of O_2 to H_2O_2 and dioxygen, another ROS (McCord and Fridovich, 1969). The reactions (1 and 2) that take place in the presence of SODs are:

$O_2^- + SOD\text{-}M^{+2} \rightarrow O_2 + M^+$ Reaction 1

$O_2^- + 2H^+ + SOD\text{-}M^+ \rightarrow H_2O_2 + M^{+2}$ Reaction 2

The sum of these reactions (1 and 2) is given in Reaction 3.

$2O_2^- + 2H^+ \rightarrow H_2O_2 + O_2$ Reaction 3

The products of the reaction are H_2O_2 and molecular O_2. H_2O_2, also toxic, is removed by catalase and/or ascorbate peroxidase (APX, EC 1.11.1.7). APX is present in plants, cyanobacteria and algae (Asada, 1992). In higher plants at least three different forms of APX have been characterized. These are thylakoid-bound, stromal and cytosolic APXs. Ascorbate is the required electron donor for chloroplastic forms of APX, and this enzyme is highly labile if ascorbate is not present (Chen and Asada, 1989; Miyake et al. 1991). The cytosolic form of this enzyme is known to be more stable in the absence of the donor, and has a broader donor range (Mittler and Zilinskas, 1991). Toxicity of H_2O_2, like that of SODs, is through a metal ion dependent conversion into hydroxyl radicals that have the ability to mutate DNA and start lipid peroxide reactions (Bowler et al. 1991; Salin, 1988). A schematic of the formation and removal of reduced O_2^- species in the chloroplast is given in Figure 1. Once formed, O_2^- radicals are removed by SODs in the stroma and in the thylakoid membrane. H_2O_2 formed as a result of this reaction is scavenged by ascorbate peroxidase, also located both in the stroma and thylakoid membrane. Monodehydroascorbate reductase (MDAR, EC 1.6.5.4), dehydroascorbate reductase (DHAR), and glutathione reductase, using NADPH produced as a result of electron transport, are also involved in this scavenging function. The chemical disproportion of MDA to DHA and ascorbate is very fast at the pH of chloroplast storma in the light. Therefore any MDA escaping the reduction is disproportionated quickly to DHA and ascorbate. DHA is unstable at physiological pH, and it is reduced to

ascorbate. This reaction is catalyzed by DHA reductase in the presence of glutathione. The end product of the reaction is disulfide glutathione (GSSG). GSSG then is reduced by glutathione reductase (GR, EC 1.6.4.2) back to two GSH molecule at the expense of NADPH.

3. Superoxide Dismutases (SODs)

In the cell, O_2^- is produced at any location where an electron transport chain is present. Takahashi and Asada (1983) showed that phospholipid membranes are impermeable to charged O_2^- molecules. Therefore, it is crucial that SODs are present for the removal of O_2^- in the compartments where O_2^- radicals are formed (Takahashi and Asada, 1983). Based on the metal co-factor used by the enzyme, SODs are classified in to three groups, and these SODs are located in different compartments of the cell (Figure 4). Fe SOD is located in the chloroplast, Mn SOD in the mitochondrion and Cu-Zn SODs in the chloroplast and cytosol. Deduced amino acid sequences from these three different types of SODs suggest that Mn and Fe SODs are more ancient types of SODs, and these enzymes most probably have arisen from the same ancestral enzyme, whereas Cu-Zn SODs have no sequence similarity to Mn and Fe SODs and probably have evolved separately in eukaryotes (Kanematsu and Asada, 1990; Smith and Doolittle, 1992). The evolutionary reason for the separation of SODs with different metal requirements is probably related to the different availability of soluble transition metal compounds in the

Figure 4. Subcellular localization of SOD proteins. SODs are found in different compartments within the cell. All three SOD forms are nuclear-encoded. Mn SOD is located in both mitochondria and peroxisomes. Fe SOD is located in the chloroplasts and Cu-Zn SOD is located in apoplast, chloroplast, and cytosol.

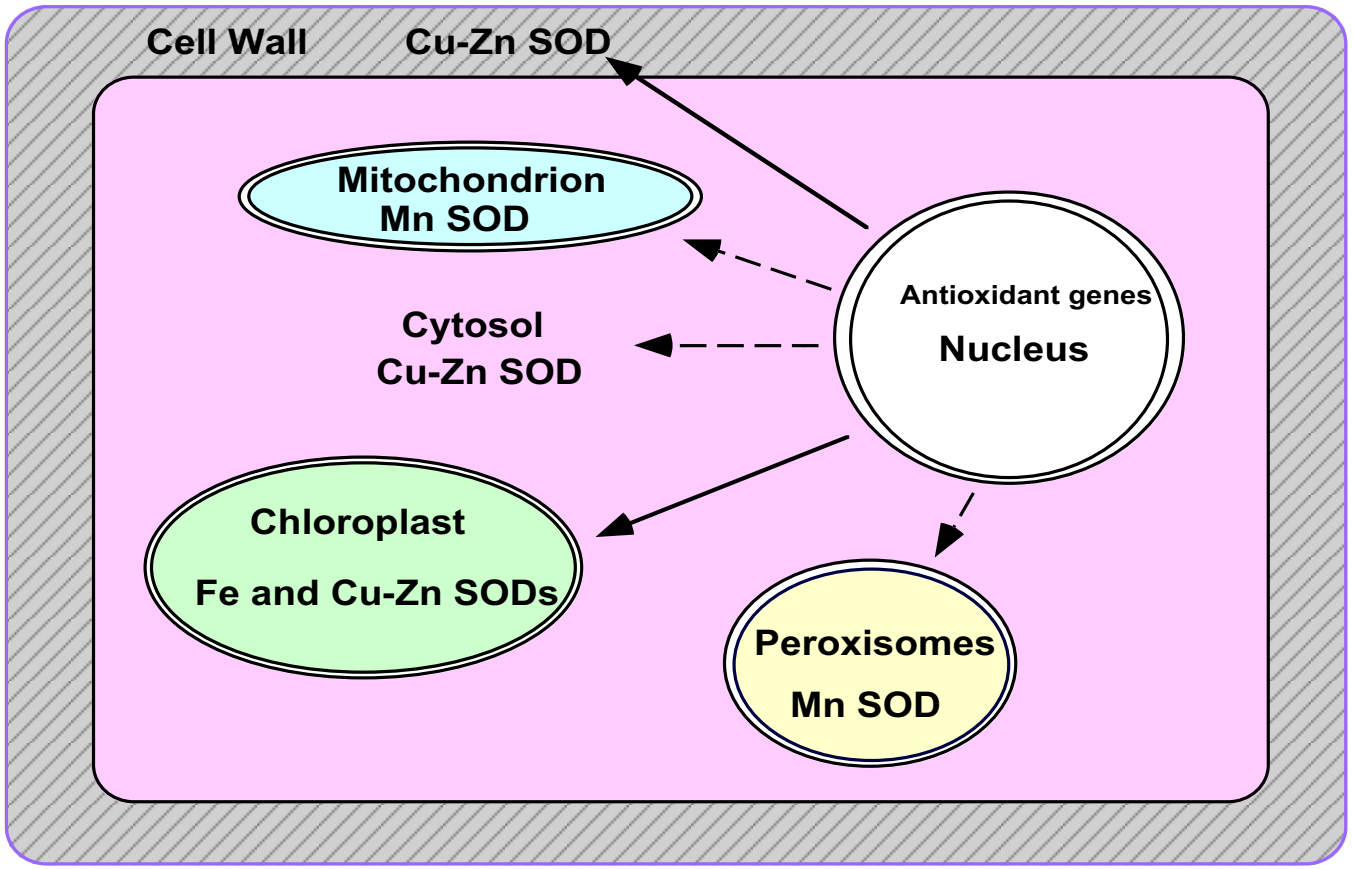
Cell Wall
Cu-Zn SOD
Mitochondrion
Mn SOD
Cytosol
Cu-Zn SOD
Antioxidant genes
Nucleus
Chloroplast
Fe and Cu-Zn SODs
Peroxisomes
Mn SOD

biosphere in relation to the O_2 content of the atmosphere in different geological eras (Bannister et al. 1991). Bannister et al (1991) suggested that iron was probably the first metal used as a metal cofactor at the active site of the first SOD. At the time, iron was abundant in soluble Fe (II) form. As the levels of O_2 in the environment increased, the mineral components of the environment started to be oxidized. The decrease in available Fe (II) in the environment caused a need for the use of another available metal which was more available--Mn (III). When the atmosphere was completely replenished with oxygen, Fe (II) was almost completely unavailable in the atmosphere and insoluble Cu (I) was converted into soluble Cu (II). At this stage, Cu (II) began to be used as the metal cofactor at the active sites of SODs. Since Fe SODs and Mn have similar electrical properties, there was no need for a change in the structure of the protein. Thus, Mn and Fe SODs are structurally very similar. The existence of archaic Mn/Fe[1]-containing SODs supports this theory. However electrical properties of Cu-Zn[2] SODs are completely different than Fe and Mn SODs, therefore a major change in the structure of the protein occurred after Cu become a metal cofactor (Bannister et al. 1991). Fe and Mn SODs are present both in prokaryotic and in eukaryotic organisms whereas Cu-Zn SODs have been found mostly in eukaryotes. However, Cu-Zn SODs have been demonstrated in some bacteria, including *Photobacterium leiognathi*, *Caulobacter crescentus*, and

[1] Every molecule of Mn and Fe SOD contains either an atom of manganese or an atom of iron depending on the species and/or the availability of the metal in archaic SODs, and is denoted as such by a slash, Mn/Fe.
[2] Every molecule of the Cu-Zn SOD enzyme contains both an atom of copper and one zinc, as denoted by the hyphen.

pseudomonads. The presence of Cu-Zn SOD in prokaryotes may be explained with the three hypotheses described below:

1. Independent evolution of Cu-Zn SODs took place in prokaryotes and eukaryotes.

2. Cu-Zn SOD first originated in the eukaryotes and then the gene was transferred into the prokaryotes. This theory was first proposed by Martin and Fridovich (1981) and then was supported by Bannister and Parker (1985) because of the 30% similarity between the amino acid sequences of a ponyfish and its symbiont *Photobacterium leiognathi*. After taking point mutations into consideration this similarity increased to 44%, bringing yet more support to the theory (Leunisssen and Jong, 1986). However, the presence of Cu-Zn SOD in *Caulobacter crescentus* (Steinman, 1982) and pseudomonads which are not symbionts (Steinman, 1985) has raised some questions about this theory.

3. Cu-Zn SOD first originated in prokaryotes and then was transferred to eukaryotes. However, this theory suggests that prokaryotic and eukaryotic enzymes have a common ancestor, which is unlikely, due to the unavailability of Cu (II) in the atmosphere before prokaryotes and eukaryotes were separated.

In addition to these three common SODs, two unusual SODs were reported in *Methanobacterium bryantii* and *Streptomyces* sp. An Fe-Zn SOD was reported in *M. bryantii* (Kirby et al. 1981), *Streptomyces coelicolor* (Kim et al. 1996), and *Nocardia*

asteroides (Beaman et al. 1983). This enzyme is a tetramer of 22.2 kD subunits. The amino acid sequences of the Fe-Zn SODs from these two species have similarities to one another as well as to known Mn and Fe SODs, but the roles of the cofactors of Fe-Zn SODs are not clearly identified and need further investigation (Kim et al. 1996). *Streptomyces* strain-IMSNU-1 contains only one SOD, which has a Ni atom in its active center (Youn et al. 1996). *S. coelicolor* has a Ni SOD in addition to its Fe-Zn containing isoform. This enzyme is a homotetramer of 13.4 kD subunits. The presence of Ni in the environment seems to play an important role in the regulation of SODs in *S. coelicolor*. When Ni is in the environment there is a significant decrease in the amount of Ni SOD apoenzyme, accompanied by a significant increase in the amount of Fe-Zn containing apoenzyme. The mechanism by which Ni regulates the synthesis of each apoenzyme is not understood and has yet to be explored (Kim et al. 1996). Streptomycetes live in the soil, where Ni is abundant as a soluble metal source (Andrews et al. 1988). This abundance of Ni may be the reason for the evolution of a new Ni-containing SOD. Ni SOD has no sequence similarity to known SODs (Kim et al. 1996). The phylogenetic relationship of Ni SOD to other SODs requires further research.

3.1. Copper-Zinc Superoxide Dismutase (Cu-Zn SOD):

Cu (II) and Zn (II) atoms in Cu-Zn SODs are noncovalently associated with the apoprotein and connected to each other by a disulfide bond (Fridovich, 1989). Cu (II) is the functionally crucial atom, and its replacement with another metal, or omission from

the structure, causes enzyme inactivation (Bordo et al. 1994; Cudd and Fridovich, 1982, Marino et al. 1995). In bovine erythrocyte, Cu-Zn SOD Cu (II) is ligated to the imidazole rings of histidines (His 44, 46, 61, and 118). There are two lysine residues (Lys 120 and Lys 134) at 12-13 Å respectively from the Cu ion. These two lysine residues (Lys 120 and Lys 134) and an arginine (Arg 141) residue are found to be conserved in mammalian Cu-Zn SODs. (Bordo et al. 1994). Cu-Zn SOD has approximately 150 times the surface area of Cu (II). Therefore the interaction between O_2^- and the enzyme has to be with an electrostatic guidance to attract the O_2^- molecule to the active site of the enzyme. Native and chemically-modified Cu-Zn SODs were used to test this hypothesis (Cudd and Fridovich, 1982). It was shown that the positively charged lysine residues provide electrostatic guidance to negatively charged O_2. Cu (II) is ligated to imidazole groups of the histidines. As a result of interaction between O_2^- and Cu (II), Cu (II) ion is released from the structure, and then, after the successive reduction and re-oxidation by O_2^-, it may re-ligate to the structure. When the reduced Cu (I) leaves the active center, the highly basic imidazole draws away a proton from the solution. Following this, the proton reacts with the O_2 formed as a result of Cu (II) interaction with O_2^-, forming a HO_2^- which in turn is protonated and converted to H_2O_2 (Figure 5) (Fridovich, 1986).

Cu-Zn SOD is the most common SOD in higher plants. It is inhibited by potassium cyanide (KCN) which is related to the participation of copper in the active

Figure 5. The illustration of successive reduction and reoxidation of Cu (II) at the active center of Cu-Zn SOD by O_2^- radical. Im^- Imidazole of histine residue at the active center, Zn (II) Zinc atom at the active site of Cu-Zn SOD.

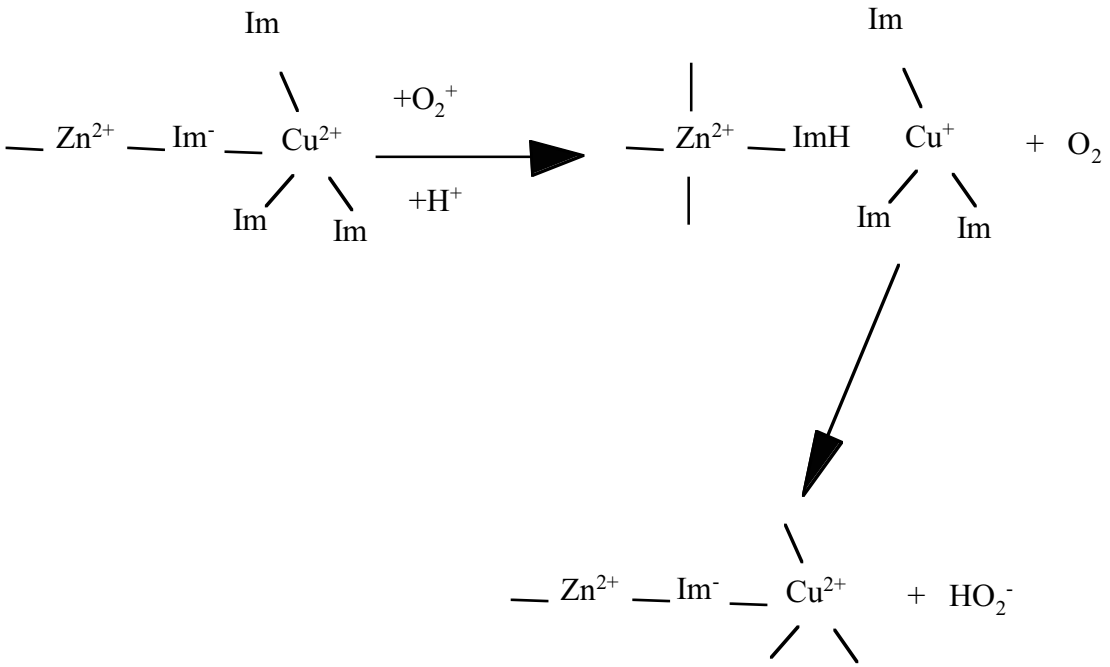
Im
Zn2+
Im-
Cu2+
Im
Im
+O2+
+H+
Zn2+
ImH
Im
Cu+
Im
Im
+ O2
Zn2+
Im-
Cu2+
+ HO2-

center (Asada et al. 1974). It is also inactivated by H_2O_2. Since the end product of the dismutation reaction of O_2^- radicals is H_2O_2, inactivation of Cu-Zn SODs by H_2O_2 has physiological importance. Chloroplastic Cu-Zn SOD (Cu-Zn SOD_{chl}) has been shown to be less sensitive to H_2O_2 than cytosolic Cu-Zn SOD (Cu-Zn_{cyt}) (Baum et al. 1983; Kwiatowski and Kaniuga, 1986).

Getzoff et al. (1992) increased the local positive charge between Cu (II) and protein by creating site-specific mutations in human Cu-Zn SOD in order to increase reaction rates. Electrostatic guidance of O_2^- on the holoenzyme depends on the Glu 132, Glu 133, and Lys 136 residues. Getzoff et al. (1992) created Glu→Gln and Glu→Lys mutations which increased the positive charge of the enzyme. However, this increase was insufficient to produce a faster reaction rate. This is probably due to structural changes resulting from electrostatic repulsion between the introduced Lys 133 and the neighboring Lys 136 (Getzoff et al. 1992).

The role of Zn (II) in Cu-Zn SODs is structural rather than functional. Replacement of Zn (II) with Co (II), Hg (II), Cd (II) or Cu (II) does not affect activity (Bordo et al. 1994; Cudd and Fridovich, 1982, Marino et al. 1995). Even complete removal of Zn (II) from the protein has little effect on activity. Zn (II) probably confers structural stability to the active site (Bordo et al. 1994, 1994, Marino et al. 1995). In contrast to Cu (II) there is a positive interaction between Zn (II) and the imidazole rings.

Dismutation of O_2^- by SODs (Figure 5) is reversible when H_2O_2 levels are high

(Reaction 4-6). The rate of the reverse reaction increases when the pH is elevated, indicating that the reactant is HO_2^-, not H_2O_2 (Fridovich, 1989).

$$\text{E-Cu (II)} + HO_2^- \rightarrow \text{E-Cu (I)-}O_2H \qquad \text{Reaction 4}$$

$$\text{E-Cu (I)-}O_2H \rightarrow \text{E-Cu (I)} + H^+ + O_2^- \qquad \text{Reaction 5}$$

$$\text{E-Cu (I)} + O_2 \rightarrow \text{E-Cu (II)} + O_2^- \qquad \text{Reaction 6}$$

The reduction of Cu (II) by H_2O_2 is a rapid process that causes the irreversible inactivation of the enzyme especially at high pH levels (Hodgson and Fridovich, 1973).

There are two different groups of Cu-Zn SODs. The first group consists of cytoplasmic and periplasmic forms, which are homodimeric. The second group comprises the chloroplastic and extracellular Cu-Zn SODs, which are homotetrameric (Bordo et al. 1994). The active sites of each subunit function independently. When these subunits are separated and then coupled with an inactive subunit, newly formed enzymes showed full activity, providing evidence that the functional interactions between the subunits are not essential for full catalytic activity (Fridovich, 1986).

Tetrameric extracellular SOD (EC-SOD) has been found exclusively in mammals to date and has a unique structure. The enzyme is a glycoprotein, and is primarily located in the interstitial matrix of tissues and the glycocalyx of cell surfaces, anchored to heparin sulfate proteoglycans (Carlsson et al. 1995). Only a small fraction of EC-SODs are found in extracellular fluids such as plasma, lymph, synovial fluid, and cerebrospinal fluid

(Carlsson et al. 1995). Carlsson et al. (1995) disrupted the expression of EC-SOD by homologous recombination in embryonic stem (ES) cells. They observed that these mice showed no abnormality and no induction of other SODs or other antioxidant enzymes up to 14 months of age. However, when they subjected these mice to oxidative stress by exposure to high O_2 concentrations, the null mutant mice displayed a remarkably reduced tolerance. This shows that under unstressed conditions, there is enough protection provided in extracellular space against O_2 (Carlsson et al. 1995).

There are at least two forms of Cu-Zn SOD in plant cells, chloroplastic and cytosolic. Deduced amino acid sequences of these two isoforms show approximately 68% similarity, whereas there is approximately 90% similarity among the chloroplastic Cu-Zn SODs (Cu-Zn SOD_{chl}), and 80-90% similarity among the cytosolic Cu-Zn SODs (Cu-Zn SOD_{cyt}). Cu-Zn $SODs_{chl}$ have a transit peptide sequence for targeting the protein to the chloroplast, but such a sequence is not present in the Cu-Zn SOD_{cyt} (Bowler et al,. 1994). One Cu-Zn SOD_{chl} isoform (Ogawa et al. 1996) and two proposed "cytoplasmic" isoforms (Kanematsu and Asada, 1990) have been identified in spinach (*Spinacia oleracea*). Cu-Zn SOD_{chl} is a soluble enzyme and is localized in the stroma (Asada et al. 1973). Localization studies performed with an immunogold-labeled antibody raised against Cu-Zn SOD_{chl} from spinach leaves showed that this soluble enzyme was not uniformly distributed in the chloroplast, but localized mainly on the stromal face of thylakoid membranes (Ogawa et al. 1995) where photosystem I (PSI) is located. The two

other Cu-Zn SODs are considered “cytoplasmic” because these are not isoforms present in intact chloroplasts (Ogawa et al. 1996). However, when immunogold-labeled antibodies raised against “cytosolic” Cu-Zn SOD were used in localization experiments, it was shown that these enzymes were located in the nucleus and apoplast (Ogawa et al. 1996). More than 40% of the immunogold particles were found in the apoplast and approximately 25% was found in the nucleus (Ogawa et al. 1996). Researchers proposed that Cu-Zn SOD in the apoplast functions in lignification, and that in the nucleus it protects the cell against fatal mutations caused by O_2^- molecules (Ogawa et al. 1996 & 1997). Occurrence of a peroxisomal Cu-Zn SOD from watermelon, which represented about 18% of the total SOD activity in the cell, was also previously reported (Sandalio and del Rio, 1987). Presence of such a peroxisomal Cu-Zn SOD also was shown in rat liver cells (Dhaunsi et al. 1992).

3.2. Manganese Superoxide Dismutase (Mn SOD):

Mn SODs carry only one metal atom per subunit. These enzymes cannot function without the Mn atom present at the active site. Even though Mn and Fe SODs have a high similarity in the primary, secondary and tertiary structure, these enzymes have diverged sufficiently that Fe (II) could not restore the activity of Mn SOD and vice versa (Fridovich 1986). Catalysis by Mn SODs is through the attraction of negatively-charged O_2^- molecules to a site formed from positively charged amino acids present at the active site of the enzyme, similar to Cu-ZnSODs. Then, the metal present in the active

site donates an electron directly to the O_2^-, reducing one O_2^- molecule, which in turn forms H_2O_2 by reacting with a proton molecule (Asada, 1994; Bowler et al. 1994).

Mn SOD is either a homodimeric or a homotetrameric enzyme with one Mn (III) atom per subunit. The enzyme is not inhibited by potassium cyanide (KCN) or inactivated by H_2O_2 and is present in both eukaryotes and prokaryotes. Plant Mn SODs have approximately 65% sequence similarity to one another, and these enzymes also have high similarities to bacterial Mn SODs (Bowler et al. 1994). Although Mn SOD is known as the mitochondrial enzyme of eukaryotes, a Mn-containing SOD has also been located in the peroxisomes. del Rio et al. (1992) showed the presence of one peroxisomal and one mitochondrial Mn SOD by using immunolocalization assays in watermelon. Four genes that encode Mn SOD were reported in maize (*Zea mays*) (Zhu and Scandalios, 1993). Deduced amino acid sequences from these four isoenzymes have a mitochondrial targeting sequence, indicating that all are located in the mitochondria. In *Nicotiana plumbaginifolis,* two nuclear-encoded Mn SOD genes were isolated and the tissue-specific expression Mn SOD was shown by analyzing promoter fusion with GUS in transgenic plants (Van Camp et al. 1996). Multiple transcripts for Mn SOD have been reported in human (*Homo sapiens*) tissues. These different transcripts have been found to be the product of the same gene but result from alternative polyadenylylation or alternative splicing and polyadenylylation (Zhu and Scandolios, 1993). In addition to maize, Mn SOD has been found in the mitochondria of tobacco (*Nicotiana tabaccum;* Bowler et al.

1989), mung beans (*Vigna mungo;* Reddy and Venkaiah, 1982), watermelon (Sandalio and del Rio, 1987), carnations (*Dianthus caryophyllus;* Droillard and Paulin, 1990), peas (*Pisum sativum;* Foster and Edwards, 1980), spinach (*Spinacia oleracea*; Jackson et al. 1978), and some other plants. del Rio (1983) and Sandalio et al. (1987) reported a peroxisomal Mn SOD in pea for the removal of O_2 formed as a result of xanthine oxidase action (Sandalio et al. 1987; del Rio et al. 1998), but none of the known Mn SOD sequences appear to have a transit peptide sequence for peroxisomal targeting (Bowler, 1994).

In green algae and cyanobacteria, Mn SOD is found in the thylakoid membrane (Kanematsu and Asada, 1979; Okada et al. 1979). Although a thylakoid bound form of Mn SOD was reported in spinach plants (Hayakawa et al. 1985), after further investigation it was suggested that this Mn SOD activity was the result of a non-specific or mimic Mn SOD activity (Palma et al. 1986), and that Mn SOD is present only in the mitochondria and peroxisomes of the plant cells.

3.4. Iron Superoxide Dismutase (Fe SOD):

Fe SOD is found in prokaryotes and eukaryotes. In eukaryotes it has been isolated from *Euglena gracilis* (Kanametsu and Asada, 1979) and higher plants. Fe SOD is inactivated by H_2O_2 and is resistant to KCN inhibition. In all plant species examined to date, it is inferred to be located in the chloroplast. Bridges and Salin (1981) raised polyclonal antibodies against water lily (*Nuphar luteum*) Fe SOD. When these antibodies

were incubated with protoplasts from water lilies, it was shown that the antibodies predominantly associated with the chloroplasts (Salin, 1988). Fe SOD also has been localized in the chloroplast in *N. luteum* , and a potential chloroplastic targeting sequence was found in soybean Fe SOD. The absence of Fe SOD in animals has given rise to the proposal that the Fe SOD gene originated in the plastid, but that during the evolutionary process it moved to the nuclear genome. Support of this theory comes from the existence of several conserved regions that are present in plant and cyanobacterial Fe SOD sequences, but absent in non-photosynthetic bacteria (Bowler, 1994). Previously, it was thought that Fe SOD was not present in all plants. The presence of Fe SOD activity in Gingkoaceae, Nymphaceae, and Cruciferae was concluded to be a random occurrence of the enzyme in the plant kingdom (Bridges and Salin, 1981). More recently Fe SOD genes were isolated in three plant species which do not have phylogenetic relationships to one another: *N. plumbaginifolia*, *A. thaliana* (Van Camp et al. 1990), and *Glycine max* (Crowell and Amasino, 1991). All three Fe SOD plant sequences encode a unique tripeptide (SRL for *N. plumbaginifolia* and *G. max* and ARL for *A. thaliana*) close to the carboxyl terminus of the enzyme. Although this sequence has shown to direct the proteins to peroxisomes in other proteins, it has yet to be determined whether this is a functional sequence or not. The conserved SRL/ARL sequence is not present in the prokaryotic Fe SOD proteins showing that it is not obligatory for the enzyme function (Van Camp et al. 1994). SOD populations in rice *(Oryzae sativa)* and maize have been

extensively studied, but there have been no reports of the presence of Fe SOD in either rice or maize.

There are two distinct groups of Fe SOD. The first group is a homodimer formed from two identical 20 kD subunit proteins, with 1-2 gram atom of iron in the active center. This type of Fe SOD has been isolated from *Escherichia coli* (Yost and Fridovich, 1973); *Photobacterium sepoa* and *P. leiognathi* (Puger and Michelson, 1974); the facultative anaerobe, *Thiobacillus denitrificans* (Baldensperger, 1978); the purple sulfur bacterim, *Chromatium vinosum* (Kanematsu and Asada, 1978); and the plant species, *Ginkgo biloba, Brassica calpestris,* and *Nuphar luteum* (Salin and Bridges, 1980). The second group is a tetramer of four equal subunits with a molecular weight of 80-90 kD. Members of this group of Fe SOD contain 2-4 grams atom of iron in the active center. Proteins in this group have been isolated from three prokaryotes, *Mycobacterium tuberculosis* (Kusunoe et al. 1976), *Thermoplasma acisophilum* (Searcy and Searcy, 1981), and *Methanobacterium bryantii*, (Kirby et al. 1981) and a eukaryote, *Tetrahymena pyriformis* (Barro et al. 1990).

Comparative crystallography studies with Fe SODs showed that three primary chemical functions are necessary for Fe SOD to catalyze a dismutation reaction (Zhang et al. 1991):

1. The Fe center must have a minimum of one coordination site available for binding O_2^- in two adjacent oxidation states.

2. The iron redox couple, governed in part by the primary coordination sphere as well as the surrounding protein matrix, must lie between the redox potentials of O_2^- oxidation (0.16 v) and O_2- reduction (0.89 v).

3. The iron center must be able to cycle between the Fe (II) and Fe (III) oxidation states more rapidly than the rate of the spontaneous dismutation reaction.

Some bacterial species can use a common SOD for both Fe and Mn and utilize either of these two metals as the active metal cofactor, according to availability of the metal. A great similarity in primary, secondary, and tertiary structures of Fe and Mn SODs have been observed. The metal ligands and other structurally- and functionally-important residues are highly conserved between these enzymes. In addition, the similar electrical properties of Fe and Mn allow the enzyme to function with either metal without a conformational change in its protein structure. Similarly, a hybrid SOD produced by using *E. coli* Fe and Mn subunits, which shown to be partially inhibited with H_2O_2 treatment in proportion to its content of Fe (Clare et al. 1984). Three dimensional structures of Mn and Fe SODs also show high similarity, further demonstrating the homology present between these two enzymes (Stallings, 1984).

4. OXIDATIVE STRESS:

The damage caused by O_2 and its radicals is called oxidative stress. A variety of stresses, both biotic (Hammond-Kosack and Jones, 1996; Snijder et al. 1996) and abiotic

(Burdon et al. 1996; Fadzilla et al. 1997, Hernandez et al. 1995, Kangasjarvi et al. 1994, Wellburn and Wellburn, 1996), increase the activity of O_2 scavenging enzymes.

4.1. Abiotic Stress

4.1.1. Ozone

The site of action for ozone has been suggested to be in the apoplast, but when Mn SOD was overexpressed in the chloroplasts of tobacco plants, less damage was observed in the leaves. When the over production of the enzyme was in the mitochondria, less protection was observed. Also, it was shown that high levels of chloroplastic Mn SOD activity protected the plant from visible injury caused by ozone, suggesting that ozone may cause oxidative stress in the chloroplast, as well as the apoplast (Van Camp et al. 1994).

4.1.2. Salt

Plants exposed to salt stress showed increased levels of Mn and Cu-Zn SOD activity as well as increased levels of H_2O_2 (Fadzilla et al. 1997; Hernandez et al. 1993 & 1995). There are several biochemical and physiological effects of salinity on plants, but the inhibition of photosynthetic capacity under salinity stress may be through the closure of stomata, which limits transpiration. The effect of salinity in oxidative stress may also be through closure of the stomata. In this case, CO_2 intake is limited and there is less NADPH available as the electron acceptor. In this case O_2 acts as the alternative electron

acceptor, which results in formation of O_2^- (Hernandez et al. 1995).

4.1.3. Herbicides

In plants the bipyridinium herbicides cause the formation of increased ROS, which is called oxidative burst. (Bolwell, 1996). Bipyridinium herbicides can bind to the thylakoid membrane of the chloroplasts and transfer the electrons to O_2 in a chain reaction causing continuous formation of O_2^-. As a result $NADP^+$ cannot be reduced and carbon fixation ceases. Methyl viologen (1,1'-dimethyl-4,4'-bipyridilium dichloride or methyl viologen), whose site of action is the chloroplast, is a bipyridylium herbicide (Dodge, 1994). This herbicide is widely used in plants to study O_2^--mediated damage in the chloroplast. Methyl viologen also affects electron-transducing reactions in the endoplasmic reticulum and in mitochondria. Methyl viologen treatment affects the level of chloroplastic SOD as well as mitochondrial and cytosolic SODs (Dodge, 1994; Van Camp et al. 1994).

4.1.4. High Light Stress

The effect of high light stress is inhibition of photosystem II through D1 protein, which is associated with PS II electron transduction reactions (Foyer and Mullineaux, 1994). Photoinhibition of PS II is not well understood. However, it has been shown that plants with an elevated level of SOD are tolerant to high light stress photoinhibition of PS II (Van Camp et al. 1994).

4.1.5. Sulfur Dioxide (SO_2)

The site of action of SO_2 is the chloroplast. After SO_2 enters the chloroplast it is hydrated, and HSO_3^-, SO_3^- and H^+ are formed. Sulfite can affect a number of different functions in the chloroplast including carbon fixation, glycolate oxidase activity, and cyclic and noncyclic photophosphorylation. It has been proposed that sulfite and bisulfite, in a chain reaction, can interact with the O_2^- radicals formed as a result of the Mehler reaction and increase production of O_2^- in the chloroplast (Asada and Kiso, 1973).

4.2. Biotic Stress

Production of reactive O_2 species (oxidative burst) appears to be a universal defense mechanism against pathogen attacks in eukaryotes. Formation of O_2^- for defense seems to be quite different than that of side reactions of metabolism and electron leakage. Under unstressed conditions plants are capable of providing efficient protection against free radicals and active O_2 species (Asada and Takahashi, 1987). In the case of stress conditions, including pathogen attack, this system is overridden by the rapid production of large amounts of active O_2 species. This may be an indication that this system has evolved as a defense mechanism, and that the toxic reactive O_2 species are produced against pathogen invasion.

The oxidative burst that occurs after pathogen invasion has two phases (Hammond-Kosack and Jones, 1996). The first phase is a rapid and non-specific occurrence of ROS. Amount of ROS formed in this case is not so high as to cause serious

damage to the plant, but it may be significant enough to kill the pathogen (Hammond-Kosack and Jones, 1996). The second phase when occurs is a delayed, but more specific, response against micro-organisms called the hypersensitive response (HR). In this case, tissues around the site of pathogen attack rapidly die, so that the pathogen cannot advance further (Hammond-Kosack and Jones, 1996).

The role of ROS in defense may be through changes in membrane permeability (Adam et al. 1989), cross-linking of cell wall proteins (Brisson et al. 1994), lignification (Peng and Kuc, (1992), phytoalexin accumulation (Sharma et al. 1992), direct killing of the plant cells, hypersensitivity reaction (Levine et al. 1994), direct killing of the pathogen, and ROS acting as a second messenger in the induction of systemic resistance (Peng and Kuc, 1992).

In the case of pathogen attack, the oxidative burst has been frequently observed in the extracellular space (Dixon et al. 1994). An NADPH oxidase gene from rice was isolated. The function of this enzyme is to generate O_2^- and pump the radicals to the extracellular space when there is a pathogen attack to the plant. It is suggested that it is functionally analogous to NADPH oxidase in mammalian phagocytes (Groom et al. 1996).

5. Role of SODs in Controlling Oxidative Stress in Plants

When the consequences of excessive amounts of O_2^- formation are taken into

account, it is clear that this defense mechanism can cause significant damage, not only to the pathogen, but also to the plant itself. Thus, these plants need to manifest a protective mechanism against possible damage from ROS to themselves.

Reactive O_2 species are produced in both unstressed and stressed cells. Plants have well-developed defense systems against ROS. This defense involves either limiting the formation and/or instituting the removal of ROS. Under unstressed conditions, formation and removal of O_2 are balanced. However, under stress conditions, because of increased ROS formation, this defense system is overwhelmed. Plants respond to this stress with increased enzymatic or non-enzymatic antioxidant processes (Alscher and Hess, 1993), but the mechanism underlying this process is not well understood.

The studies clearly show that the age of the plant, subcellular localization, type, and amount of imposed stress have significant effects on the level of oxidative damage and tolerance (Donahue et al. 1997; Doulis et al. 1998; Iturbe-Ormaetxe et al. 1998; Thomas et al. 1998). In addition, plants overexpressing SODs and other scavenging enzymes have been engineered with the goal of increasing stress tolerance. However, the scavenging pathway is quite complex. Therefore, both successful and unsuccessful results have been obtained from attempts to create resistant plants (Perl et al. 1993; Slooten et al. 1995, Tepperman and Dunsmuir 1990, Van Camp et al. 1996).

Effects of oxidative stress have been studied in different organisms. A Fe SOD mutant of cyanobacterium *Synechocicces* sp. strain PCC7942 was used to examine the

effects of oxidative stress (Thomas et al. 1998). Strain PCC7942 has two SODs—thylakoid-associated Mn SOD and cytosolic Fe SOD (Herbert et al. 1992). Methyl viologen treatment caused a significant decrease in the growth rate of the wild type strain. Under the same conditions *sod*B$^-$ did not show any growth at all. When wild type and mutant strains were exposed to norflurazon (NF), the mutant *sod*B$^-$ unexpectedly showed a higher growth rate under increased stress conditions than did the wild type (Thomas et al. 1998). In previous studies, however, increased Mn SOD activity was observed in the *sod*B$^-$ mutant compared to the wild type strain (Herbert et al. 1992). Mn SOD in *sod*B$^-$ is thylakoid-associated, whereas Fe SOD is a cytosolic enzyme. Therefore, it was concluded that the increased activity of Mn SOD may provide further protection against thylakoid located ROS formation in the mutant strain (Thomas et al. 1998). This suggests that subcellular localization of SODs is important for defense against ROS.

The effects of methyl viologen and water deprivation on SOD enzyme activities were investigated in the late vegetative growth stage of pea leaves (Iturbe-Ormaetxe et al. 1998). Plants that were moderately deprived of water (D1) and sprayed with 100 μM methyl viologen (PQ) showed an increase in total Cu-Zn activity, but a decrease in the amount of Fe SOD activity was observed after treating the plants with methyl viologen and water deprivation. Mn SOD activity was unchanged under both conditions. It was concluded that the Fe SOD activity was being inhibited by methyl viologen, but the Cu-

Zn and the Mn SOD activities were not being affected (Iturbe-Ormaetxe et al. 1998).

Donahue et al. (1997) also detected responses of antioxidants to methyl viologen in pea leaves. It was observed that there is a positive correlation between leaf age and susceptibility to methyl viologen. The younger leaves had higher SOD, APX, and GR activity in methyl viologen treated and control plants. These authors reported the presence of Fe SOD in pea plants for the first time. It was also reported that the changes they observed in the enzyme activity level as a result of stress treatment did not always correlate with the changes in the mRNA levels.

Bowler et al. (1991) targeted *N. plumbaginiafolis* mitochondrial Mn SOD sequence into *N. tabacum* mitochondria and chloroplasts. When the transformed plants were treated with methyl viologen, it was observed that the plants that had Mn SOD expressed in their chloroplast had remarkable protection, accompanied by an increased SOD activity against methyl viologen stress compared to control plants in light. This protective effect was less observable in plants that were kept in the dark, since the H_2O_2 scavenging system is not activated without light (Foyer and Halliwell, 1976; Nakano and Asada, 1980). Even though Mn SOD is not inactivated by H_2O_2, the balance between generated O_2^- and H_2O_2 is disrupted in these transgenic plants, which may increase the formation of $OH^{\cdot}$. Although increased protection was observed in plants that had foreign Mn SOD targeted into the mitochondria, this effect was not as remarkable compared to plants that had Mn SOD targeted into the chloroplasts. This may be due to the majority

of the O_2 being generated in the chloroplast in plants exposed to methyl viologen in light (Bowler et al. 1991). The effects of methyl viologen treatment in pea protoplasts were also investigated. The levels of total SOD activity remained unchanged for 9 h after methyl viologen treatment, but after 12 h a significant increase was observed. This increase was mainly in Mn SOD enzyme activity, whereas chloroplastic Cu-Zn SOD showed a decrease, and cytosolic Cu-Zn SOD activity remained constant. It was suggested that the decrease in chloroplastic SOD is caused by increased H_2O_2 formation as a result of increased SOD activity (Doulis et al. 1998).

Tsang et al. (1991) investigated the effects of methyl viologen in *N. plumbaginifolia*. In these studies a significant increase was observed in the amount of mRNA levels for Mn, Fe and cytosolic Cu-Zn SODs in methyl viologen-treated plants that were kept in light. In the plants that were kept in the dark following the treatment Mn and Fe SOD transcript levels did not change, but an increase in the amount of cytosolic Cu-Zn SOD mRNA was observed (Tsang et al. 1991). The effect of methyl viologen treatment was not investigated at the enzyme or protein level, however.

When an *A. thaliana* Fe SOD gene was targeted into *N. tabacum* cv Petit Havana SR1 chloroplasts, an increased protection against O_2 generated both in the plasmalemma and photosystem II was observed (Van Camp et al. 1996). In contrast, when mitochondrial Mn SOD was targeted to the chloroplasts of tobacco plants, protection was only observed against stress generated in the plasmalemma. An increase in the

activity of APX and DHAR and MDAR, other scavenging pathway enzymes, was also observed. It was concluded that the protection provided by overproduction of Mn SOD was dependent on whether the other enzymes-DHAR and MDAR- were present in elevated levels or not (Slooten et al. 1995). Localization of imposed stress as well as its type seems to play an important role in enhancing tolerance against oxidative stress.

When the tomato chloroplastic and cytosolic Cu-Zn SOD genes were transferred into potato plants, elevated levels of tolerance against the stress caused by methyl viologen was observed. A higher tolerance was observed in plants that carry the cytosolic Cu-Zn SOD gene compared to plants expressing the chloroplastic Cu-Zn SOD gene (Perl et al. 1993). In contrast, tobacco plants transformed with the Cu-Zn SOD gene exhibited approximately 50-fold increase in Cu-Zn SOD expression with no increased tolerance (Tepperman and Dunsmuir 1990). The authors suggest that this is due to increased formation of H_2O_2. When the overexpression results in a moderate increase in SOD activity, then it is more likely there will be tolerance against oxidative stress, since the equilibrium between O_2^- radicals and H_2O_2 is maintained (Perl et al. 1993).

The effects of SO_2 on Cu-Zn SOD enzyme activity were investigated in two pea cultivars, cv. Progress and Nugget insensitive and sensitive, respectively, to SO_2 (Madamanchi et al. 1994). After the treatment of these plants with SO_2, activities of both cytosolic and chloroplastic SODs increased in cv. Progress whereas the activities of both enzymes decreased in cv. Nugget. Chloroplastic Cu-Zn SOD mRNA levels

decreased in cv. Nugget after the treatments, whereas in cv. Progress there was a recovery in the amount of transcripts present after an initial decrease (Madamanchi et al. 1994). Similar to SODs, an increase in the amount of activity of glutathione reductase and glutathione content was observed in pea cv. Progress, suggesting that resistance to SO_2 is through increased enzymatic and non-enzymatic antioxidant levels (Madamanchi and Alscher, 1991).

6. Dissertation Research Objectives

The effects of oxidative stress on plants have been an important research topic. In this research the effect of oxidative stress on *A. thaliana* SOD populations is investigated. The three dimensional structure of the *A. thaliana* Fe SOD enzyme was also modeled by using two bacterial Fe SODs whose structures are known.

The specific objectives of my dissertation research study are;

1. To determine effects of oxidative stress on members of individual SOD isoforms at the enzyme and protein levels.

2. To characterize relationships among these effects--especially with regard to organeller localization.

3. To determine sequence similarities and evolutionary relationships between individual SOD isoforms.

4. To raise antibodies against Arabidopsis FeSOD protein.

5. To model the three dimentional structure of Arabidopsis Fe SOD by using crystallized Fe SODs as a template and compare the structure with the three dimensinal structure of other isoforms.

Chapter II

Materials and Methods

1. Cloning of Mature *A. thaliana* Fe SOD Gene into Bacterial Expression Vectors

Full length, mature *A. thaliana* Fe SOD cDNA was amplified by PCR from SOD10 (Van Camp et al., 1991). Primers (GibcoBRL, Gaithersburg, MS) with the following sequences were designed based on the published *A. thaliana* Fe SOD sequence (Figure 6):

Primer 1; 5'-CGGAATTCCCAACTACGTCCTTCAAGCC-3'

Primer 2; 5'-GCGAGCTCCTTAAGCAGAAGCAGCC-3'.

DNA amplifications were carried out in a 100 μl reaction mixture containing 5 ng Fe SOD plasmid DNA as a template. A final concentration of 100 μM primers was used for both primers. The mixture was incubated for an initial 5 minute at 95 ^{o}C for complete denaturation. Subsequently, 50 thermocycles consisting of one minute for melting at 94 ^{0}C, 45 seconds for annealing at 52 ^{o}C, and 2 minutes for synthesis at 72 ^{o}C were completed.

To characterize the amplified fragments, products from the PCR reactions were digested with *Pst*I (USB, Cleveland, OH), *Sph*I (Stratagene, La Jolla, CA), and *Pst*I + *Sph*I mixtures. Digestion reactions were separated in 0.7% agarose + 0.65% synergel/Tris-borate-EDTA (TBE) to identify the amplified fragment.

After the diagnostic test, the amplified PCR product was subcloned into a pNoTA/T7 shuttle vector (Figure 7) using Prime PCR Cloner System Kit (5 Prime → 3 Prime, Inc., Boulder, CO) according to the following procedure. Unincorporated

Figure 6. Full length *A. thaliana* Fe SOD cDNA sequence (Genebank Accession Number M55910)

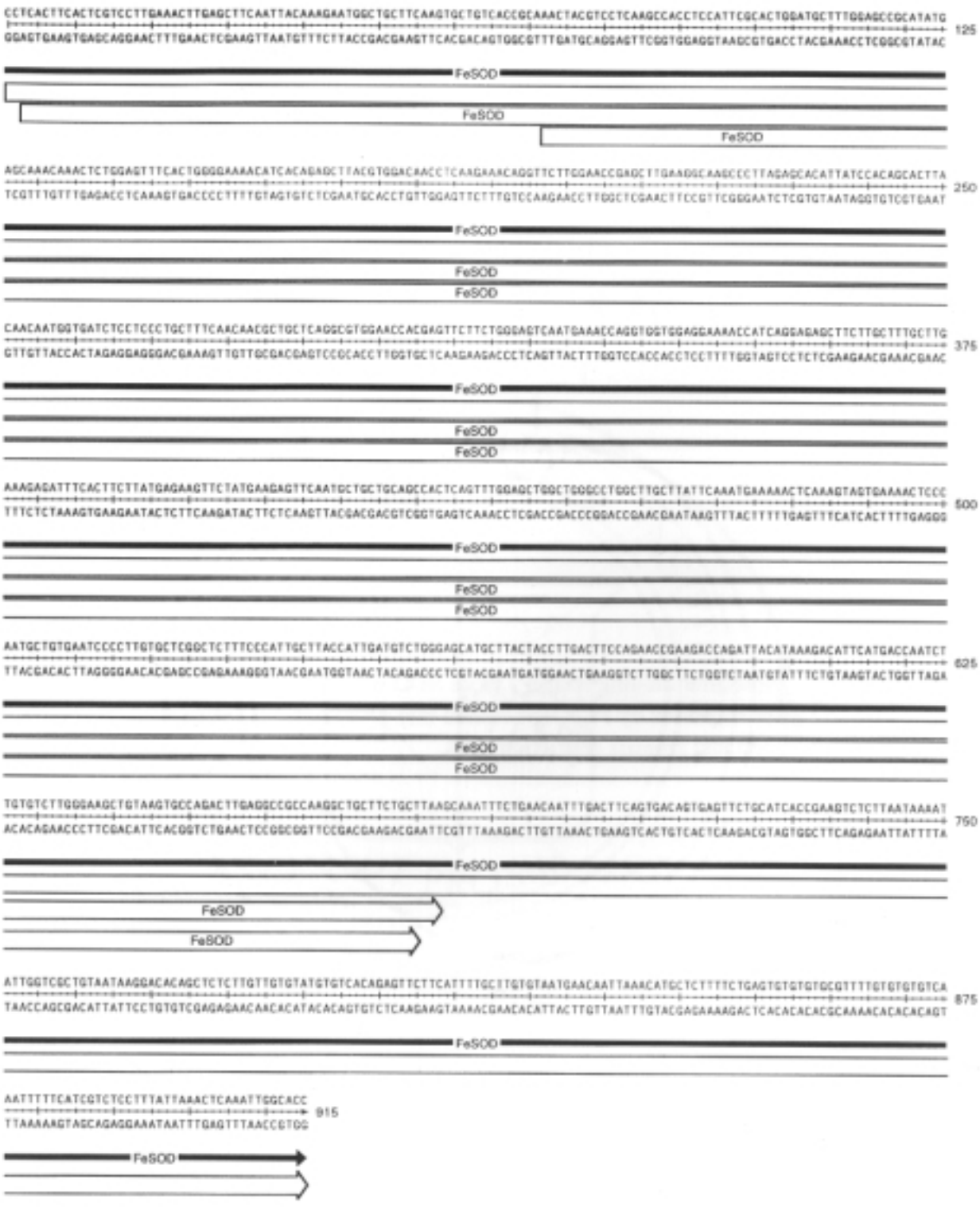
125
FeSOD
FeSOD
FeSOD
250
FeSOD
FeSOD
FeSOD
375
FeSOD
FeSOD
FeSOD
500
FeSOD
FeSOD
FeSOD
625
FeSOD
FeSOD
FeSOD
750
FeSOD
FeSOD
FeSOD
875
FeSOD
915
FeSOD

Figure 7. Molecular cloning strategy of Fe SOD cDNA into shuttle vector pNoTA/T7. Fe SOD gene amplified by PCR was cloned into pNoTA/T7 at the multiple cloning site between *Eco*RI and *Hin*dIII restriction sites.

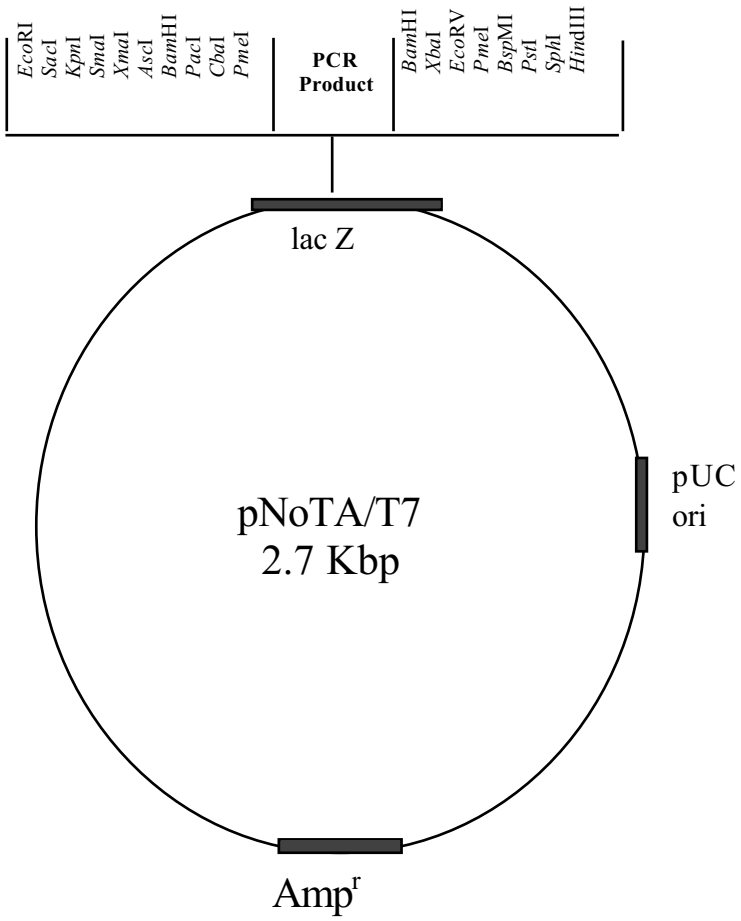
EcoRI
SacI
KpnI
SmaI
XmaI
AscI
BamHI
PacI
CbaI
PmeI
PCR Product
BamHI
XbaI
EcoRV
PmeI
BspMI
PstI
SphI
HindIII
lac Z
pNoTA/T7
2.7 Kbp
pUC ori
Ampr

deoxynucleoside triphosphates (dNTPs), residual mineral oil, polymerase, and primers, from PCR reaction were removed by passing the reaction mixture through PCR SELECT-III. The purified nucleic acid was recovered from the column by brief centrifugation at 1100 xg twice, first for 1 minute and then for 2.5 minutes in a swing rotor centrifuge into a collection tube. The collected PCR product was recovered in 100 μL Tris-EDTA (TE) at pH 8.0. The concentration of the PCR product was estimated from agarose gel electrophoresis. The ends of the recovered PCR amplified fragments were modified, and then blunt-end ligated into the dephosphorylated vector. The ligation reaction was performed at 16 ^{o}C for 15 minutes. Ligated plasmid DNA was used to transform competent cells of *E. coli* (cells provided in Prime PCR Cloner System kit) by incubation on ice for 20 minutes and then heat shocked for 90 seconds. Transformed cells were inoculated on Luria broth (LB) plates containing 100 μg/mL ampicillin, isopropyl thio-β-D-galactoside (IPTG) and 5-bromo-4-chloro-3-indolyl-β-D-galactoside (X-Gal) and the plates were incubated at 37 ^{o}C overnight. White colonies, putatively transformed with plasmid, were selected for further analyses.

The direction of the insert in transformed plasmids as well as confirming which strains had the desired DNA fragment has determined using a method modified from S. Qusus (Personal communication). Sixteen transformed colonies were inoculated onto LB containing 50 μg ampicillin /mL and incubated overnight at 37 ^{0}C. Colonies were picked with a sterile toothpick and transferred into a centrifuge tube containing 50 μL of 10 mM

EDTA pH 8.0. A volume of 50 mL fresh cracking buffer (0.2 M NaOH, 0.5% SDS, and 20% sucrose) was added to the tube, which was then resuspended by vortexing. Then it was incubated at 70 ^{0}C for 5 minutes. After it cooled to room temperature, 1.5 μl 4 M KCl and 0.5 μl 0.4% bromophenol blue were added. The mixture was vortexed for 30 seconds, left in ice for 5 minutes, and then centrifuged at 4 ^{0}C for 3 minutes. A volume of 30 μL of the mixture was separated in 0.7% agarose/Tris-acetate-EDTA (TAE) to identify the colonies with the Fe SOD sequence. Of the 16 colonies, 11 had the desired Fe SOD sequence. Plasmids from these 11 colonies carrying the Fe SOD sequence (pNoT7/TA Fe SOD_{1-11}) were isolated by using the alkaline lysis plasmid method (Sambrook et al. 1989). Orientation of the plasmid was identified by fractionating the plasmids digested with SphI in 1% agarose/TAE.

Two of the six colonies (pNoT7/TA Fe SOD_7 and pNoT7/TA Fe SOD_9) that had the *A. thaliana* Fe SOD ligated at T7→TA direction were used to isolate plasmids using a QIAGEN (Chatsworth, CA) plasmid preparation kit according to the manufacturer's manual. pNoT7/TA Fe SOD_7 and pNoT7/TA Fe SOD_9 were digested with *Hin*dIII (BioLabs, New England, Beverly, MA) and *Eco*RI (BioLabs, New England, Beverly, MA). Inserts from both plasmids were then digested with *Sph*I, *Pst*I, and *Sph*I + *Pst*I mixture to confirm the identify the fragments. The products from *Sph*I, *Pst*I, and *Sph*I+*Pst*I digestions were fractionated in 0.7% agarose + 0.65% synergel/TBE, and the orientation and the identity of the fragments were confirmed. PNoT7/TA Fe SOD_9,

which had the insert in right orientation and size, was digested with *Hin*dIII and *Eco*RI. Fragments recovered from this digestion were fractionated in 0.7% low melting point agarose/TAE gel. The DNA band containing the Fe SOD fragment was excised from an ethidium bromide-stained agarose gel with a razor blade. To view the DNA in the gel long-wavelength UV light was used for a short time in order to minimize the effects of UV on DNA. The sliced gel was placed into a tube and the fragment was purified by from the gel using Gene Clean II (Bio 101, Vista, CA) kit according to the following procedure.

The gel slice containing DNA fragment was crushed into small pieces in the tube, and NaI stock solution was added to a final concentration of 4 M into the tube. The tube was placed in 45-55^{o} C for five minutes with occasional mixing. After the agarose gel had completely dissociated, Gene Clean (Bio 101, Vista, CA) Glassmilk silica particles were added into the solution, and the mixture was incubated on ice for five minutes to allow binding of the DNA to the silica matrix, mixing every 1-2 minutes to ensure that the Glassmilk stayed suspended. Then the mixture was centrifuged at 4^{o}C for five seconds. The supernatant was discarded and the pellet was washed with 80% ethyl alcohol three times. DNA then was eluted from Glassmilk with TE buffer.

pET32c (Novagen, Madison, WI) was transformed into Novablue (Novagen, Madison, WI) competent cells. Plasmid preps from transformed Novablue cultures were carried out using a QIAGEN (Chatsworth, CA) plasmid prep kit according to the following procedure. QIAGEN (Chatsworth, CA) plasmid purification protocols were

carried out by using cultures grown in standard LB medium overnight to a cell density of approximately $1x10^9$ cells/ml (A_{600}= 1-1.5). After bacterial cells were harvested by centrifugation at 6,000xg for 15 minutes at 4°C, the supernatant was drained by inverting the tube. After resuspending bacterial pellet in resuspension buffer (50 mM Tris-HCL, pH 8.9; 10mM EDTA) with 100μg/ml RNase A, lysis buffer (200 mM NaOH, 1% SDS) was added to the resuspended cells. The mixture was incubated at room temperature for no more than five minutes to allow the lysis reaction. Chilled neutralization buffer (3.0 M potassium acetate, pH 5.5) was added to the lysate and the mixture was mixed by gentle inversion of the tube and then centrifuged at 20,000xg for 30 minutes at 4°C. Supernatant was removed promptly and then was centrifuged again at 20,000xg for 15 minutes at 4 °C in order to remove any particulate material left in the supernatant. After this step the supernatant was passed through a QIAGEN (Chatsworth, CA) column by gravity flow. The column was washed with wash buffer (1.0M NaCl; 50 mM MOPS, pH 7.0; 15% ethanol) at room temperature four times. Then, DNA was eluted with elution buffer (1.25 M NaCl; 50 mM Tris-HCl, pH 8.5; 15% ethanol) at room temperature. Elution was precipitated with 0.7 volume of isopropanol and immediately centrifuged at 15,000xg for 30 minutes at 4°C. DNA was washed with 70% ethanol, air-dried for 5 minutes, and redissolved in TE Buffer (10 mM Tris-HCl, pH 8.0, 1 mM EDTA). Isolated pET32c prep was digested with *Hin*dIII and *Eco*RI. The digestion product was fractionated in 0.7% low melting point agorose gel and then cleaned with

Gene Clean II (Bio 101, Vista, CA). Purified Fe SOD fragments were ligated into pET32c to create pET32c-$FeSOD_7$ and pET32c-$FeSOD_9$.

2. Expression and Purification of Enzymatically Active Recombinant Fe SOD Enzyme from *E. coli*

Ligation products were transformed into Novablue competent cells according to the manufacturer's protocol. A single colony from each transformation mixture was used to isolate pET32c-$FeSOD_7$ and pET32c-$FeSOD_9$ by the QIAGEN (Chatsworth, CA) plasmid preparation. Isolated plasmids were transformed into BL21DE3 competent cells containing pLyseS plasmid (Novagen, Madison, WI). These cells were grown in LB broth containing 100 μg/mL ampicillin and 34 μg/mL chloramphenicol at 37 ^{0}C at 170 rpm overnight. A volume of 5 mL of these cultures was used for inoculation of a fresh 500 mL LB broth containing 100 μg/mL ampicillin and 34 μg/mL chloramphenicol at 37 ^{0}C at 170 rpm. When the turbidity ($O.D._{550nm}$) of the culture reached to 0.5-0.7, 5 mL samples from the cultures were taken. Then IPTG was added to a 250 mM final concentration to induce the expression of Fe SOD recombinant protein. Cultures were grown for three additional hours. A volume of 5 mL samples were taken at hourly intervals. Three hours later samples were centrifuged at 3300xg at 4 ^{0}C for 10 minutes, resuspended in the SDS sample buffer and fractionated in 12% PAGE (polyacrylamide gel electrophoresis) to determine the degree of expression.

pET32c-$FeSOD_7$ (Figure 8) line was used as a source of the recombinant protein.

Figure 8. Molecular cloning strategy of Fe SOD cDNA into pET-32c(+) vector. Fe SOD gene was harvested from pNoTA/T7-Fe SOD vector at *Eco*RI and *Hin*dIII regions, and then ligated into pET-32c(+) vector to create pET32c-FeSOD_{10}. Histidine (his)-tag and thioredoxin (thx)-tag: Sequences for rapid detection, quantitation, and alternative affinity purification of thioredoxin-*A. thaliana* Fe SOD fusion protein.

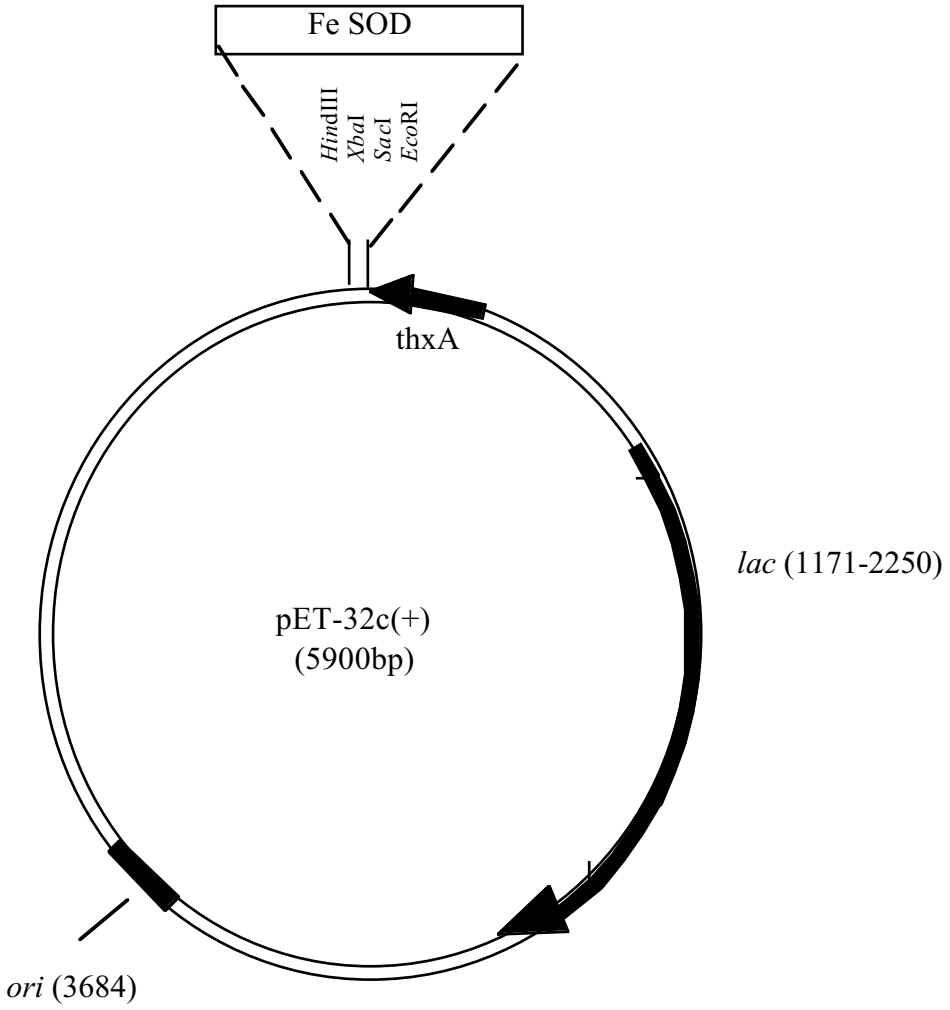
Fe SOD
HindIII
XbaI
SacI
EcoRI
thxA
lac (1171-2250)
pET-32c(+)
(5900bp)
ori (3684)

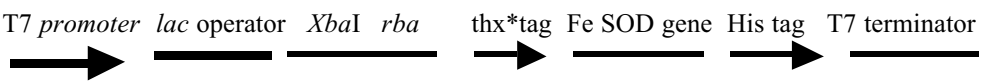
T7 promoter
lac operator
XbaI
rba
thx*tag
Fe SOD gene
His tag
T7 terminator

Centrifuged cells were resuspended in the ice-cold lysis buffer (20 mM Tris, 100 mM After three hours incubation the cells were centrifuged at 3300xg at 4 ^{0}C for 10 minutes. NaCl) using 40% of the original volume. The resuspended cells were recentrifuged at 3300xg at 4 ^{0}C for 10 minutes. The pellets were placed in -70 ^{0}C for one hour. One hour later frozen pellets were dissolved in the lysis buffer, using 3.5 mL lysis buffer per g pellet. Phenylmethylsulfonylfluoride (PMSF, Sigma, Milwaukee, WI) to 1 mM final concentration, DNaseI (Boehringer Manheim, Indianapolis, IN) to 40 μM/mL, and $MgCl_2$ to 10 mM final concentration were added to the solution. The mixture was incubated on ice for 40 minutes with occasional mixing until the solution was no longer viscous. The mixture was centrifuged at 15,000xg in Beckman SK50 rotor at 4 ^{0}C for 10 minutes to pellet insoluble proteins. Supernatant was removed and centrifuged at 58,000xg for 10 minutes at 4 ^{0}C. A 14 mL volume of supernatant containing recombinant Fe SOD protein was incubated with 1 mL of Talon metal affinity resin (Clontech, San Fransisco, CA) for one hour at room temperature. The resin was washed four times at room temperature with the lysis buffer (50 mM NaH 2 PO 4 (pH 8.0), 10 mM Tris-HCl (pH 8.0), 6 M 8 M Guanidinium-HCl, 100 mM NaCl, final pH adjusted to 8.0). Then the resin was centrifuged at 700 x g for two minutes and the sample was added immediately. After 10 minutes incubation with gentle shaking, the mixture was centrifuged at 700 x g for two minutes and the recombinant protein was eluted with the lysis buffer containing 100 mM EDTA and 200 mM imidazole. The elute was subjected to denaturing and non-denaturing

PAGE and stained for protein and SOD activity in order to determine the purity of the samples.

3. Antibody Production

Chicken (*Gallus gallus*) polyclonal antibodies were raised against 500μg thioredoxin-Fe SOD fusion protein (Cocalico Biologicals, Reamstown, PA). Serum obtained from blood was used as the source of the antibody against Fe SOD protein.

4. Plant Material

Wild-type *Arabidopsis thaliana* ecotype Columbia seeds were imbibed in a Murashige and Skoog basic salt mix (Sigma, Milwukee, WI), pH 5.7 for three days at 4 ^{0}C in the dark. These imbibed seeds were mixed with 0.15% agar (about 100 seeds/mL) and were pipeted uniformly into soil (Metro Mix 100, Wetzel Seeds, Virginia Beach, VA). The pots were covered with a sterile net, and the nets were attached to the pots with rubber bands to prevent the soil discharge into the treatment solutions when intact *A. thaliana* plants are dipped for the stress treatments.

After planting the seeds, pots were transferred into the growth chamber (Environmental Growth Systems, Chagrin Falls, OH) and covered with a transparent lid. The plants were grown under 120 μE m^{-2} sec^{-1} continuous light, 21 ^{0}C, and 70-80% relative humidity. Every other day the plants were watered.

5. Determination of Optimum Surfactant Concentration

In order to spread the solvents uniformly on the leaf surface and increase the

penetration of the solvents into the leaf, Ortho-X 77 (Valent USA Corp., Walnut Creek, CA) was applied to the plant surface as the surfactant. In order to use a concentration that causes minimal or no detectable effect on the plants, three different concentrations, 0.05%, 0.1%, and 0.15% of Ortho-X 77 (Valent USA Corp., Walnut Creek, CA) were applied to *A. thaliana* plants and these plants were observed for injury.

6. Stress Treatments

Sixteen day old *A. thaliana* plants were divided into five groups. The first group, $Control_1$ (C_1), did not receive any treatments. The second group, surfactant (C_2), was treated with 0.05% Ortho-X 77 (Valent USA Corp., Walnut Creek, CA). The next two groups were treated with methyl viologen. A $2x10^{-5}$ M methyl viologen concentration causes minimal visible injury in *A. thaliana* plants (R. Alscher, unpublished data). In our experiments, methyl viologen treatments were made in two groups—one with a concentration that causes visible injury, and the second that does not cause any visible injury. The third group was treated with a lower concentration than that which causes minimal visible injury, $5x10^{-6}$ M. The fourth group was treated with a higher concentration than that which causes minimal visible injury, $5x10^{-5}$ M. And the last group was treated with 10 μM DCMU (Figure 9). Four sets of 0.2 g samples were collected from each group, wrapped in aluminum foil, and frozen immediately in liquid nitrogen. These samples were then promptly transferred into the freezer (-70 ^{0}C) and kept there until the time of assays.

Figure 9. Treatments of *A. thaliana* plants with the appropriate solvents. Treatments were done with $5x10^{-5}$ M and $1x10^{-6}$ M methyl viologen, 10 μm DCMU, and 0.05% Ortho-X 77, surfactant (Valent USA Corp., Walnut Creek, CA).

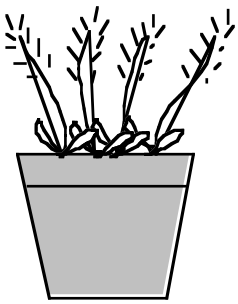

Sample collection
(0h)

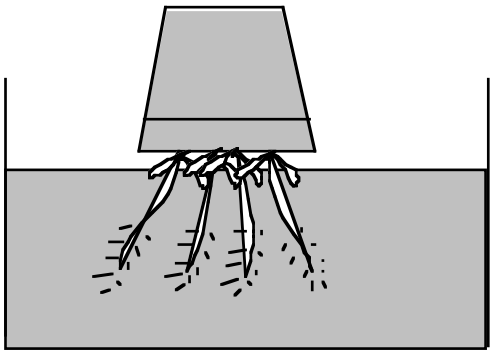

Treatments with the
stress reagent.

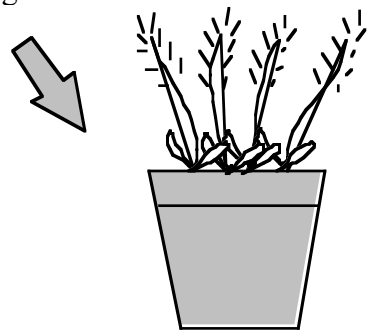

Samples collected at
5, 17, 27 and 41 hrs
following the treatments.

Enzyme activity and protein assays.

The plants were treated with the appropriate solvents right after the collection of the first samples, and then the pots were transferred back to the growth chamber. 0.2 g samples were collected from each group 5, 17, 27, and 41 hours after the treatments as described above. Non-denaturing and denaturing PAGE were performed with the collected samples in order to determine the effects of stress treatment at the enzyme and protein levels of SODs respectively.

7. Effects of Light on Stress Treated Plants

Sixteen day old plants were divided into two groups. Before the treatments, 0.2 g samples were taken from the pots as described above. Following sample collection, half of the plants were treated with 0.05% Ortho-X 77 (Valent USA Corp., Walnut Creek, CA) and the other half with $5x10^{-5}$ M methyl viologen containing 0.05% Ortho-X 77 (Valent USA Corp., Walnut Creek, CA). Then the plants were transferred into the growth chamber under constant light. Samples from both groups were taken 5 and 10 hours following the treatment. The same experiment was performed under the same conditions except that this time the plants were kept in constant dark for 10 hours. Non-denaturing PAGE was performed on these samples in order to determine the effects of light and dark conditions on stress treated plants.

8. DNA Gel Blot Analysis

Mature Fe SOD sequence amplified by PCR was used to perform DNA gel blot analysis. The PCR product described previously (Chapter I, Section 1) was run in 0.7%

low melting point agarose/TAE gel. The band corresponding to the Fe SOD containing sequence was excised from the gel and used as the template. Hybridization probe was generated from the gel-purified DNA fragments by labeling with 50 μCi of [α-^{32}P]dATP (Dupont, Wilmington, DE,) in a 20 μl reaction using random primer labeling procedure (Boehringer Mannheim, Indianapolis, IN). Genomic *A. thaliana* DNA, digested with *Eco*RI, *Hin*dIII or *Xba*I, transferred into 0.2μm nylon membranes (Bio Rad, Richmond, CA) was used for DNA gel blot analysis (provided by Janet Donohue). This membrane was prehybridized at 55 ^{0}C for 4 hours, and hybridized with the radioactively-labeled probe at 65 ^{0}C for 2 days at high stringency. The membrane was washed at 65 ^{0}C with 2XSSC, 0.1% SDS for 30 minutes, 1XSSC, 0.1% SDS twice for 30 minutes, and 0.1XSSC. 0.1% SDS for 30 minutes. The membrane was exposed to X-ray film at -70 ^{0}C using an intensifying screen. For low stringency hybridization the membrane was prehybridized at 55 ^{0}C for 4 hours, hybridized with the radioactively labeled probe at 55 ^{0}C for 2 days, washed at 55 ^{0}C with 2XSSC, 0.1% SDS for 30 minutes, 1XSSC, 0.1% SDS for 30 minutes, and 0.1xXSSC, 0.1% SDS for 30 minutes. The membrane was exposed to X-ray film at -70 ^{0}C using an intensifying screen.

9. Preparation of Plant Material for Denaturing and Non-Denaturing PAGE

Frozen leaf material (0.2 g) was placed into prechilled mortars. These mortars were filled with liquid nitrogen. After the nitrogen evaporated, the leaf material was ground quickly to a fine powder. The powder was transferred to a glass tube, and 1.2 mL

ice cold extraction buffer, containing 50 mM K_2HPO_4, pH 7.6, 10% glycerin, 0.1% Triton X-100, 1 mM EDTA, 1 mM EGTA, 1 mM PMSF, 0.05 % 2-mercaptoethanol, and 0.1 mg/mL BSA was added. After homogenizing with a Tekmar homogenizer at setting 30 for 20 seconds, the suspension was transferred to a clean microfuge tube and centrifuged at 16,000 x g at 4 °C for 30 minutes. The supernatant was transferred to a clean microfuge tube and placed on ice. The amount of the protein present in the supernatant was calculated by using the Bradford method (Bradford, 1976). The grinding buffer was prepared fresh each time.

10. Specificity of the Antibodies

Gel electrophoresis of proteins was carried out using the Miniprotean II system (Bio Rad, Richmond, CA). Stacking and separating gels were prepared according to the manufacturer's protocol, with the exception of 10% glycerol being added to the final solution. Both denaturing and non-denaturing PAGE gels were carried out according to Laemmli (1970). In non-denaturing gels, SDS and 2-mercaptoethanol were omitted from all solutions except the extraction buffer. The non-denaturing gels were electrophoresed at 4 ^{0}C for 2-3 hours at 35 mA per gel. The denaturing gels were electrophoresed at room temperature for 1-2 hours at 35 mA per gel.

The non-denaturing gels were stained for activity. Three identical sets of the samples were separated in the non-denaturing gels. The first set was stained without SOD inhibitors. The second set was stained in the presence of H_2O_2, which inactivates

Cu-Zn and Fe SODs. The last set was stained in the presence of KCN, which inhibits only Cu-Zn SODs. Protein (50 μg) was loaded into each of the lanes that were not treated with SOD inhibitors (Figure 10). This set was incubated with 50 mL SOD assay buffer (50 mM KH_2PO_4/K_2HPO_4 pH 7.8, 0.1 mM EDTA, 16 mg nitroblue tetrazolium, 1 mg riboflavin, and 0.2 mL TEMED). Gels that were treated with the inhibitors received 75 μg of protein per lane. The first set of inhibitor-treated gels was incubated in SOD assay buffer containing 5 mM H_2O_2. The second set was stained in SOD assay buffer containing 2 mM potassium cyanide (KCN). Incubation of the gels in SOD assay buffer was carried out in the dark for 20 minutes with gentle shaking. After the incubation, the gels were rinsed with distilled water and exposed to light to observe band development.

A semi-dry blotting apparatus (Millipore, Bedford, MA) was used to transfer proteins from the denaturing gels to 0.2 μm nitrocellulose membrane (Bio Rad, Richmond, CA) according to the manufacturer's protocol. Detection of the SOD proteins on the membrane was carried out according to Ausubel et al. (1988) using a 1:500 dilution of primary antibody and horseradish peroxidase conjugated rabbit (*Oryctolagus cuniculus*)-anti-chicken IgG (Jackson Immunologicals). Color development was with 4-chloro-1-naphthol (Bio Rad, Richmond, CA).

11. Densitometric Scanning of the Non-Denaturing Gels and Western Blots

The gels and membranes were scanned by using a Kaiser® Fototechnik scanner

Figure 10. Sensitivities of SOD enzymes to different inhibitors. Mn SOD is resistant to both, KCN and H_2O_2. Fe SOD and Cu-Zn SOD are sensitive to H_2O_2, therefore both SODs are inhibited in the presence of H_2O_2 and only the Mn SOD band is observed. Cu-Zn SOD is sensitive to KCN, therefore in KCN-treated gels Mn and Fe SOD bands are observable.

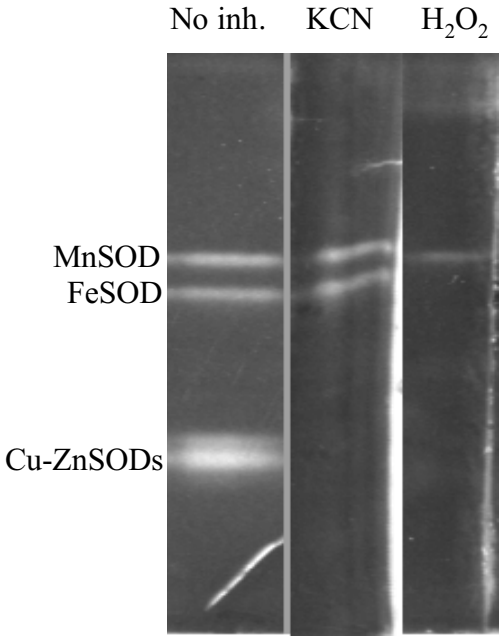
No inh.
KCN
H_2O_2
MnSOD
FeSOD
Cu-ZnSODs

(Kaiser, Fototechnik, Buchen, Germany). The intensity of the bands was determined using spot densitometry analysis in AlphaEase™ (Version 3.3a, Alpha Innotech Corporation, Serial # 930951).

12. Comparison of Sequences

Amino acid sequences of known SODs were downloaded from the National Center for Biotechnology Information, GenBank Sequence Database (http://www.ncbi.nlm.nih.gov/Entrez/protein.html). Pairwise alignment, multiple alignment, and phylogenetic trees were generated using the Lasergene computer program (version 1.61; DNASTAR Inc., Madison, WI) according to the Clustal Methods.

13. Modeling of the Three Dimensional Structure of *A. thaliana* Fe SOD Protein

The three-dimensional structure of *A. thaliana* Fe SOD protein was modeled using the amino acid sequences from previously crystallized *E. coli* and *Pseudomonas ovalis* Fe SOD proteins as templates (Figure 11). The sequences of crystallized Fe SOD, PDBid (Protein Data Bank identification code) 1isa for *E. coli* and 3sdp for *P. ovalis*, were downloaded from Brookhaven National Protein Databank (http://www.pdb.bnl.gov/pdb-bin/pdblite). Modeller 4 was used to generate the model (Sali and Blundell, 1993).

Five models were built and were observed by visual inspection to be similar to one another. The root mean square deviation (rmsd) among the models did not exceed 3.5 Å. Thus, a single average structure was created from the five models. The Leap module of AMBER (Perlman et al., 1995) was used to create the topology and coordinate files

Figure 11: Alignment of amino acid sequences of; A. *E. coli* (PDBid,1isa), B. *Pseudomonas ovalis* (PDBid, 3sdp), and C. *A. thaliana* aligned to generate the three dimensional structure of *A. thaliana* Fe SOD. Residues shaded with solid deep red color match the *A. thaliana* Fe SOD (Genebank accession number M55910) sequence exactly and residues with solid bright cobalt color match *E. coli* sequence exactly.

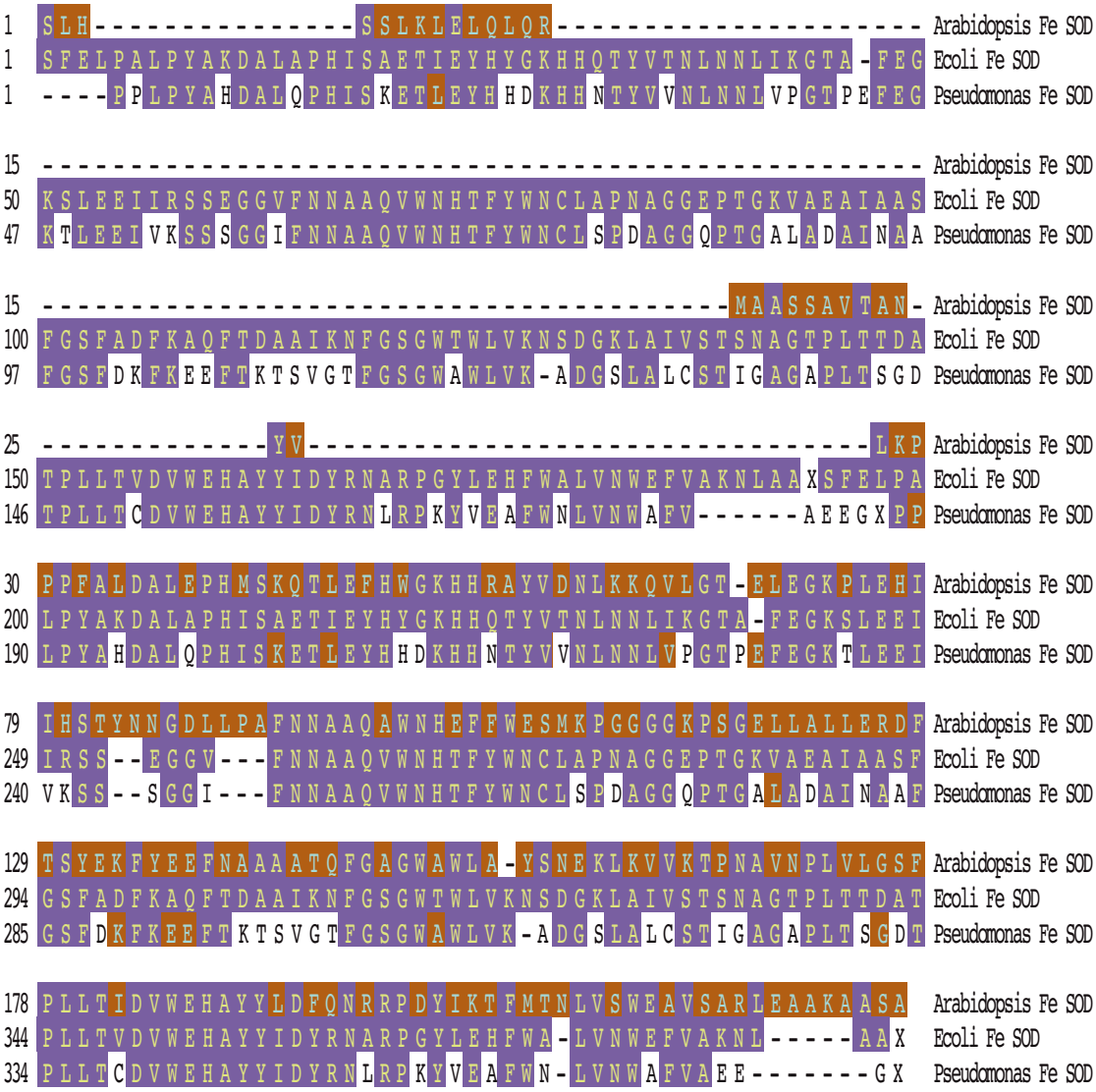
1 SLH SSLKLELQLQR Arabidopsis Fe SOD
1 SFELPALPYAKDALAPHISAETIEYHYGKHHQTYVTNLNNLIKGTA-FEG Ecoli Fe SOD
1 ----PPLPYAHDALQPHISKETLEYHHDKHHNTYVVNLNNLVPGTPEFEG Pseudamonas Fe SOD
15 Arabidopsis Fe SOD
50 KSLEEIIRSSEGGVFNNAAQVWNHTFYWNCLAPNAGGEPTGKVAEAIAAS Ecoli Fe SOD
47 KTLEEIVKSSSGGIFNNAAQVWNHTFYWNCLSPDAGGQPTGALADAINAA Pseudamonas Fe SOD
15 MAASSAVTAN- Arabidopsis Fe SOD
100 FGSFADFKAQFTDAAIKNFGSGWTWLVKNSDGKLAIVSTSNAGTPLTTDA Ecoli Fe SOD
97 FGSFDKFKEEFTKTSVGTFGSGWAWLVK-ADGSLALCSTIGAGAPLTSGD Pseudamonas Fe SOD
25 YV LKP Arabidopsis Fe SOD
150 TPLLTVDVWEHAYYIDYRNARPGYLEHFWALVNWEFVAKNLAAXSFELPA Ecoli Fe SOD
146 TPLLTCDVWEHAYYIDYRNLRPKYVEAFWNLVNWAFV------AEEGXPP Pseudamonas Fe SOD
30 PPFALDALEPHMSKQTLEFHWGKHHRAYVDNLKKQVLGT-ELEGKPLEHI Arabidopsis Fe SOD
200 LPYAKDALAPHISAETIEYHYGKHHQTYVTNLNNLIKGTA-FEGKSLEEI Ecoli Fe SOD
190 LPYAHDALQPHISKETLEYHHDKHHNTYVVNLNNLVPGTPEFEGKTLEEI Pseudamonas Fe SOD
79 IHSTYNNGDLLPAFNNAAQAWNHEFFWESMKPGGGGKPSGELLALLERDF Arabidopsis Fe SOD
249 IRSS--EGGV---FNNAAQVWNHTFYWNCLAPNAGGEPTGKVAEAIAASF Ecoli Fe SOD
240 VKSS--SGGI---FNNAAQVWNHTFYWNCLSPDAGGQPTGALADAINAAF Pseudamonas Fe SOD
129 TSYEKFYEEFNAAAATQFGAGWAWLA-YSNEKLKVVKTPNAVNPLVLGSF Arabidopsis Fe SOD
294 GSFADFKAQFTDAAIKNFGSGWTWLVKNSDGKLAIVSTSNAGTPLTTDAT Ecoli Fe SOD
285 GSFDKFKEEFTKTSVGTFGSGWAWLVK-ADGSLALCSTIGAGAPLTSGDT Pseudamonas Fe SOD
178 PLLTIDVWEHAYYLDFQNRRPDYIKTFMTNLVSWEAVSARLEAAKAASA Arabidopsis Fe SOD
344 PLLTVDVWEHAYYIDYRNARPGYLEHFWA-LVNWEFVAKNL-----AAX Ecoli Fe SOD
334 PLLTCDVWEHAYYIDYRNLRPKYVEAFWN-LVNWAFVAEE-------GX Pseudamonas Fe SOD

structures (1isa and 3sdp) were visualized by using Visual Molecular Dynamics (VMD) needed for geometry optimization (energy minimization). Geometry optimization, consisting of 600 steps of steepest descent minimization, was done using the Sander module of AMBER.

The visualization of the created model and Fe SODs with known crystallized (http://www.ks.uiuc.edu/Research/vmd/), Ras Mol Molecular Visualization Freeware (http://www.umass.edu/microbio/rasmol), and Chime Resources (http://www.umass.edu/microbio/chime). Secondary structures for nine crystallized SODs were downloaded from the CATH (Class, Architecture, Topology, Homologous superfamily) Data Bank (http://www.biochem.ucl.ac.uk/bsm/cath/CATH.html) and the secondary structure of modeled *A. thaliana* Fe SOD was generated by using these structures as templates.

Chapter III

Results

1. Expression of *A. thaliana* Fe SOD protein in *E. coli*

E. coli containing pET32c vectors with a full length *A. thaliana* Fe SOD gene were used to express *A. thaliana* Fe SOD protein. Samples were taken from *E. coli* cultures induced with IPTG at hourly time intervals and separated by SDS PAGE to test for expression of the *A. thaliana* Fe SOD protein (Figure 12). No accumulation of the fusion protein was observed before inducing the cultures with IPTG. The accumulation of a protein was observed starting from the first hour after the induction and the highest accumulation of this protein at the predicted molecular weight for the fusion protein was observed three hours after induction.

2. Production of Anti-Fe SOD antibodies

A. thaliana full-length Fe SOD cDNA containing pET32 vectors were introduced into *E. coli*. thioredoxin (Trx)-Fe SOD fusion protein was purified by using Talon metal affinity chromatography from these cultures. The resin was eluted three times, and then the eluted samples were separated by SDS PAGE (Figure 13). Nearly 1 mg of Trx-Fe SOD was purified from a 1 liter culture in the first elution. Purified samples were separated in a native gel electrophoresis gel and stained for SOD activity. Purified fusion protein, containing *A. thaliana* Fe SOD and bacterial Trx, was found to be enzymatically active by this technique (Figure 14).

The purified Trx-Fe SOD fusion protein was used to raise antibodies in chickens. The serum drawn following three injections was used as the source of the antibody.

Figure 12: Trx-Fe SOD protein expression in *E. coli*. Electrophoretic separation of crude lysates of *E. coli* containing Trx-Fe SOD fusion protein by SDS-PAGE. Duplicate lanes contain a crude extract from two different *E. coli* colonies independently transformed with the fusion construct. The arrow shows the position of the Trx-Fe SOD fusion protein which migrates at the predicted molecular weight. Lane 1 is the molecular weight markers, lanes 2 and 3 have the samples taken at T= 0h, before IPTG induction, lanes 4-9 contain samples taken at one hour intervals.

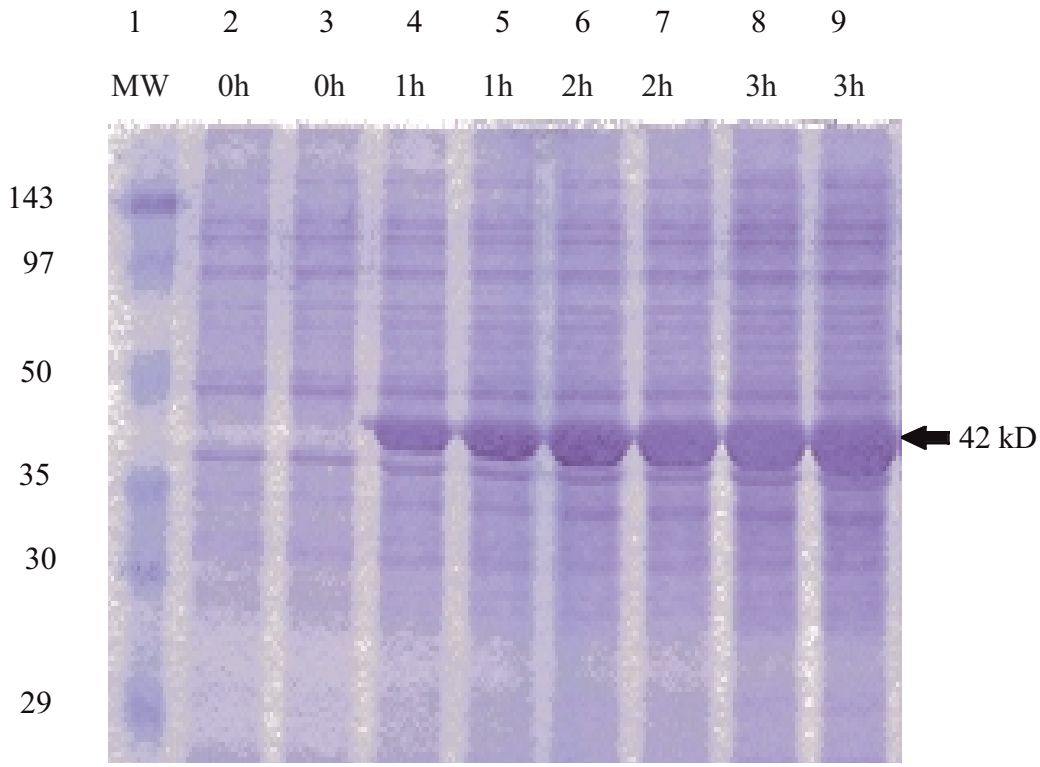
1 2 3 4 5 6 7 8 9
MW 0h 0h 1h 1h 2h 2h 3h 3h
143
97
50
35
30
29
42 kD

Figure 13. SDS PAGE of purified Thx-Fe SOD fusion protein. Electrophoretic separation of the bacterial extract purified using affinity chromatography. The arrow indicates the position of the fusion protein at the predicted molecular weight. Lane 1 shows molecular weight markers, lanes 2-8 the BSA dilutions, lane 8 the purified fusion protein (first elution from the affinity column), lane 9 the purified fusion protein (second elution from the affinity column). Only one protein was observed in the purified samples.

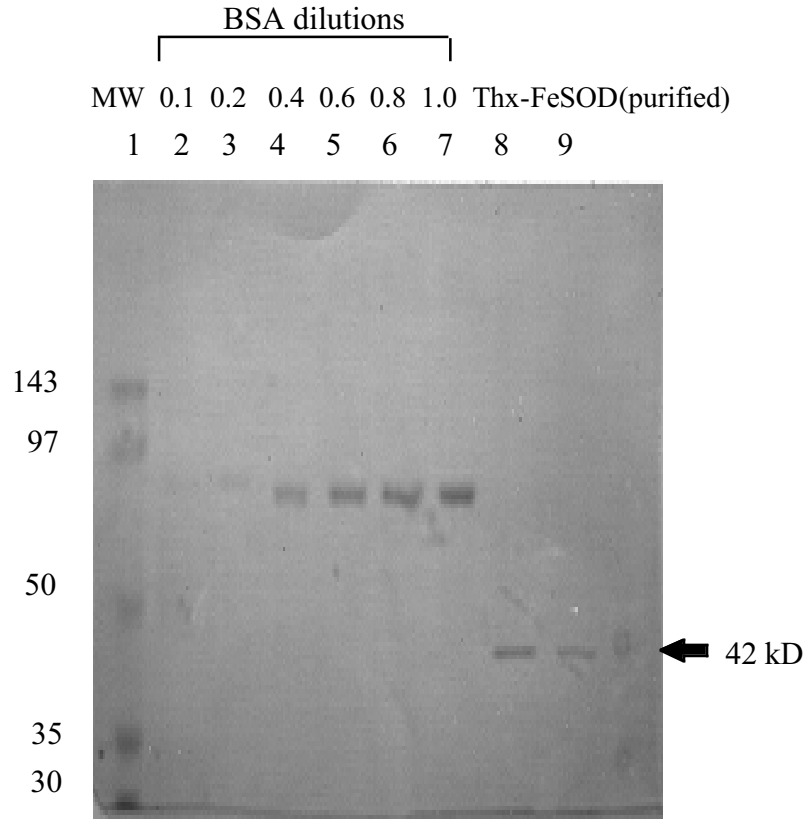
BSA dilutions
MW 0.1 0.2 0.4 0.6 0.8 1.0 Thx-FeSOD(purified)
1 2 3 4 5 6 7 8 9
143
97
50
35
30
42 kD

Figure 14. Enzyme activity of purified Trx-Fe SOD protein. 10% non-denaturing PAGE was performed with the purified samples. The gel was stained for SOD activity. SOD activity was observed both in the second elution (lane 1) and in the first elution (lane 2) of the affinity column.

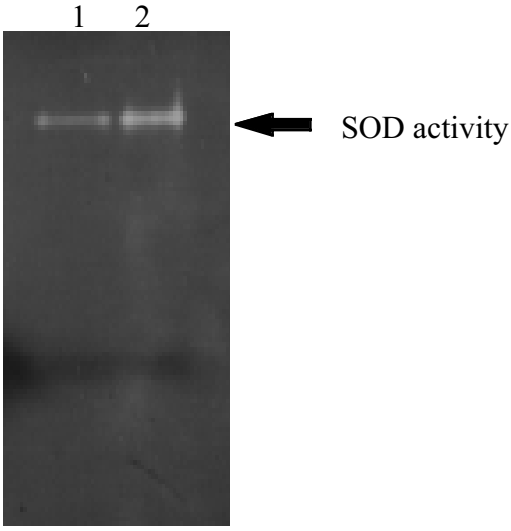
1
2
SOD activity

Dilution of 1:20, 1:200, and 1:2000 of this serum were tested against the *A. thaliana* plant extracts in immonoblot analysis (Figure 15). A band of the predicted molecular weight for the Fe SOD protein was observed in testbleed obtained from the injected chicken, but not in the prebleed (Figure 15). After three dilutions of the antibody were tested with the plant extracts, a 1:200 dilution was chosen as the working concentration.

In order to determine the specificity of the antibodies, non-denaturing gels containing *A. thaliana* extract were transferred to a nitrocellulose membrane. The membrane then was incubated with the antibodies, but the Fe SOD band was not observed using a colorimetric detection method. In order to further examine the specificity of the antibodies, non-denaturing gels were soaked in 10 % SDS to denature the proteins and then transfer to nitrocellulose membrane was performed. However, again the Fe SOD band was not observed using colorimetric detection. The gel containing the *A. thaliana* extract was boiled after soaking in 10 % SDS and β-mercaptoethonol to denature proteins and then proteins were transferred to a nitrocellulose membrane. Colorimetric detection did not show any hybridization of the probe with the Fe SOD band in these membranes either. The data indicate that the Fe SOD antisera did not recognize the native form of the protein (data not shown).

3. Fe SOD gene copy number in the *A. thaliana* genome

In order to determine the copy number of Fe SOD genes in the *A. thaliana* genome, low and high stringency DNA gel blot analysis was performed. Full length

Figure 15. Protein blot of *A. thaliana* leaf extract probed with Fe SOD anti-sera raised in chickens. Lanes 1-3 were probed with immune sera. Lane 1 1:2000, lane 2 1:200, and lane 3 1:20 dilution of the serum. Lanes 4-5 were probed with preimmune sera. Lane 4 1:2000, lane 5 1:200, and lane 6 1:20 dilution of the serum. 25 kD: Predicted molecular weight of *A. thaliana* Fe SOD protein. 25kD: Predicted molecular weight of *A. thaliana* Fe SOD protein.

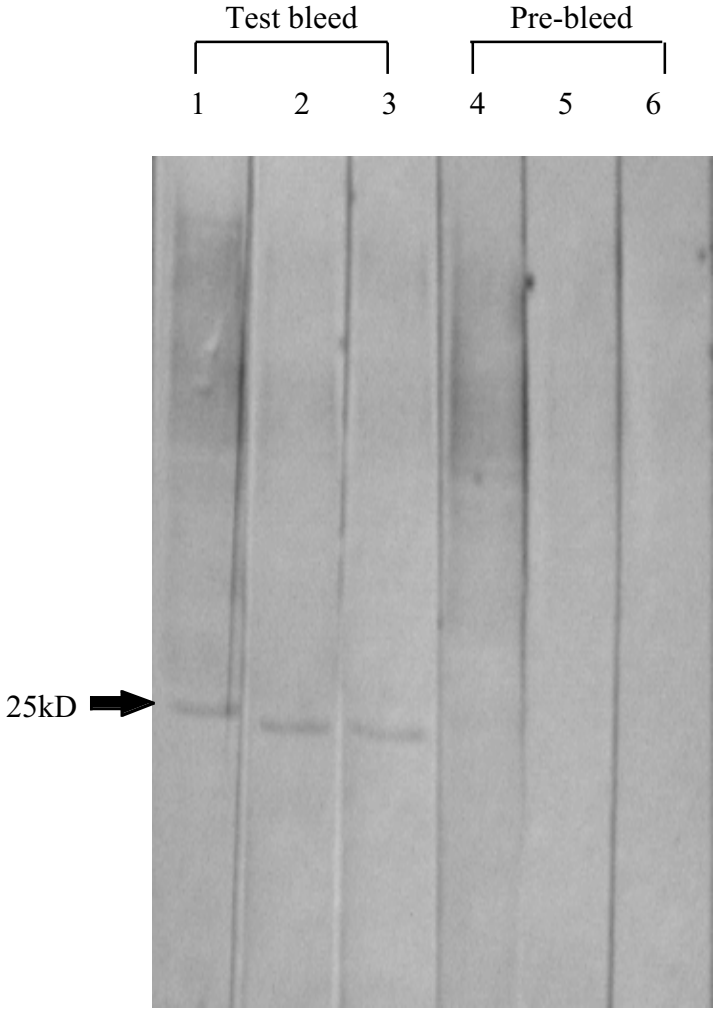
Test bleed
Pre-bleed
1
2
3
4
5
6
25kD

mature Fe SOD sequences (GenBank M55910) were used as the probe (kindly provided by Dr. Marc Van Montagu, Universiteit Gent, Belgium). Under both high (65 ^{0}C) and low (55 ^{0}C) stringency conditions, the Fe SOD probe hybridized with only one fragment in *Eco*RI, *Hin*dIII, and *Xba*I digests (Figure 16). When these results were compared with the DNA gel blots performed using Mn SOD, Cu-Zn SOD_{cyt} and Cu-Zn SOD_{chl} ESTs (Donahue and Alscher, unpublished data) no cross hybridization of the Fe SOD probe with other SODs was identified (data not shown).

4. Oxidative Stress Treatments

Ortho-X 77 (Valent USA Corp., Walnut Creek, CA) was used as the surfactant in *A. thaliana* in order to increase the penetration of methyl viologen into the plant cells. In order to determine the surfactant concentration that does not cause an effect on *A. thaliana*, three different concentrations (0.15 %, 0.1% and 0.05 %) of Ortho-X 77, a surfactant, were applied to sixteen day old plants. Samples were taken 6, 12 and 24 hours following treatment. Plants treated with 0.05 % surfactant showed no signs of injury, whereas 0.1 % and 0.15 % surfactant-treated plants had moderate to severe bleaching in their leaves (Figure 17).

Enzyme activities and protein levels were determined in 16-day old whole *A. thaliana*. Under our experimental conditions, after sixteen days, floral parts of the plants are observed. Therefore, when the samples were taken the same size, and non-flowering plants were taken for the assays. Activity gels and immunoblots were performed from

Figure 16. Gel blot of wildtype *A. thaliana* genomic DNA. DNA was cleaved with the restriction enzymes *Hind*III (H), *EcoR*I (E) and *Xba*I (X). Lanes 1, 2, and 3 were probed with the full length Fe SOD cDNA under high stringency conditions, whereas lanes 4, 5, and 6 were probed under low stringency conditions. The probe hybridized with one and the same fragment under both conditions.

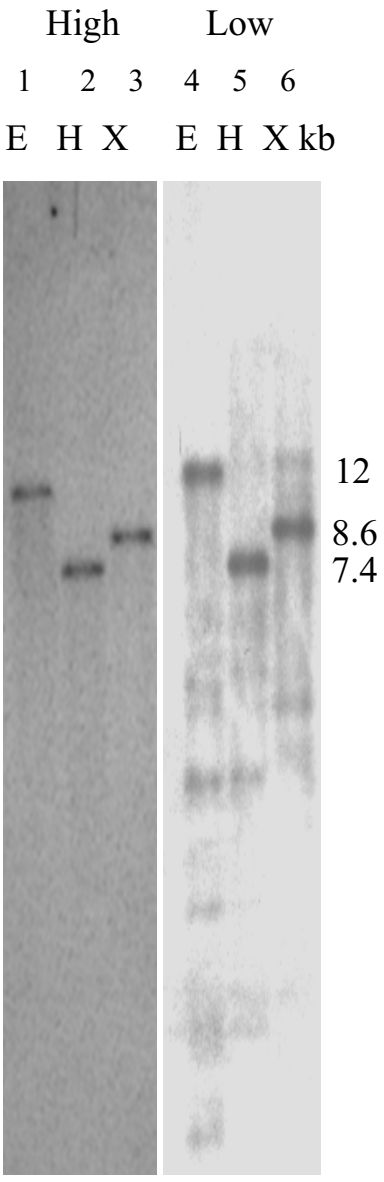
High
Low
1 2 3 4 5 6
E H X E H X kb
12
8.6
7.4

Figure 17. Effects of surfactant (Ortho X-77, Valent USA Corp., Walnut Creek, CA). treatment on *A. thaliana* seedlings. Plants were treated with three different surfactant concentration. 0.05% surfactant did not cause any visible damage, whereas 0.1 and 0.15% caused bleaching of the leaves. X-77: Surfactant (Ortho X-77, Valent USA Corp., Walnut Creek, CA).

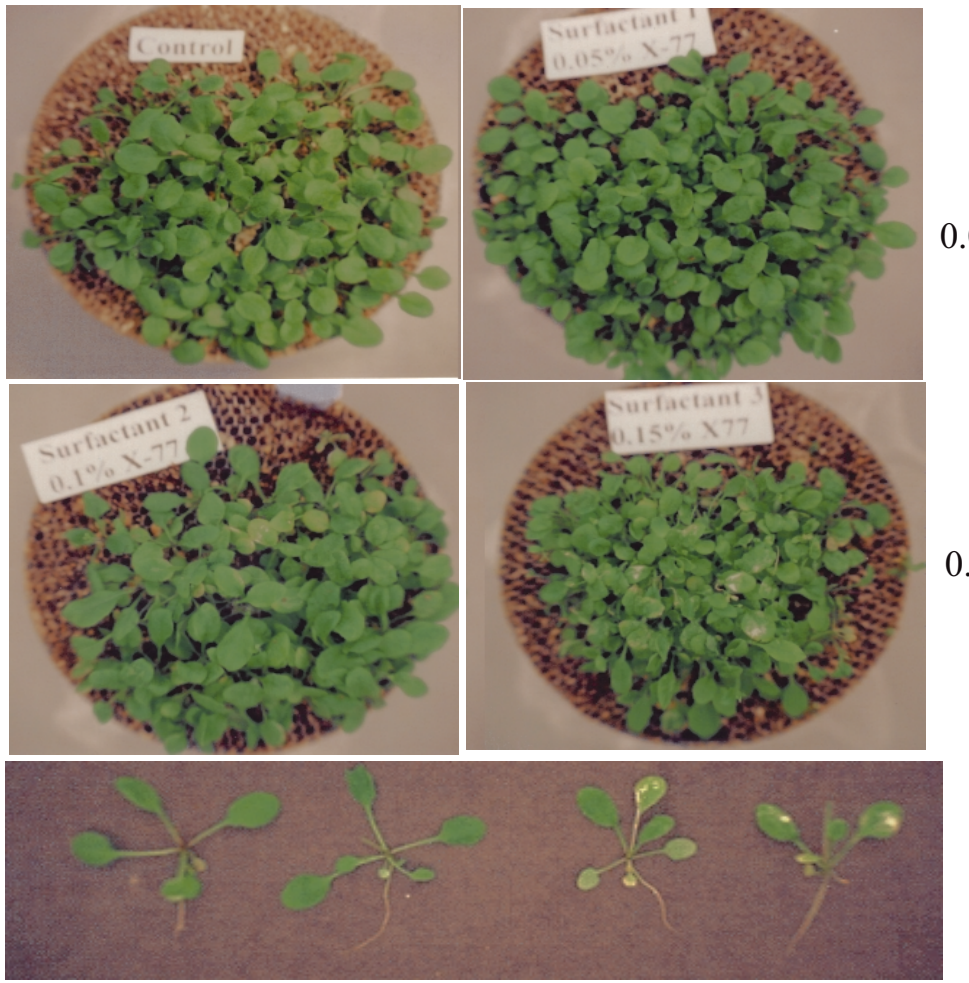
Control
Surfactant 1
0.05% X-77
Surfactant 2
0.1% X-77
Surfactant 3
0.15% X77
Control
0.05% X-77
0.1% X-77
0.15% X-77

these samples. Two control groups, untreated and 0.05 % surfactant treated groups, two methyl viologen-treated groups ($1x10^{-6}$ M and $5x10^{-5}$ M), and one DCMU-treated group ($1x10^{-5}$ M) were used as the experimental groups. Treatments were repeated three times with different set of plants and replicate samples were taken from each treatment group. One set of these replicas was used for the activity experiments and the other set was used for immonoblot experiments. Each experiment was repeated three times and one representative picture of these experiments is presented in the figures. Histograms were generated from the data obtained from all three experiments. Bands from the gels stained for activity and from the immunoblots were scanned in the densitometer in order to determine changes that had occurred in the amount of activity and of protein for Fe, Mn and Cu-Zn SODs. Amount of activity and of protein at T=0 h was set to 100 and changes in the amount of activity and of protein was determined by taking T=0 h as the control.

4.1. Effects on Fe SOD

Both concentrations of methyl viologen caused an increase in the amount of Fe SOD enzyme, whereas DCMU treatment caused an initial decrease followed by an increase (Figure 18). After the methyl viologen treatment, the maximum increase in Fe SOD activity was observed 5 hours after the treatments for both methyl viologen-treated groups and the level of activity in both groups was similar. Fe SOD activity in the DCMU-treated group showed an initial decrease at 17 hours following the treatment, but

Figure 18. Effects of methyl viologen and DCMU treatments on Fe SOD of *A. thaliana*. C_1: Untreated plants; C_2: Surfactant-treated plants; MV_1: $5x10^{-5}$ M methyl viologen-treated; MV_2: $1x10^{-6}$ M methyl viologen-treated. A. Histogram generated from Fe SOD activity assays shown in panel C. B. Histogram generated from Fe SOD protein blots shown in panel C. C. SOD activity gels. Slower migrating band Mn SOD activity, faster migrating band Fe SOD activity. D. Fe SOD immunoblots using anti Fe SOD (25 kD protein)

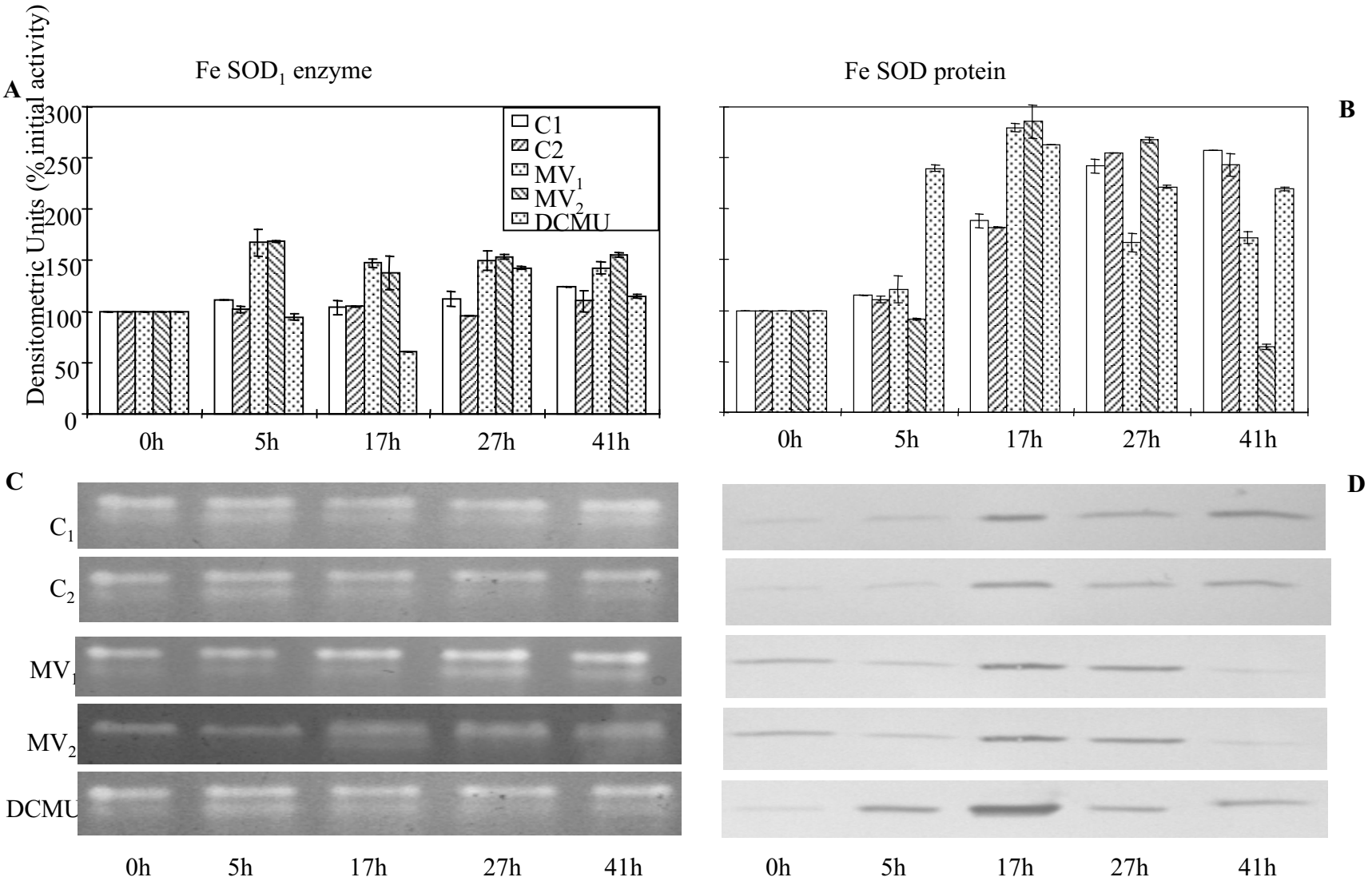
A
Fe SOD$_1$ enzyme
Densitometric Units (% initial activity)
300
250
200
150
100
50
0
C1
C2
MV$_1$
MV$_2$
DCMU
0h
5h
17h
27h
41h
B
Fe SOD protein
0h
5h
17h
27h
41h
C
C$_1$
C$_2$
MV$_1$
MV$_2$
DCMU
0h
5h
17h
27h
41h
D
0h
5h
17h
27h
41h

increased to the same level as in methyl viologen-treated plants 27 hours after the treatments, and then decreased to the level of the control plants.

Another Fe SOD response to stress is the appearance of novel Fe SOD activity bands (Figure 19). These bands were observed both in DCMU- and in methyl viologen-treated plants. Densitometric scanning showed that the novel Fe SOD enzyme activity was present five hours after the treatment, and it showed a consistent increase over the 41 hour time course. These bands were not observed in the control plants.

Denaturing gel electrophoresis was performed using the collected samples in order to determine the effects of stress treatment at the protein level. Proteins from denaturing gel electrophoresis were transferred to the nitrocellulose membranes. After these membranes were incubated with the Fe SOD antibody, one band at 25 kD was observed. Although second and third Fe SOD activity bands were observed in methyl viologen and DCMU-treated plants, no secondary bands were observed in immunoblots in any of the treatment groups, at any time point. The protein bands were scanned using a densitometer in order to quantify these results. Although an increase in the protein level was observed in both the methyl viologen- and DCMU-treated groups, protein amounts increased in both control groups as well (Figure 18), suggesting that this increase was not a result of the oxidative stress treatments.

4.2. Effects on Mn SOD

Treatment of *A. thaliana* with methyl viologen resulted in an increase in the

Figure 19. Appearance of two novel Fe SOD activity bands after treatment of *A. thaliana* with methyl viologen and DCMU. A. SOD activity gels. C_1: Untreated plants; C_2:Surfactant-treated plants; MV_1:$5x10^{-5}$ M methyl viologen-treated; MV_2:$1x10^{-6}$ M methyl viologen-treated. B. Histogram generated from Fe SOD_2 activity assays shown in panel A.

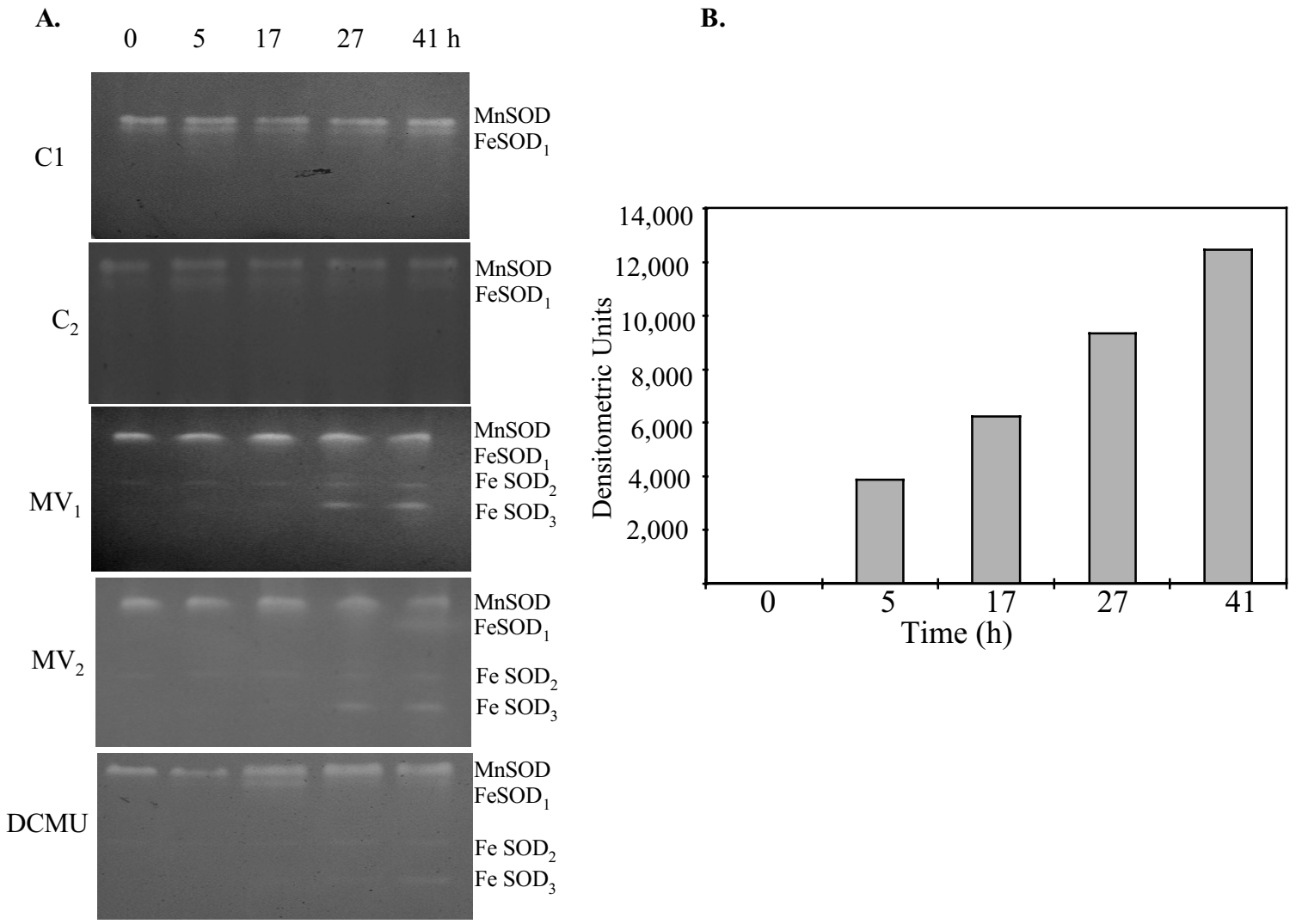
A.
0
5
17
27
41 h
C1
MnSOD
FeSOD1
C2
MnSOD
FeSOD1
MV1
MnSOD
FeSOD1
Fe SOD2
Fe SOD3
MV2
MnSOD
FeSOD1
Fe SOD2
Fe SOD3
DCMU
MnSOD
FeSOD1
Fe SOD2
Fe SOD3
B.
Densitometric Units
14,000
12,000
10,000
8,000
6,000
4,000
2,000
0
5
17
27
41
Time (h)

amount of mitochondrial Mn SOD enzyme activity. Increase in the activity was between 50-75 % for both $5x10^{-5}$ M and for $1x10^{-6}$ M methyl viologen-treated plants. No change in the activity was observed in the control groups or the DCMU-treated group over the 41-hour time course (Figure 20). Activity changes caused by methyl viologen were similar in both Mn and Fe SOD enzymes. In contrast to the changes observed in Fe SOD activity, DCMU did not cause any changes in Mn SOD enzyme activity.

Immunoblots were performed with anti Mn SOD (kindly provided by Dr. Robert Last and Dr. Daniel Kleibenstein at Boyce Thompson Institute, Ithaca, NY) in order to determine the effects of oxidative stress on Mn SOD protein levels. Immunoblots performed for Mn SOD showed that the blots incubated with the Mn SOD antibody had only one band of 26 kD. The $1x10^{-6}$ M methyl viologen-treated group responded to this stress with an increase in the amount of protein. The observed increase was about 50 % of the initial protein amount, and it remained the same over the 41 hour time course. The amount of protein observed in the $5x10^{-5}$ M methyl viologen-treated group stayed at the same level as the control groups. Although a small change in the DCMU-treated group was observed, the Mn SOD protein level remained very close to that of the control groups (Figure 20).

The increase observed in the Mn SOD protein level was followed by an increase in the activity of this enzyme in the $1x10^{-6}$ M methyl viologen-treated group. In contrast, in the $5x10^{-5}$ M methyl viologen-treated group, increased Mn SOD activity (~75 %) was

Figure 20. Effects of methyl viologen and DCMU treatments on Mn SOD of *A. thaliana*. C_1: Untreated plants; C_2: Surfactant treated plants; MV_1: $5x10^{-5}$ M methyl viologen-treated; MV_2: $1x10^{-6}$ M methyl viologen-treated. A. Histogram generated from Mn SOD activity assays shown in panel C. B. Histogram generated from Fe SOD protein blots shown in panel C. C. SOD activity gels. D. Fe SOD immunoblots using anti Mn SOD (25.8 kD protein)

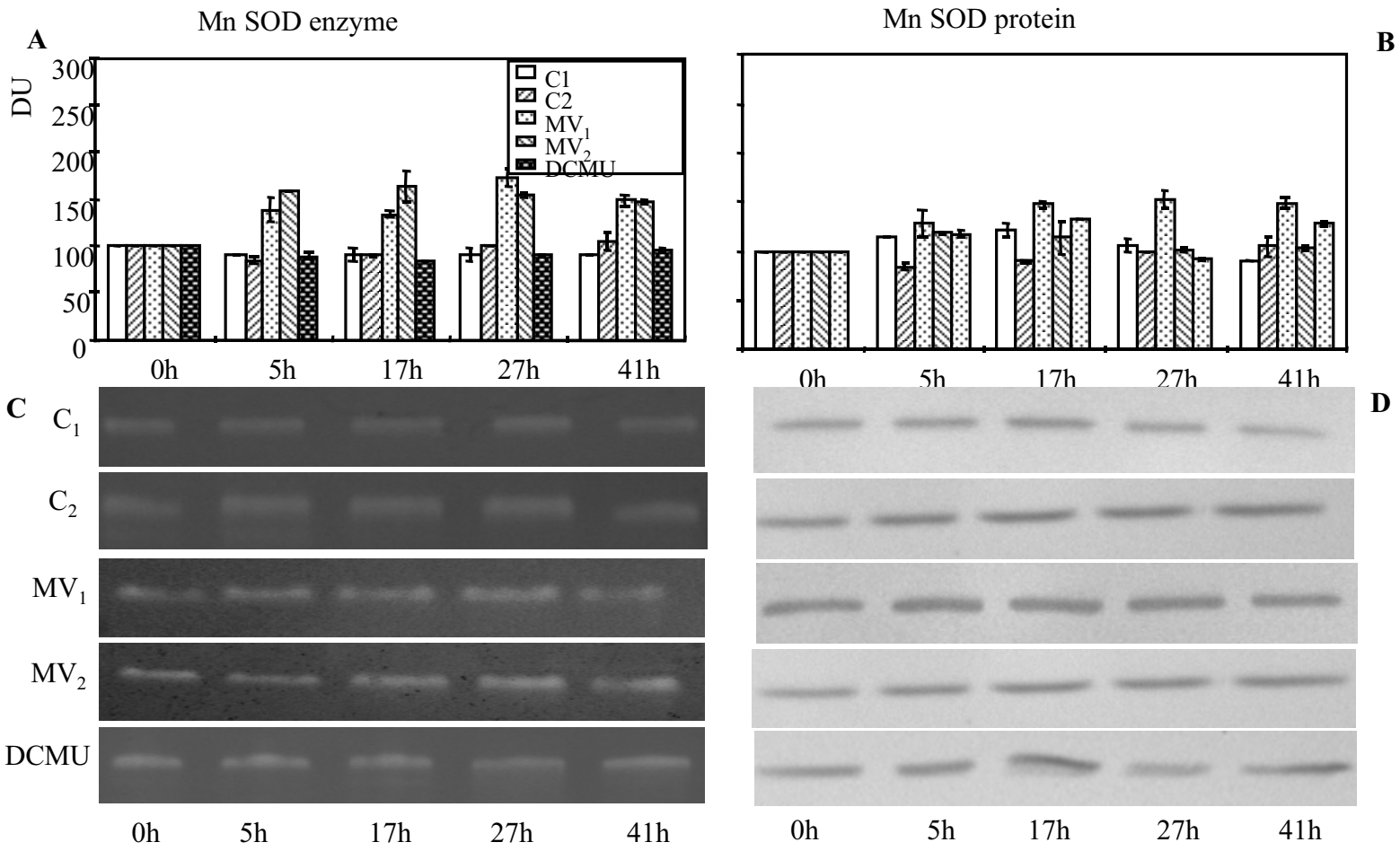
A
Mn SOD enzyme
DU
300
250
200
150
100
50
0
C1
C2
MV1
MV2
DCMU
0h
5h
17h
27h
41h
B
Mn SOD protein
0h
5h
17h
27h
41h
C
C1
C2
MV1
MV2
DCMU
0h
5h
17h
27h
41h
D
0h
5h
17h
27h
41h

not accompanied by a similar increase in protein level. Similar to Mn SOD enzyme activity, the level of Mn SOD protein remained the same as that of the control groups in the DCMU-treated group (Figure 20).

4.3. Effects on Cu-Zn SOD

Treatment of *A. thaliana* with oxidative stress in the form of methyl viologen and DCMU did not cause any changes in the amount of either total Cu-Zn SOD enzyme activity and cytosolic and chlroplastic Cu-Zn SOD protein levels (Figure 21). Immunoblots were performed with anti chloroplastic and cytosolic Cu-Zn SODs (kindly provided by Dr. Robert Last and Dr. Dan Kleibenstein at Boyce Thompson Institute, Ithaca, NY) in order to determine the effects of oxidative stress on Cu-Zn SOD protein levels. When the immunoblots were incubated with the Cu-Zn SOD antibody, two bands (22 kD and 15 kD) were observed. The 22 kD band is the chloroplastic Cu-Zn SOD (Cu-Zn SOD_{chl}) and the 15 kD band is the cytosolic Cu-Zn SOD (Cu-Zn SOD_{cyt}) (Kleibenstein et al. 1998). Changes in the amount of Cu-Zn SOD_{chl} and Cu-Zn SOD_{cyt} were measured separately. A small decrease in the amount of 22 kD Cu-Zn SOD_{chl} was observed after methyl viologen treatments. At T=5 h, 17 h and 27 h, however, the amount of protein was the same as in the control groups at T=47 h. Whereas the DCMU-treated group showed a small increase at T=27, the level of protein decreased to that of the controls at T=47 h. Overall, an inconsistent change in the amount of Cu-Zn SOD_{chl} protein was observed for all treatment groups.

Figure 21. Effects of methyl viologen and DCMU treatments on Cu-Zn SOD of *A. thaliana*. C_1: Untreated plants; C_2: Surfactant-treated plants; MV_1: $5x10^{-5}$ M methyl viologen-treated; MV_2: $1x10^{-6}$ M methyl viologen-treated. A. Histogram generated from Cu-Zn SOD activity assays shown in panel D. B. Histogram generated from chloroplastic Cu-Zn SOD immunoblots using anti Cu-Zn shown in panel E (22 kD protein). C. Histogram generated from cytosolic Cu-Zn SOD immunoblots using anti Cu-Zn shown in panel F. D. SOD activity gels. E. Chloroplastic SOD immunoblots using anti Cu-Zn SOD. F. Cytosolic SOD immunoblots using anti Cu-Zn SOD (15 kD protein).

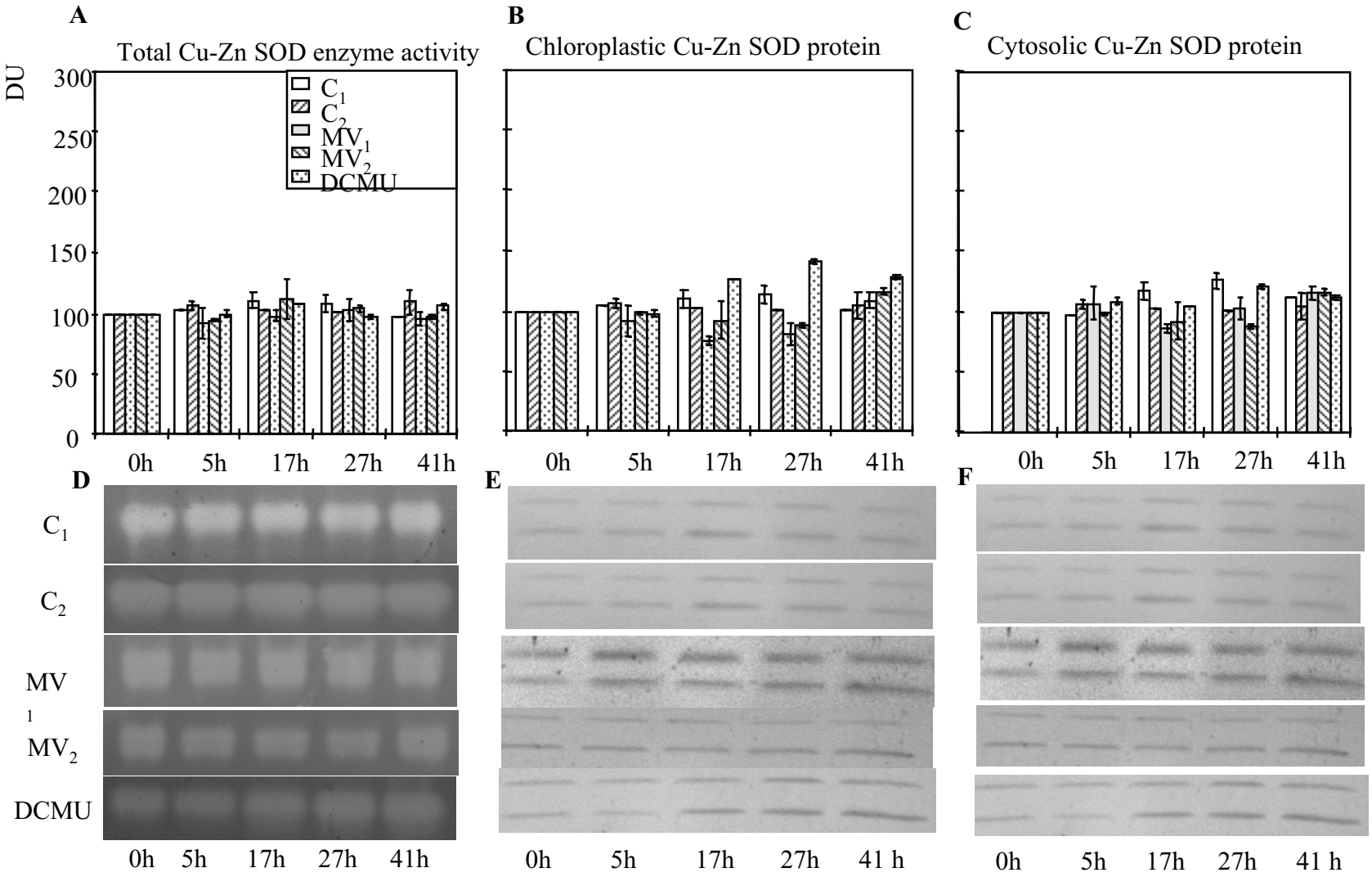
A
Total Cu-Zn SOD enzyme activity
DU
300
250
200
150
100
50
0
C1
C2
MV1
MV2
DCMU
0h
5h
17h
27h
41h
B
Chloroplastic Cu-Zn SOD protein
0h
5h
17h
27h
41h
C
Cytosolic Cu-Zn SOD protein
0h
5h
17h
27h
41h
D
C1
C2
MV1
MV2
DCMU
0h
5h
17h
27h
41h
E
0h
5h
17h
27h
41 h
F
0h
5h
17h
27h
41 h

The 15 kD Cu-Zn SOD_{cyt} responded in a similar way, with a small decrease in the level of protein after methyl viologen treatment, but no significant change in the amount of this enzyme overall. That no change was observed in the amount of either Cu-Zn SOD protein correlates with the finding that no changes in the amount of Cu-Zn SOD enzyme was observed after any of the treatments (Figure 21).

4.4. Effects of Light on Oxidative Stress Responses

In order to test the effects of light on oxidative stress responses of SODs, half of the $5x10^{-5}$ M methyl viologen-treated plants and half of the surfactant-treated plants (C_2), were transferred to a growth chamber where the plants were kept under constant light for 10 hours. The remaining plants were transferred to a growth chamber where they were kept in the dark for 10 hours.

The response of Fe SOD to methyl viologen was light-independent. Plants respond similarly to methyl viologen treatment under both light and dark conditions. The activity of the novel Fe SOD bands (Fe SOD_2 and Fe SOD_3) was observed both in dark and light kept plants (Figure 22). A similar response was observed for Cu-Zn SOD. Regardless of the light conditions, the level of Cu-Zn SOD enzyme activity remained similar that of the controls (Figure 22). However, Mn SOD enzyme showed a light dependent response to methyl viologen treatment. The plants that were kept in light showed a higher activity when compared to the control and methyl viologen-treated plants kept in the dark (Figure 22).

Figure 22. Effects of light and methyl viologen on SOD activities in *A. thaliana*. One group of methyl viologen-treated plants was kept in light and the other group was kept in the dark for 5 hours before the activities were measured. A. SOD activities measured in *A. thaliana*. B. Histogram generated from the data on panel A. MV= $5x10^{-5}$ M methyl viologen, C_2 0.05% OrthoX77. MV; methyl viologen, C_2; surfactant.

A.

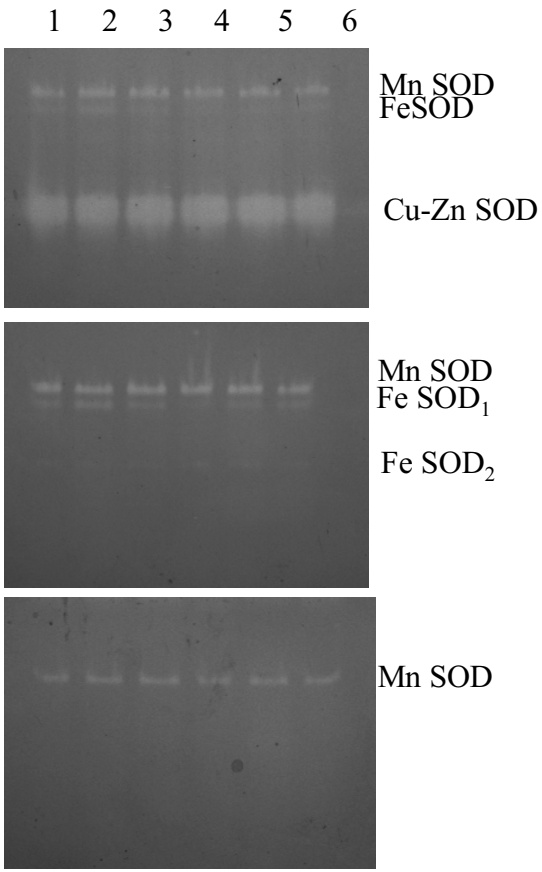
1 2 3 4 5 6
Mn SOD
FeSOD
Cu-Zn SOD
Mn SOD
Fe SOD1
Fe SOD2
Mn SOD

B.

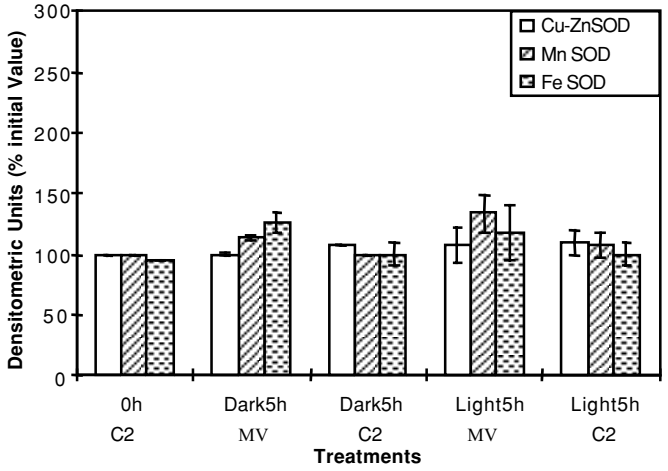
Cu-ZnSOD
Mn SOD
Fe SOD
Densitometric Units (% initial Value)
300
250
200
150
100
50
0
0h
C2
Dark5h
MV
Dark5h
C2
Light5h
MV
Light5h
C2
Treatments

5. Comparison of SOD Sequences

Phylogenetic trees were constructed for twelve cytosolic Cu-Zn, five chloroplastic Cu-Zn, and six Mn/Fe plant superoxide dismutases in order to determine the evolutionary relationships among superoxide dismutases in the same group. Three samples were randomly chosen from each group for construction of this phylogenetic tree.

Amino acid sequences from twelve cytosolic and five chloroplastic Cu-Zn SODs were aligned to identify the overall similarities using the DNASTAR MEGALIGN computer program (version 1.61) according to the Clustal method. An 85 % similarity was found among twelve plant cytosolic Cu-Zn SODs. Chloroplastic Cu-Zn SODs showed about 77 % similarity to each other. However the similarity falls to 61 % when chloroplastic and cytosolic Cu-Zn SOD sequences are compared to one another (Figure 23) and is clearly seen in the phylogenetic tree (Figure 24).

When deduced Fe SOD amino acid sequences from three plant species were compared, a 79 % overall similarity was observed. Mn SOD sequences from three different plant species had 76 % similarity was found. When Fe and Mn SODs were compared, the similarity dropped to 35 % (Figure 25), and the phylogenetic tree again shows that there is a clear difference between Fe and Mn SODs (Figure 26).

When amino acid sequences of three representative species from each group were

Figure 23. Comparison of amino acid sequences of known chloroplastic and cytosolic plant Cu-Zn SODs using the Clustal method with PAM 250 residue weight table. Residues decorated with solid deep red are the residues that match *A. thaliana* cytosolic Cu-Zn SOD, residues decorated with solid bright cobalt are the residues that match aspen chloroplastic Cu-Zn SOD. The first twelve sequences are cytosolic Cu-Zn SODs and the last five sequences are chloroplastic Cu-Zn SODs. The sequences for this study were derived from Gene Bank and have the following accesion numbers: arabidopsis, *A. thaliana* Cu-Zn SOD_{cyt}, X60935; cabbage, *Brassica oleracea* Cu-Zn SOD_{cyt}, P09678; iceplant, *Mesembryanthemum crystallinum* Cu-Zn SOD_{cyt}, P93258; iceplant2, *Mesembryanthemum crystallinum* Cu-Zn SOD_{cyt}, O49044; maize, *Zea mays* Cu-Zn SOD_{cyt}, P23346; maize2, *Zea mays* Cu-Zn SOD_{cyt}, P23345; rice, *Oryza sative* Cu-Zn SOD_{cyt}, P28757; rice2, *Oryza sative* Cu-Zn SOD_{cyt}, P28756; sweet potato, *Ipomoea batatas* Cu-Zn SOD_{cyt}, X73139; tobacco, *Nicotiana plumbaginifolia* Cu-Zn SOD_{cyt}, P27082; tomato1, *Lycopersicon esculemtum* Cu-Zn SOD_{cyt}, P143779; tomato2, *L. esculemtum* Cu-Zn SOD_{cyt}, Q43799; aspen, *Populus tremuloides* Cu-Zn SOD_{chl}, U08097; pea, *Pisum sativum* Cu-Zn SOD_{chl}, X56435; petunia, *Petunia x hybrida* Cu-Zn SOD_{chl}, P10792; scotch pine, *Pinus sylvestris* Cu-Zn SOD_{chl}, P24707; spinach, *Spinacia oleracea* Cu-Zn SOD_{chl}, P22233.

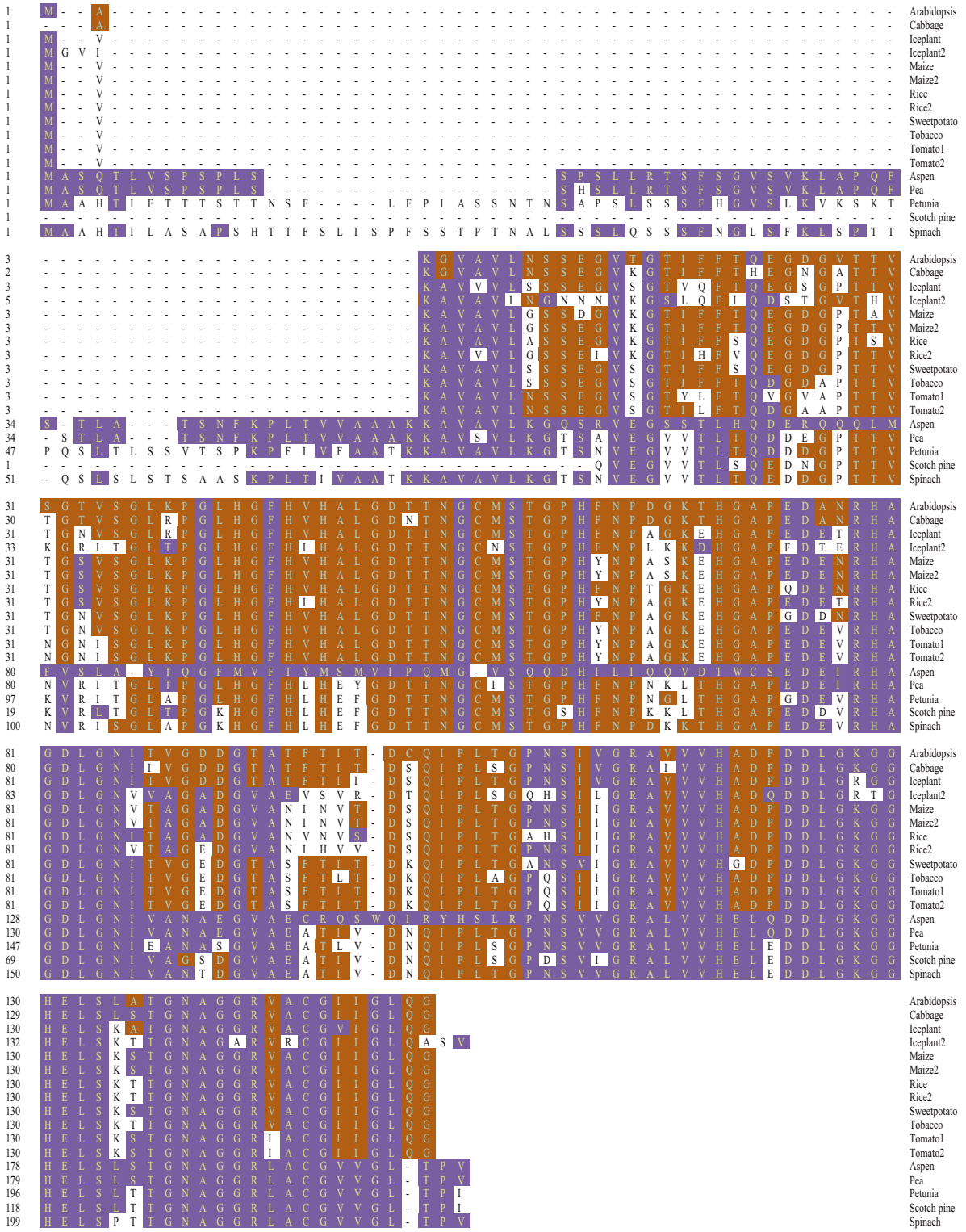
Arabidopsis
Cabbage
Iceplant
Iceplant2
Maize
Maize2
Rice
Rice2
Sweetpotato
Tobacco
Tomato1
Tomato2
Aspen
Pea
Petunia
Scotch pine
Spinach

Figure 24. Phylogenetic tree of plant Cu-Zn SODs generated using amino acid sequence alignment from figure 23. A. Sequence distances, B. Phylogenetic tree. The sequences for this study were derived from Gene Bank and have the following accesion numbers: arabidopsis, *A. thaliana* Cu-Zn SOD_{cyt}, X60935; cabbage, *Brassica oleracea* Cu-Zn SOD_{cyt}, P09678; iceplant, *Mesembryanthemum crystallinum* Cu-Zn SOD_{cyt}, P93258; iceplant2, *Mesembryanthemum crystallinum* Cu-Zn SOD_{cyt}, O49044; maize, *Zea mays* Cu-Zn SOD_{cyt}, P23346; maize2, *Zea mays* Cu-Zn SOD_{cyt}, P23345; rice, *Oryza sative* Cu-Zn SOD_{cyt}, P28757; rice2, *Oryza sative* Cu-Zn SOD_{cyt}, P28756; sweet potato, *Ipomoea batatas* Cu-Zn SOD_{cyt}, X73139; tobacco, *Nicotiana plumbaginifolia* Cu-Zn SOD_{cyt}, P27082; tomato1, *Lycopersicon esculemtum* Cu-Zn SOD_{cyt}, P143779; tomato2, *L. esculemtum* Cu-Zn SOD_{cyt}, Q43799; aspen, *Populus tremuloides* Cu-Zn SOD_{chl}, U08097; pea, *Pisum sativum* Cu-Zn SOD_{chl}, X56435; petunia, *Petunia x hybrida* Cu-Zn SOD_{chl}, P10792; scotch pine, *Pinus sylvestris* Cu-Zn SOD_{chl}, P24707; spinach, *Spinacia oleracea* Cu-Zn SOD_{chl}, P22233.

Percent Similarity

	1	2	3	4	5	6	7	8	9	10	11	12	13	14	15	16	17		
1		92.1	86.2	65.1	82.9	84.2	82.2	80.3	86.2	84.9	83.6	84.2	35.5	64.5	65.1	65.2	68.4	**1**	Arabidopsis
2	8.4		84.1	64.2	80.8	82.1	79.5	77.5	82.8	81.5	80.1	80.8	36.4	63.6	64.2	65.2	66.2	**2**	Cabbage
3	15.3	17.9		65.1	82.9	84.2	82.2	84.2	86.8	86.8	85.5	85.5	34.9	65.8	65.1	65.2	68.4	**3**	Iceplant
4	45.5	48.3	45.5		68.4	68.4	70.4	68.4	63.8	65.1	64.5	65.1	34.0	60.9	61.5	63.1	60.3	**4**	Iceplant2
5	19.5	22.2	19.5	39.8		98.7	90.8	91.4	85.5	86.2	83.6	84.2	37.5	63.8	63.8	63.1	66.4	**5**	Maize
6	17.8	20.5	17.8	39.8	1.3		91.4	92.8	86.8	87.5	84.9	85.5	37.5	64.5	64.5	63.8	67.1	**6**	Maize2
7	20.3	24.0	20.3	36.6	9.8	9.1		88.2	86.8	84.9	80.9	81.6	36.2	61.8	64.5	64.5	65.8	**7**	Rice
8	23.0	26.8	17.8	39.8	9.1	7.6	12.9		83.6	85.5	82.2	82.9	35.5	63.2	64.5	65.2	67.1	**8**	Rice2
9	15.3	19.6	14.5	47.9	16.1	14.5	14.5	18.6		90.8	88.2	88.8	34.9	63.2	64.5	66.0	66.4	**9**	Sweetpotato
10	16.9	21.4	14.5	45.5	15.3	13.7	16.9	16.1	9.8		92.8	94.1	34.9	61.8	65.8	63.8	65.8	**10**	Tobacco
11	18.6	23.1	16.1	46.7	18.6	16.9	22.1	20.3	12.9	7.6		98.0	34.2	64.5	63.8	63.8	67.1	**11**	Tomato1
12	17.8	22.2	16.1	45.5	17.8	16.1	21.2	19.5	12.1	6.2	2.0		34.9	65.1	64.5	63.8	67.1	**12**	Tomato2
13	108.0	109.5	108.0	107.1	98.7	98.7	103.2	105.6	110.5	108.0	108.0	105.6		65.2	43.8	45.4	46.8	**13**	Aspen
14	45.9	48.8	43.5	51.4	47.1	45.9	50.8	48.3	48.3	50.8	45.9	44.7	38.5		72.8	84.4	75.7	**14**	Pea
15	44.7	47.5	44.7	51.4	47.1	45.9	45.9	45.9	45.9	43.5	47.1	45.9	78.5	30.1		86.5	73.5	**15**	Petunia
16	44.8	44.8	44.8	50.4	48.7	47.4	46.1	44.8	43.5	47.4	47.4	47.4	75.2	17.5	14.9		87.2	**16**	Scotch pine
17	39.0	43.9	39.0	52.7	42.4	41.3	43.5	41.3	42.4	43.5	41.3	41.3	71.5	26.5	29.4	14.0		**17**	Spinach
	1	**2**	**3**	**4**	**5**	**6**	**7**	**8**	**9**	**10**	**11**	**12**	**13**	**14**	**15**	**16**	**17**		

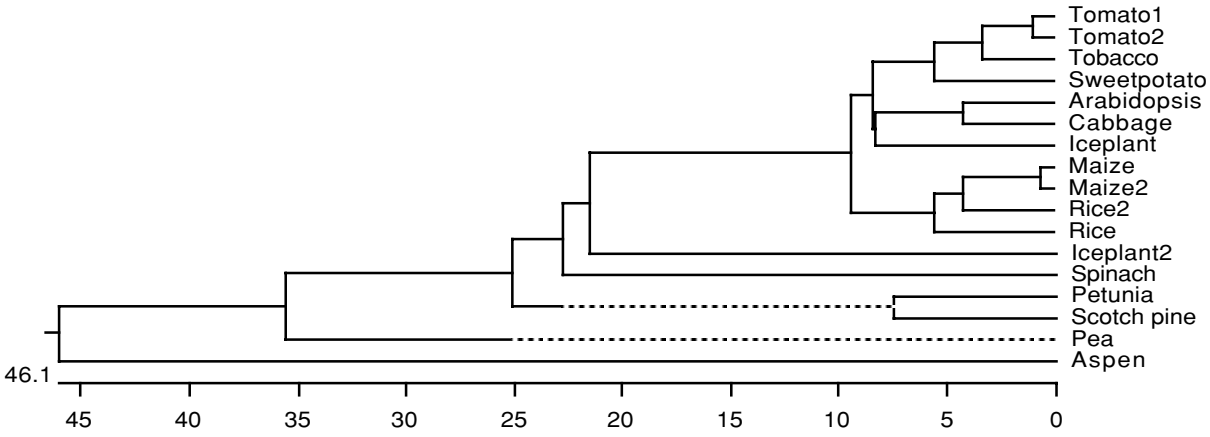

Figure 25. Comparison of amino acid sequences of twelwe plant and prokaryotic Fe and Mn SODs using the Clustal method with PAM 250 residue weight table. Residues decorated with solid deep red are the residues that match *A. thaliana* Fe SOD exactly, residues decorated with solid bright yellow match *E. coli* Fe S OD exactly, residues decorated with solid dark green are the residues that match *A. thaliana* Mn SOD exactly, residues decorated with solid bright cobalt match *E. coli* Mn SOD exactly. The sequences for this study were derived from Gene Bank and have the following accesion numbers: arabidopsis Fe, *A. thaliana* Fe SOD, M55910; soybean Fe, *Glycine max* Fe SOD, M64267; tobacco Fe, *Nicotiana plumbaginifolia* Fe SOD, M55909; *E. coli* Fe, *E. coli* Fe SOD, P09157; mycobacterium Fe, *Mycobacterium tuberculosis* Fe SOD, P17670; pseudomonas Fe, *P. ovalis* Fe SOD, P09223; arabidopsis Mn, *A. thaliana* Mn SOD, T44258; hevea Mn, *Hevea brasiliensis* Mn SOD, L11707; tobaco Mn, *Nicotiana plumbaginifolia* Mn SOD, A05335; *E. coli* Mn, *E. coli* Mn SOD, P00448; acinetobacter Mn, Acinetobacter sp. Mn SOD, Z46863; chlamdia Mn, *Chlamydia trachomatis* Mn SOD, AE001302.

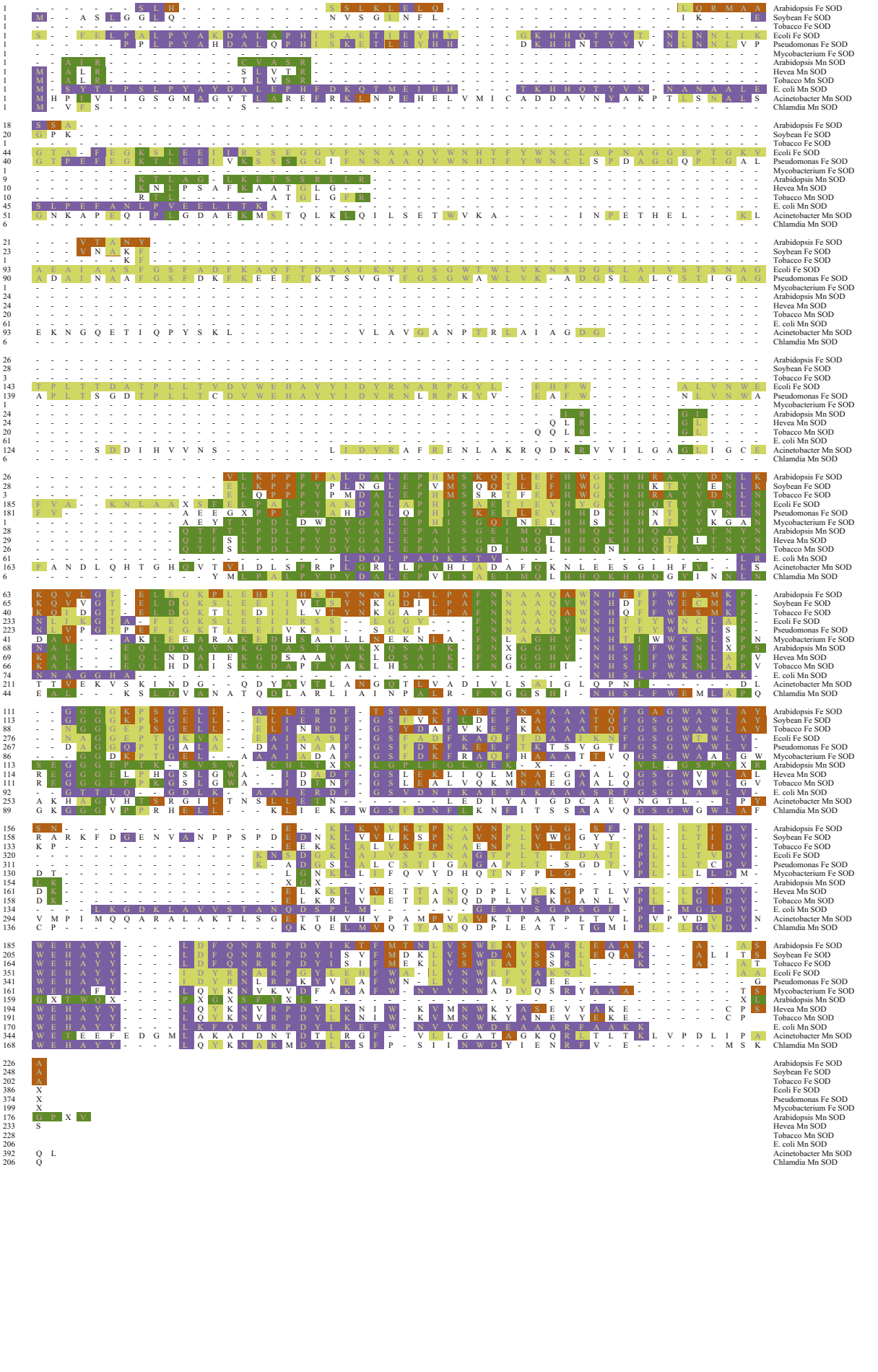

Figure 26. Phylogenetic tree of plant and bacterial Fe and Mn SODs generated using amino acid sequence alignment from figure 25. A. Sequence distances, B. Phylogenetic tree. The sequences for this study were derived from Gene Bank and have the following accesion numbers: arabidopsis Fe, *A. thaliana* Fe SOD, M55910; soybean Fe, *Glycine max* Fe SOD, M64267; tobacco Fe, *Nicotiana plumbaginifolia* Fe SOD, M55909; *E. coli* Fe, *E. coli* Fe SOD, P09157; mycobacterium Fe, *Mycobacterium tuberculosis* Fe SOD, P17670; pseudomonas Fe, *P. ovalis* Fe SOD, P09223; arabidopsis Mn, *A. thaliana* Mn SOD, T44258; hevea Mn, *Hevea brasiliensis* Mn SOD, L11707; tobaco Mn, *Nicotiana plumbaginifolia* Mn SOD, A05335; *E. coli* Mn, *E. coli* Mn SOD, P00448; acinetobacter Mn, Acinetobacter sp. Mn SOD, Z46863; chlamdia Mn, *Chlamydia trachomatis* Mn SOD, AE001302.

Percent Similarity

	1	2	3	4	5	6	7	8	9	10	11	12		
1		65.9	73.8	37.6	37.6	32.2	15.6	25.7	24.3	37.9	14.2	28.2	**1**	Arabidopsis Fe SOD
2	37.6		72.8	28.2	32.7	30.7	15.1	25.3	24.1	34.5	12.5	31.1	**2**	Soybean Fe SOD
3	28.2	28.6		46.5	41.6	33.2	16.8	30.7	29.7	35.6	13.9	30.7	**3**	Tobacco Fe SOD
4	88.6	87.6	69.2		65.0	36.2	19.6	27.9	27.2	36.4	10.9	32.0	**4**	Ecoli Fe SOD
5	88.6	85.8	77.0	38.9		37.2	22.3	28.3	26.8	36.9	11.2	29.1	**5**	Pseudomonas Fe SOD
6	112.7	112.3	124.9	108.2	103.4		26.3	41.7	40.2	35.7	16.6	35.2	**6**	Mycobacterium Fe SOD
7	186.0	184.7	181.3	170.8	172.9	115.1		48.0	49.2	24.0	13.4	30.2	**7**	Arabidopsis Mn SOD
8	122.8	119.9	122.0	129.3	132.8	91.5	58.1		82.5	36.4	13.3	48.1	**8**	Hevea Mn SOD
9	135.5	131.7	124.9	135.2	141.7	97.1	51.1	15.3		35.0	13.2	46.1	**9**	Tobacco Mn SOD
10	96.5	113.3	95.8	101.5	94.1	111.5	268.0	138.5	134.9		13.1	36.9	**10**	E. coli Mn SOD
11	260.0	261.0	281.0	321.0	323.0	476.0	254.0	292.0	257.0	380.0		13.1	**11**	Acinetobacter Mn SOD
12	128.9	123.3	119.8	120.9	130.9	115.1	107.6	76.0	81.2	109.8	328.0		**12**	Chlamdia Mn SOD
	1	**2**	**3**	**4**	**5**	**6**	**7**	**8**	**9**	**10**	**11**	**12**		

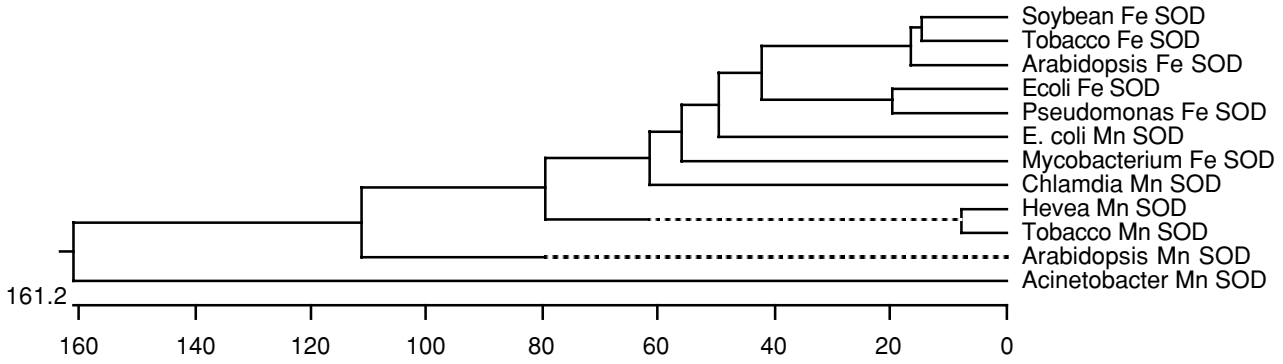

compared to one another, a clear distinction between these Cu-Zn SODs and Mn/Fe SODs were observed (Figure 27). The similarity between plastidic Cu-Zn SODs and Fe SOD sequences is approximately 7 % and between Cu-Zn SODs and Mn SODs approximately 6 %. It is clear from the phylogenetic tree that Fe and Mn SODs are closely related to each other. Similarly, chloroplastic and cytosolic Cu-Zn SODs are closely related to each other, whereas the relationship between Fe/Mn and Cu-Zn SODs are more distantly related (Figure 28).

6. Generation of the Three-Dimensional Structure of *A. thaliana* Fe SOD Protein

The three-dimensional structures of prokaryotic Fe SODs, prokaryotic and eukaryotic Mn SODs and eukaryotic Cu-Zn SODs have been determined using X-ray crystallography. Discovery of Fe SODs in eukaryotes is relatively new, and the three-dimensional structure of plant Fe SODs is not known. In order to compare the three-dimensional structures of SODs, the three-dimensional structure of *A. thaliana* Fe SOD protein was modeled using the amino acid sequences from previously crystallized *E. coli* (1isa) and *Psuedomonas ovalis* (3sdp) Fe SOD proteins as templates (Figure 29).

The *A. thaliana* Fe SOD sequence has two identical chains, each with 203 amino acids and 3207 atoms. Eight α-helices, three β-strands, and twenty-five β-turns are present as well as an Fe atom at the active site of the subunit. The three β-strands together form an anti-parallel β-pleated sheet. The secondary structure of *A. thaliana* Fe SOD protein was investigated and compared to that of the bacterial Fe SOD, Mn SOD

Figure 27. Comparison of amino acid sequences of plant Fe, Mn, chloroplastic Cu-Zn, and cytosolic Cu-Zn SODs using the Clustal method with PAM 250 residue weight table. Residues decorated with solid bright yellow are the residues that match *A. thaliana* Fe SOD exactly, residues decorated with solid deep red match *A. thaliana* chloroplastic Cu-Zn SOD, residues decorated with solid bright cobalt match *A. thaliana* Mn SOD, and the residues decorated with solid dark green match *A. thaliana* cytosolic Cu-Zn SOD. The sequences for this study were derived from Gene Bank and have the following accesion numbers: arabidopsis Fe, *A. thaliana* Fe SOD, M55910; soybean Fe, *Glycine max* Fe SOD, M64267; tobacco Fe, *Nicotiana plumbaginifolia* Fe SOD, M55909; arabidopsis Mn, *A. thaliana* Mn SOD, T44258; hevea Mn, *Hevea brasiliensis* Mn SOD, L11707; arabidopsis, *A. thaliana* Cu-Zn SOD_{cyt}, X60935; pea, *Pisum sativum* Cu-Zn SOD_{cyt}, M63003; tobacco, *Nicotiana plumbaginifolia* Cu-Zn SOD_{cyt}, P27082; arabidopsis, *A. thaliana* Cu-Zn SOD_{chl}, T21001; pea, *Pisum sativum* Cu-Zn SOD_{chl}, X56435; tomato, *Lycopersicon esculentum* Cu-Zn SOD_{chl}, M37151.

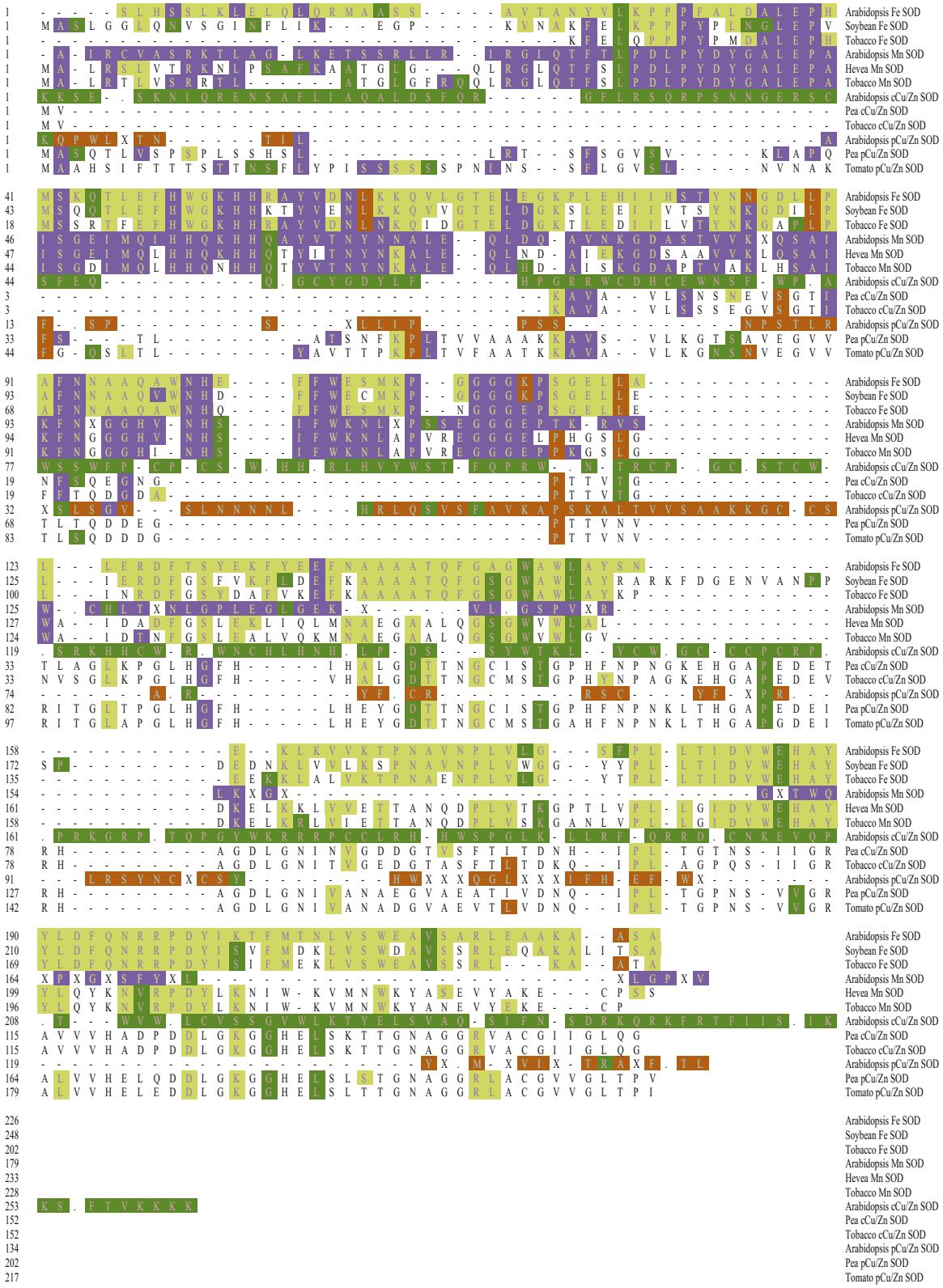
Arabidopsis Fe SOD
Soybean Fe SOD
Tobacco Fe SOD
Arabidopsis Mn SOD
Hevea Mn SOD
Tobacco Mn SOD
Arabidopsis cCu/Zn SOD
Pea cCu/Zn SOD
Tobacco cCu/Zn SOD
Arabidopsis pCu/Zn SOD
Pea pCu/Zn SOD
Tomato pCu/Zn SOD

Figure 28. Phylogenetic tree of plant Fe, Mn, cytosolic Cu-Zn, and chloroplastic Cu-Zn SODs generated using using amino acid sequence alignment from figure 27. A. Sequence distances, B. Phylogenetic tree. The sequences for this study were derived from Gene Bank and have the following accesion numbers: arabidopsis Fe, *A. thaliana* Fe SOD, M55910; soybean Fe, *Glycine max* Fe SOD, M64267; tobacco Fe, *Nicotiana plumbaginifolia* Fe SOD, M55909; arabidopsis Mn, *A. thaliana* Mn SOD, T44258; hevea Mn, *Hevea brasiliensis* Mn SOD, L11707; arabidopsis, *A. thaliana* Cu-Zn SOD_{cyt}, X60935; pea, *Pisum sativum* Cu-Zn SOD_{cyt}, M63003; tobacco, *Nicotiana plumbaginifolia* Cu-Zn SOD_{cyt}, P27082; arabidopsis, *A. thaliana* Cu-Zn SOD_{chl}, T21001; pea, *Pisum sativum* Cu-Zn SOD_{chl}, X56435; tomato, *Lycopersicon esculentum* Cu-Zn SOD_{chl}, M37151.

Percent Similarity

	1	2	3	4	5	6	7	8	9	10	11	12		
1		65.9	73.8	15.6	25.7	24.3	11.5	14.5	14.5	11.2	11.4	11.1	**1**	Arabidopsis Fe SOD
2	37.6		72.8	15.1	25.3	24.1	9.3	13.2	12.5	11.2	11.4	12.0	**2**	Soybean Fe SOD
3	28.2	28.6		16.8	30.7	29.7	9.4	11.8	11.8	9.0	9.9	12.4	**3**	Tobacco Fe SOD
4	187.9	196.9	152.3		48.0	49.2	8.9	11.8	11.8	9.7	11.2	11.2	**4**	Arabidopsis Mn SOD
5	139.3	128.6	118.0	58.1		82.5	9.0	13.2	13.8	11.2	13.4	12.4	**5**	Hevea Mn SOD
6	142.5	136.2	118.5	51.1	15.3		9.2	11.8	13.2	11.2	13.9	12.0	**6**	Tobacco Mn SOD
7	339.0	407.0	354.0	332.0	438.0	386.0		9.2	9.9	11.2	10.4	8.3	**7**	Arabidopsis cCu/Zn SOD
8	418.0	553.0	451.0	328.0	317.0	374.0	796.0		83.6	8.2	63.8	63.8	**8**	Pea cCu/Zn SOD
9	418.0	553.0	418.0	328.0	317.0	374.0	661.0	18.6		8.2	61.8	63.8	**9**	Tobacco cCu/Zn SOD
10	451.0	1000.0	569.0	434.0	1000.0	754.0	195.0	569.0	1000.0		14.9	14.2	**10**	Arabidopsis pCu/Zn SOD
11	456.0	430.0	438.0	291.0	321.0	311.0	553.0	47.9	51.6	447.0		75.2	**11**	Pea pCu/Zn SOD
12	461.0	447.0	560.0	368.0	389.0	414.0	524.0	47.9	47.9	403.0	27.2		**12**	Tomato pCu/Zn SOD
	1	**2**	**3**	**4**	**5**	**6**	**7**	**8**	**9**	**10**	**11**	**12**		

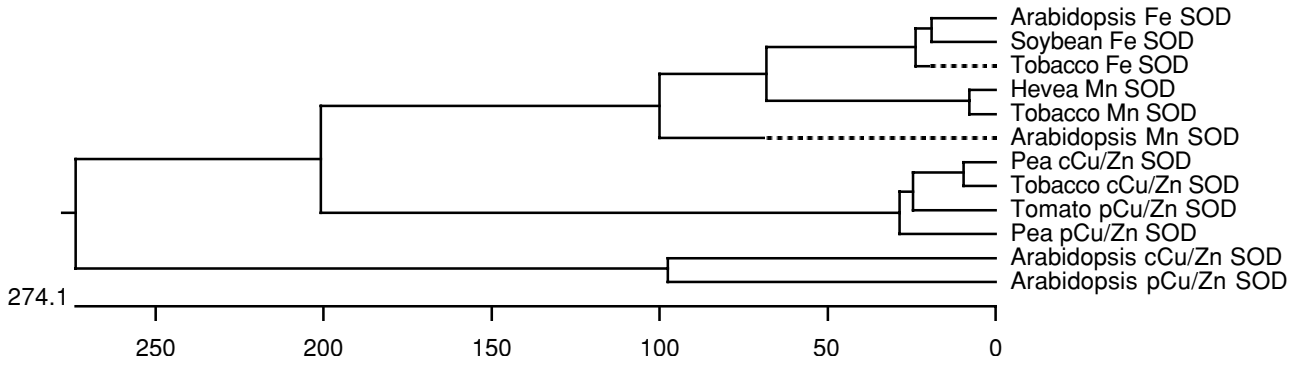

Figure 29. Stereo image of modeled *A. thaliana* Fe SOD protein. Violet, α-helices; cyan, β-strands; orange, residues at the active site; red, iron.

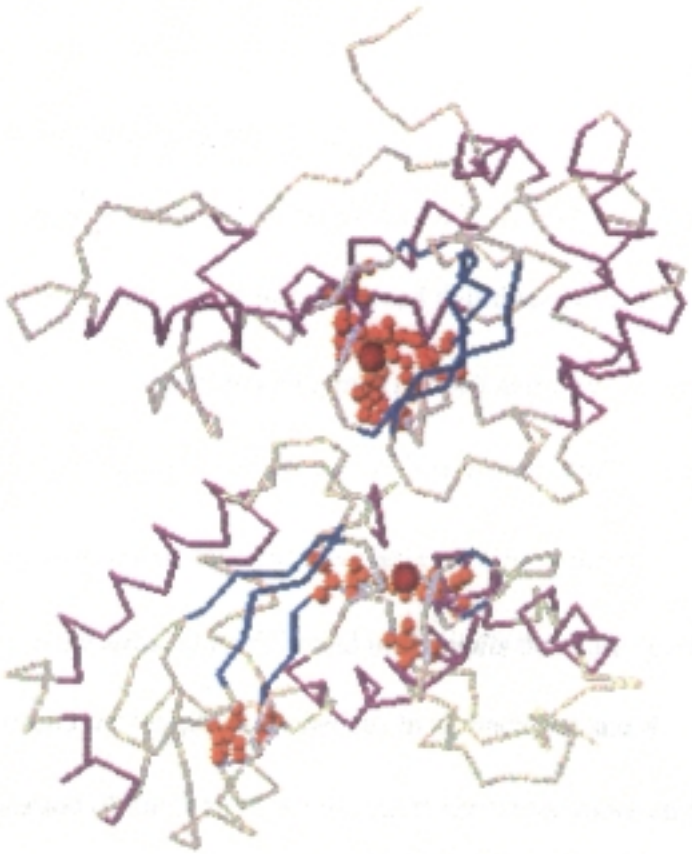

and Cu-Zn SOD proteins (Figure 30-32).

When the secondary structure of the modeled Fe SOD protein was compared with bacterial Fe SODs (Figure 30), it was observed that three β-strands forming a β-pleated sheet were present in two bacterial enzymes (*E. coli* and *Mycobacterium tuberculosis*) as well as the *A. thaliana* protein. There are no β-sheets present in *P. ovalis*. *E. coli* and *Mycobacterium tuberculosis* proteins have ten α-helices whereas in *A. thaliana* the number of helices are reduced to eight and in *P. ovalis* there are seven helices (Figure 30 A-D). Location and the length of the helices in all bacterial and *A. thaliana* protein varies whereas the location of the β-strands forming β-sheets are more conserved.

When the secondary structure of *A. thaliana* Fe SOD is compared with the Mn SOD structures from human, fish, and bacterial species (Figure 31), differences in the length of helices were observed. Mn SODs have 10-15 α-helices, and these helices are much longer than in the Fe SODs. The lengths and locations of β-strands forming the β-sheets are found to be conserved between Fe and Mn SODs (Figure 31 A-D).

The structure of Cu-Zn SODs from human, spinach, and yeast were compared to modeled *A. thaliana* Fe SOD (Figure 32). Cu-Zn SODs showed a different structure from that of Fe and Mn SOD. There are no α-helices present in Cu-Zn SOD, whereas 6-13 β-strands forming antiparallel β-sheets are in the structure. Cu-Zn SODs show a great dissimilarity to both Fe and Mn SODs (Figure 32 A-D).

Figure 30. Comparison of the secondary structure of modeled *A. thaliana* Fe SOD to known bacterial Fe SODs. A. *A. thaliana* (modeled), B. *E. coli* (PDBid, 1isa), C. *P. ovalis* (PDBid, 3sdp)D. *Mycobacterium tuberculosis* (PDBid, 1ids). H: α-Helicies, β: β-turns, ∇: Residues associated with the active center, γ: γ-turns

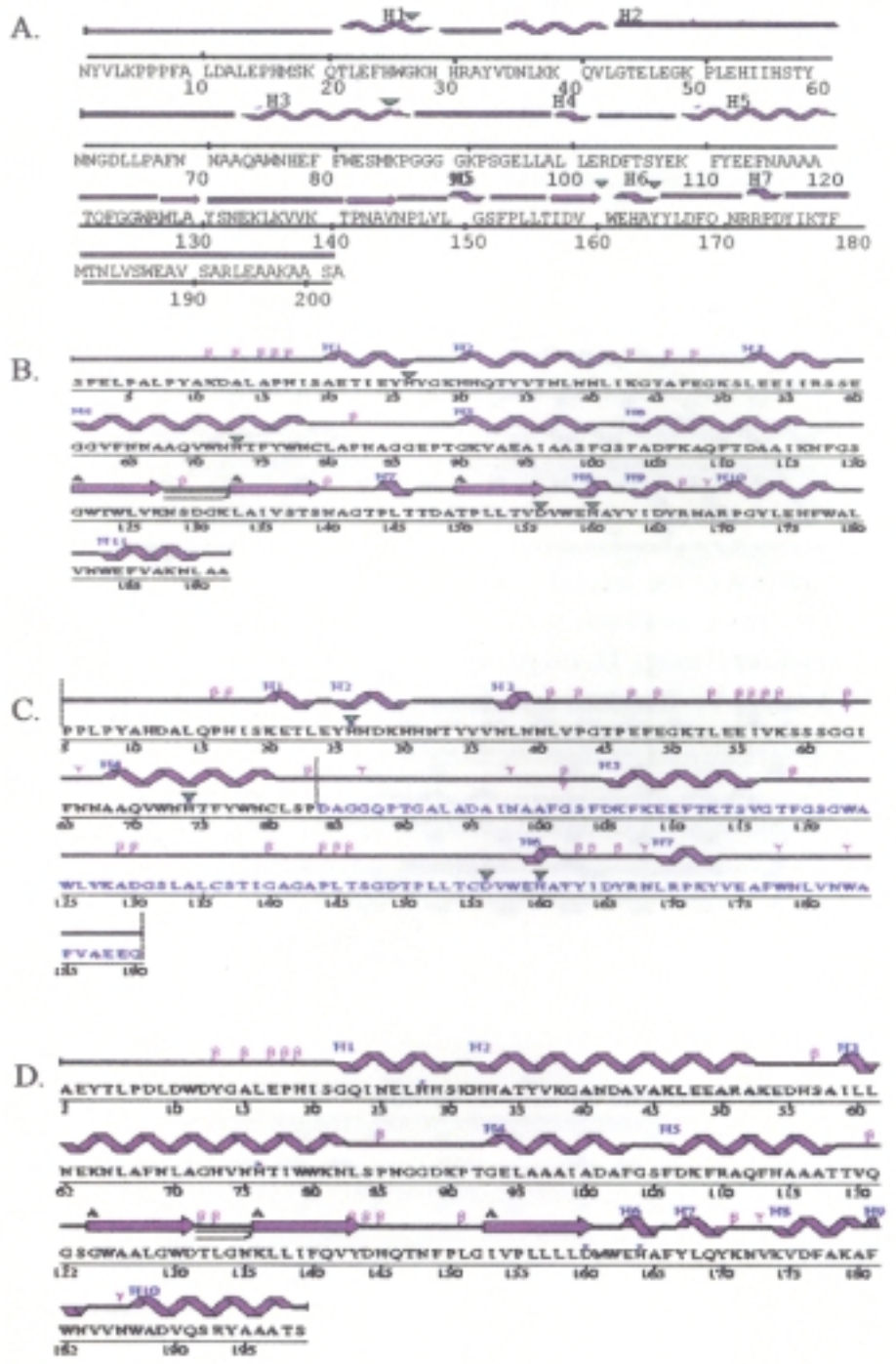
A.
B.
C.
D.

Figure 31. Comparison of the secondary structure of modeled *A. thaliana* Fe SOD to known Mn SODs. A. *A. thaliana* (modeled), B *Homo sapiens* (PDBid, 1ap5), C. *Thermus thermophilus* (1mng), D. *Propionibacterium freudemreichii* (PDBid, 1ar4). H: α-Helicies, β: β-turns, ∇: Residues associated with the active center, γ: γ-turns

A.

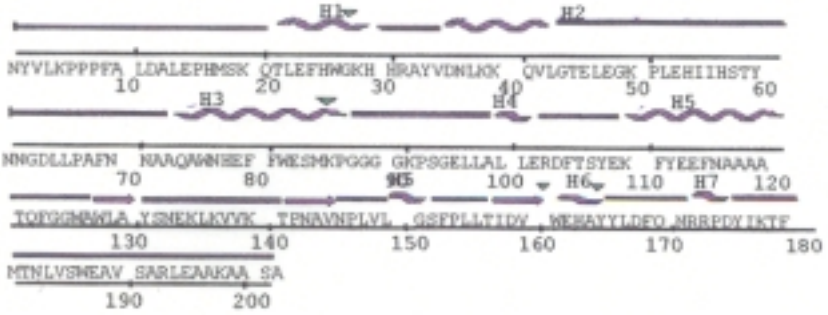

B.

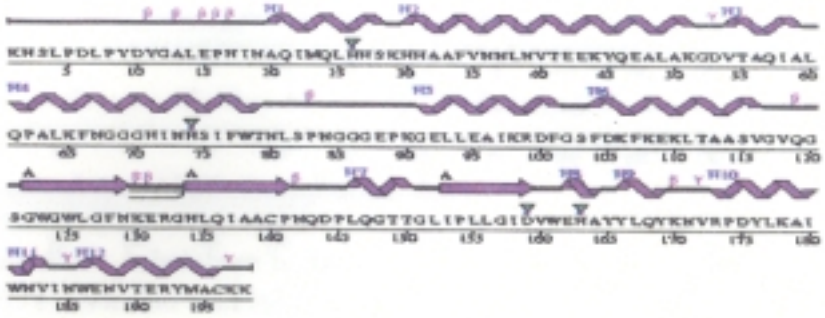

C.

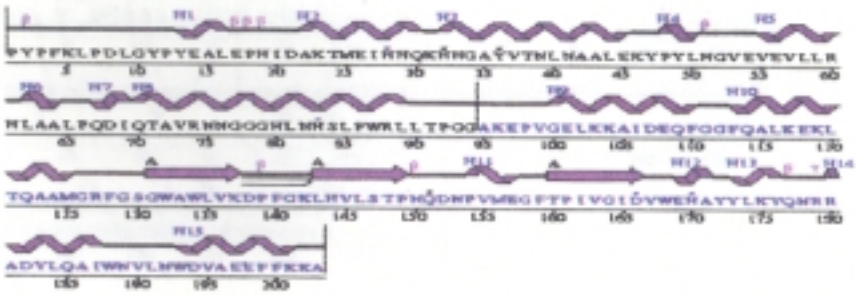

D.

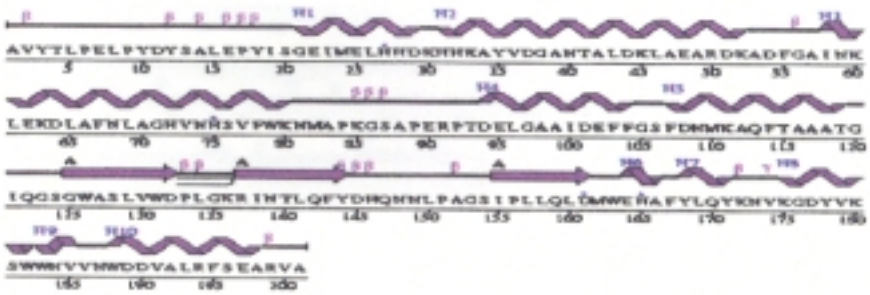

Figure 32. Comparison of the secondary structure of modeled *A. thaliana* Fe SOD to known Cu-Zn SODs. A. *A. thaliana* (modeled), B *Spinace oleracea* (PDBid, 1srd), C. *Homo sapiens* (PDBid, 1azv), D. *Saccharomyces cerevisiae* (PDBid, 1sda). H: α-Helicies, β: β-turns, ∇: Residues associated with the active center, γ: γ-turns

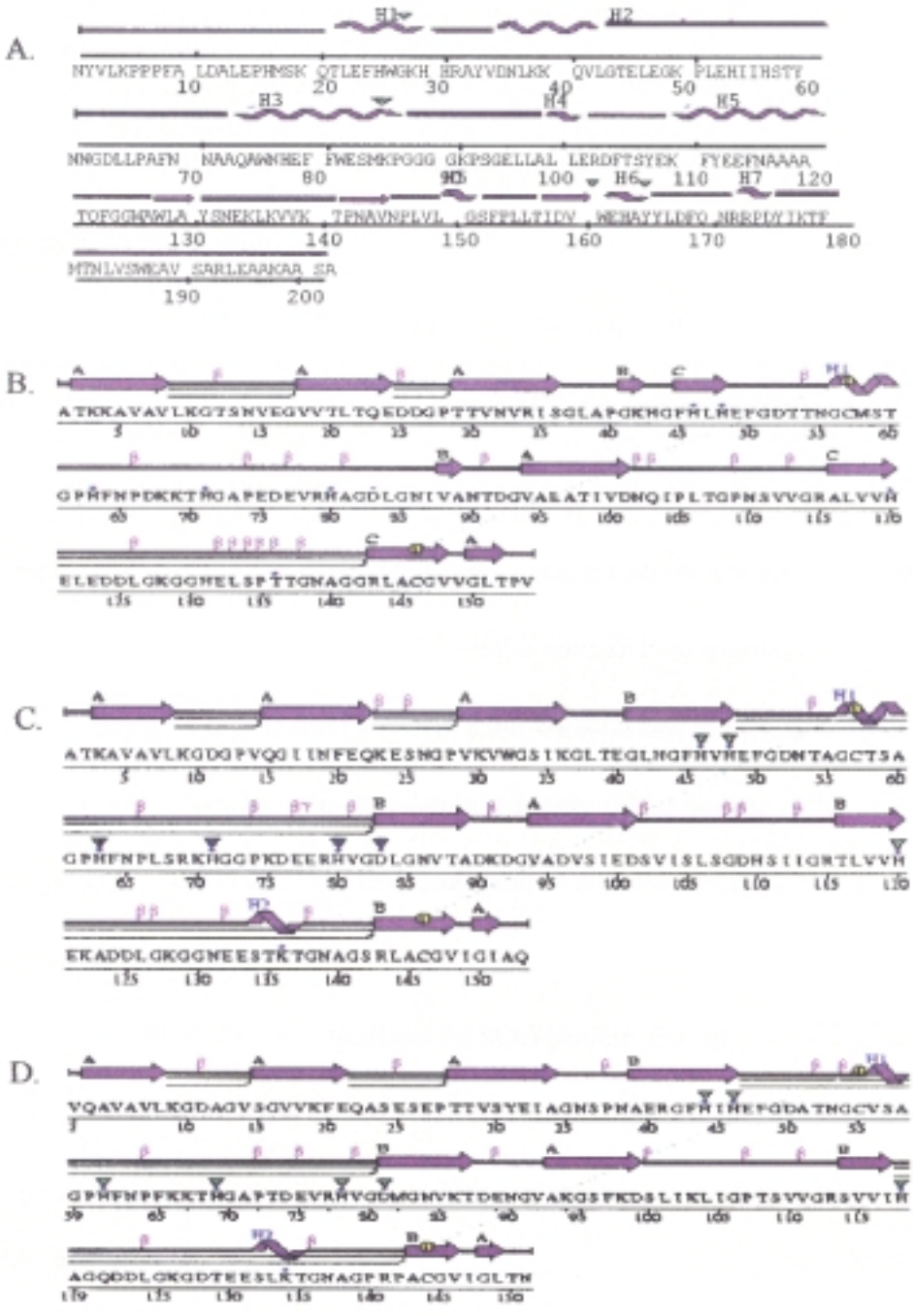
A.
B.
C.
D.

According to the novel hierarchical CATH classification system, which clusters proteins at four major levels, class(C), architecture(A), topology(T) and homologous superfamily (H), the secondary structure of *A. thaliana* Fe SOD is classified as Alpha Beta. Class, derived from secondary structure content, is assigned for more than 90 % of protein structures automatically. Proteins that have both alpha helical and β-sheet regions are classified as Alpha Beta category. Proteins in the Alpha Beta category have a cutoff of 15%≤%alpha≤55% and 10%≤beta≤45% for secondary structure composition. All Fe and Mn SODs whose three-dimensional structures have been classified in CATH have been catalogued in the Alpha Beta class, whereas all the Cu-Zn SODs, have been catalogued in the Mainly Beta class. When the secondary structure of *A. thaliana* Fe SOD was compared to Mn and Fe SODs from bacteria and plants, it is observed that the sequence at the active center of the protein is highly conserved, as is the secondary structure. The position and the structural roles of structure-essential residues are maintained the same (Figure 29).

At the active site of *A. thaliana* Fe SOD protein there are three histidine (H26, H73, H160) residue and one aspartic acid (D156) residue with an Fe atom non-covalently attached to these residues (Figure 29). This structure is conserved in all Mn and Fe SODs, whereas in Cu-Zn SODs there are eight amino acids associated with the metals at the active site. Four histidine residues interact with the Zn atom, whereas three histidine and an aspartic acid interact with the Cu atom.

When the three-dimensional structures of Fe and Mn SODs were aligned together, it was observed that the structures that are conserved in SODs are also highly conserved in the modeled *A. thaliana* Fe SOD protein (Figure 33), whereas greater differences in the three-dimensional structures of Cu-Zn SODs and the modeled *A. thaliana* Fe SOD were observed.

Figure 33. Comparison of the three dimensional structures of modeled *A. thaliana* Fe SOD with the SODs with known three dimensional structures. A. *A. thaliana* (modeled), B. *Homo sapiens* (1azv) C. *Spinace oleracea* (1srd).

A.

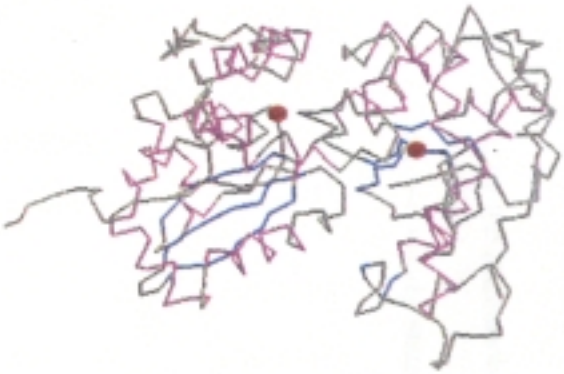

B.

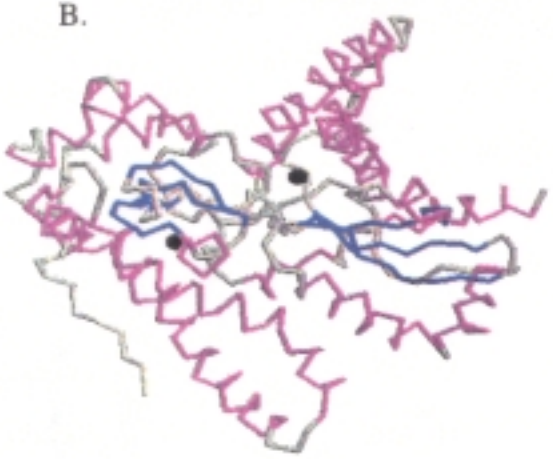

C.

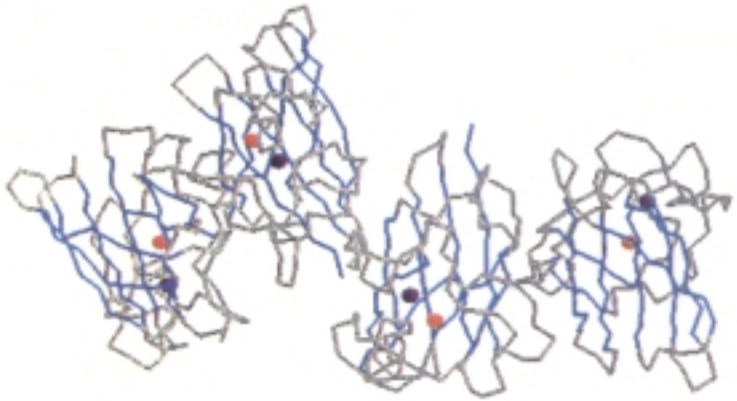

Chapter IV

Discussion

Changes in superoxide dismutase (SOD) enzyme activity and protein levels that occur in response to a chloroplast-located oxidative stress caused by methyl viologen and 3-(3,4-dichlorophenyl)-1,1'-dimethylurea (DCMU) are reported. Two concentrations of methyl viologen, which causes formation of superoxide radical (O_2^-) at the site of photosystem I (PS I) (Dodge, 1994), were used. In *A. thaliana*, $2x10^{-5}$ M methyl viologen causes the lowest visible injury (R. Alscher, unpublished data). In our experiments with *A. thalina* one concentration of methyl viologen that causes visible injury ($5x10^{-5}$ M) and a second concentration does not cause visible injury ($1x10^{-6}$ M) were used. DCMU inhibits linear photosynthetic electron transport and may reduce the generation of O_2^- radicals from the photosynthetic electron transport chain (Asada et al.1974). DCMU ($1x10^{-5}$ M) causes a decrease in SOD mRNA levels in *N. tabacum* (Tsang et al. 1991) and this concentration was used in our experiments. In this report, the relationships between oxidative stress and SODs at the protein and enzyme levels were determined by the immunoblot and activity gel electrophoresis analyses. Although we did not measure steady-state mRNA levels for the SODs in our experiments, comparisions at the transcriptional, translational, and post-translational levels were made by comparing the mRNA data from Tsang et al. (1991) with our data for protein and enzyme levels.

1. Analysis of SOD Genes in *A. thaliana*

Multiple SOD genes have been identified in *A. thaliana*. Three Cu-Zn SODs, two Fe SODs, and one Mn SOD genes are represented in the *A. thaliana* EST databank (http://genome-www2.stanford.edu/cgi-bin/AtDB/nph-blast2atdb). An additional Fe SOD gene has been reported by Kazusa DNA Research Institute, Chiba, Japan (http://www.kazusa.or.jp/arabi/). All of the seven SOD genes identify transcripts in RNA blots, indicating that they are expressed (Kliebenstein et al. 1998). Six SOD genes represented in EST databank including only two of the three Fe SOD genes. ESTs have been identify for the other four genes. Additional SODs, that are expressed in tissues that have not been used for the isolation of ESTs and/or stress responsive isoenzymes, may be present in *A. thaliana* genome.

Full-length mature *A. thaliana* Fe SOD sequences (GenBank M55910) were used to probe *A. thaliana* genomic DNA under high (65^0C) and low (55^0C) stringency conditions to determine the copy number of Fe SOD genes in *A. thaliana*. Under both conditions, our probe hybridized with only one fragment (Figure 16), showing that there is no cross hybridization of the full length M55910 Fe SOD gene with the other Fe SOD genes present in *A. thaliana* genome. Using Mn SOD, Cu-Zn SOD_{chl}, and Cu-Zn SOD_{cyt} ESTs as probes (J. Donahue and R. Alscher, unpublished data). No cross hybridization of the Fe SOD probe with the Mn and Cu-Zn SODs was detected.

2. Analysis of Multiple SOD Isoenzymes in *A. thaliana*

Five SOD activity bands were observed in *A. thaliana* plants. The slowest-migrating band has Mn SOD activity and is resistant to both SOD inhibitors, KCN and H_2O_2. The fastest migrating band has Cu-Zn SOD activity (Figure 10), and is sensitive to both inhibitors. Generally only one activity band was observed, occasionally, this band separated into two Cu-Zn activity bands (data not shown). Band separation was inconsistant due probably to experimental limitations since the growth conditions were as similar as possible for all experimental plants.

The third activity band had Fe SOD activity, and this is sensitive to H_2O_2 but not KCN. The Fe SOD band migrated slower than Cu-Zn SOD, but faster than Mn SOD activity band. Stress treatments caused the appearance of a second and a third (Figure 28 & 29) Fe SOD band, suggesting that stress-induced expression or activation of the enzyme may occur.

The presence of Cu-Zn and Mn SODs in *A. thaliana* as, in all plants, is well established (Bowler et al. 1991; Foyer and Mullineaux 1994), but the presence of Fe SOD had been controversial. Ormrod et al. (1995) reported that *A. thaliana* has only Cu-Zn and Mn SODs, but no Fe SOD, whereas Pan and Yau (1992) and Kleibenstein et al. (1998) observed Fe SOD activity as well as Cu-Zn and Mn SOD activities in *A. thaliana*.

3. Effects of Oxidative Stress on SOD Populations

An increase in the amount of antioxidant enzyme activity has been reported previously in plants exposed to oxidative stresses such as drought (Mittler and Zilinskas, 1992; Smirnoff and Colomve, 1988; Tanaka et al. 1990), high light intensity (Gilham and Dodge, 1987), photodynamic herbicides such as methyl viologen (Donahue et al. 1997; Iturbe-Ormaetxe et al. 1998; Melhorn, 1990) and norflurazon (Thomas, et al. 1998; Thomsen et al. 1992;), or air pollutants such as ozone (Madamanchi et al.1992; Melhorn, 1990) and sulfur dioxide (Kenyon and Duke, 1985). Methyl viologen is known to enhance O_2^- formation in plant cells (Dodge, 1994). Although the mechanism is not known, it has been suggested that increased formation of O_2^- may be the main cause for this increased SOD activity.

3.1. Effects of Oxidative Stress on Fe SOD Enzyme and Protein:

In our experimental system, a chloroplast-located stress caused an increase in Fe SOD enzyme activity, which is a chloroplast-located enzyme (Kliebenstein, et al. 1998). Both concentrations of methyl viologen ($5x10^{-5}$ M and $1x10^{-6}$ M) caused about a 75% increase in Fe SOD activity (Figure 18). Increased activity was observed immediately after the stress treatment and remained the same over a 41-hour time course. When the levels of protein were measured an increase in the amount of Fe SOD protein was observed 5 hours after the treatments, but after 17 hours the amount of protein increased in non-stressed controls as well (Figure 18). Therefore the increases observed in the level

of Fe SOD protein may not be a result of oxidative stress treatments. No correlation could be made between Fe SOD protein levels and enzyme activity after stress treatment.

In addition to the observed increase in Fe SOD activity, two novel Fe SOD activity bands were observed in stress-treated plants (Figure 19). This result suggests that in *A. thaliana* there is a constitutively-expressed, but stress-responsive Fe SOD isoform (Fe SOD_1) as well as two stress-induced Fe SOD isoforms (Fe SOD_2 and Fe SOD_3).

Iturbe-Ormaetxe et al. (1998) measured the effects of 100 μM methyl viologen on SOD enzyme activities in pea plants. The authors observed that this caused an increase in the amount of total Cu-Zn SOD activity and a decrease in the amount of Fe SOD activity. The authors suggested that Fe SOD is being inhibited by methyl viologen stress, but Cu-Zn SOD is not. This finding contrast with our results may be a result of the differences among the concentrations of methyl viologen that were used as well as the sensitivity of the plant species used in our experiments. Pea plants that were used by Iturbe-Ormaetxe et al. (1998) were treated with $1x10^{-4}$ M methyl viologen. This is twice the highest concentration that was used in our experiments. This high concentration may result in O_2^- leaking into the cytosol. H_2O_2 formed as a result of high SOD activity in the chloroplast may inhibit chloroplastic SODs, Fe and Cu-Zn_{chl} SODs, while O_2^- radicals leaked as a result of chloroplast breakage may caused an increase in cytosolic Cu-Zn SOD

activity. Another possibility is that increased damage to chloroplasts may generate other signals thay may induce the activation of Cu-Zn SODs in the cell.

The effects of methyl viologen on SOD populations in pea plants have been investigated (Donahue et al. 1997; Iturbe-Ormaetxe et al. 1998). Iturbe-Ormaetxe et al. (1998) used leaves from 30-day-old pea plants. Although higher total SOD activity was observed in younger leaves, leaf age did not cause a significant difference in response to oxidative stress (Donahue et al. 1997). Donahue et al. (1997) did not observe an increase in the amount of Cu-Zn SOD activity, but an increase in the amount of mRNA levels and a correlation between higher mRNA levels and resistance to oxidative stress was also observed. Donahue et al. (1997) showed that age may play a crucial role in the amount of SOD activity measured in plants. The difference observed in the response of Cu-Zn SODs in peas after the treatment with the same concentration of methyl viologen may be due to the difference in the age of plants. Young leaves may have higher basal SOD activity compared to old ones and this higher level may be enough for the young leaves to cope with the methyl viologen stress.

Donahue et al. (1997) also observed the appearance of second and third Fe SOD activity bands in native gels following treatment of peas with methyl viologen (J. Donahue, Personal communication). However, analogous bands have not been observed on anti-Fe SOD immunoblots. The antibody used in our experiments was raised against Fe SOD_1 protein. This indicated that either Fe SOD_2 and Fe SOD_3 proteins do not cross-

react with anti-Fe SOD_1, or alternatively, that all these proteins migrate to the same location in 15% SDS polyacrylamide gels.

Tobacco responses of SODs to methyl viologen or a DCMU stress at the mRNA level have been reported by Tsang et al. (1991) showed that $5x10^{-5}$ M methyl viologen caused a 40-fold increase in the amount of Fe SOD transcript. This increase was light dependent. The same concentration ($5x10^{-5}$ M) also caused an increase in the activity of Fe SOD mRNA level in our experiment with *A. thaliana*. However, we observed no increase in the amount of Fe SOD protein. Therefore, we may conclude that the observed increases in level of Fe SOD activity may be a result of enzyme rather than gene activation in response to methyl viologen treatment.

Generation of O_2^- results from electron leakage from PS I and/or ferredoxin. If electron transfer from photosystem II (PS II) is blocked, then a reduction in O_2^- formation would be expected. DCMU is a reagent that prevents reoxidation of QA (the primary electron-accepting quinone) in the PSII reaction center. Asada et al. (1974) reported that DCMU reduces the formation of O_2^- radicals from the photosynthetic electron transport chain.

In our experimental system, when *A. thaliana* were treated with $1x10^{-5}$ M DCMU, no significant change in the amount of activity was observed for any SODs, but the appearance of two novel Fe SOD bands was similar to methyl viologen-treated plants (Figure 18 & 19). One explanation for this result is that DCMU caused oxidative stress

in *A. thaliana* by increasing O_2^- formation. On the other hand, it may be possible that when the electron transport chain is disrupted, even if the formation of O_2^- is not affected, the antioxidant enzyme population is altered. As a result of disruption of the electron transport chain a signal, other than O_2^- radicals, may cause activation. When tobacco leaf discs in the dark for 3 days with or without DCMU were exposed to light, a decrease in the amount of Fe SOD transcript was observed for the DCMU-treated group, indicating that the effects of that the electron transport chain modification may be at the gene level (Tsang et al.1991). In our experimental system, the effects of $1x10^{-5}$ M DCMU were measured at the protein level and no changes as a result of DCMU treatment were observed.

3.2. Effects of Oxidative Stress on Mn SOD Enzyme and Protein:

A. thaliana mitochondrial Mn SOD enzyme responded to oxidative stress with an increase in activity after methyl viologen treatment (Figure 30). The increase observed after the treatment was 150-180% of initial Mn SOD activity. Methyl viologen $1x10^{-6}$ M -treated group responded with about 150% increase at the level of protein. However, this increase in the amount of protein was not observed in $5x10^{-5}$ M methyl viologen-treated group (Figure 20). This result was interesting because Mn SOD is a mitochondrial enzyme whereas methyl viologen is a chloroplast-specific stress. Because O_2^- cannot cross membranes, the observed Mn SOD response was unexpected. Even if damaged plastid membranes leaked O_2^-, O_2^- would still have to cross mitochondrial membranes in

order to react with Mn SODs. Therefore this unexpected response raises the question of whether the site of action for the methyl viologen is exclusively in the chloroplast or does it effect the mitochondria as well.

Alternatively, there may be coordinate regulation among antioxidant components of different subcellular compartments. Since O_2^- cannot cross membranes, O_2^- itself cannot be the molecule responsible for this intercompartmental effect. However, the presence of O_2^- may induce formation of a signal molecule that can cross the membranes. This signal molecule may be responsible from this coordinate regulation present in different compartments of the cell. Mn and Fe SODs are the more ancient family of SODs, being present both in prokaryotes and in eukaryotes, whereas Cu-Zn SOD is almost exclusively a eukaryotic enzyme. Perhaps, the response observed in the SODs are controlled at the gene level. Both prokaryotic enzymes (Fe and Mn SODs) may respond to a common signal released from the chloroplast as a stress response, but eukaryotic Cu-Zn SOD gene may not respond to this signal.

Appearance of novel Cu-Zn SOD bands following oxidative stress in peas was observed by Donahue et al. (1997). These authors did not report a change in the amount of chloroplastic Cu-Zn SOD enzyme activity, but observed the appearance of novel Cu-Zn SOD bands accompanied by a decrease in steady state mRNA level of Cu-Zn SOD enzyme after the methyl viologen treatment. Although the changes at the enzyme and

mRNA levels did not correlate, correlations between increased resistance to oxidative stress and increased mRNA was reported.

In contrast to Fe SOD, Mn SOD does not respond to DCMU stress with an increase in activity. DCMU causes oxidative stress in the chloroplast. If an intercompartmental cross-communication exists, then an increase in the amount of Mn SOD activity after DCMU treatment would be expected. Therefore, it is likely that the site of action methyl viologen is not exclusively in the chlorplast. It caused formation of O_2^- in mitochondria as well as chloroplasts and and as a result increased activity, presumably in mitochondria. Another possibility is that a signaling molecule as a result of methyl viologen stress is causing activation of mitochondrial Mn SOD, but this signal is not generated by DCMU stress.

Effects of methyl viologen on non-photosynthetic systems have been investigated. Wright et al. (1997) expressed human Mn SOD in the mitochondria of insect cells (*Spodoptera fungiparda* Sf-9). These cells were treated with the intracellular superoxide generators, methyl viologen ($3x10^{-4}$, $5x10^{-5}$, $1x10^{-5}$, and $1x10^{-6}$ M) and menadione ($1x10^{-4}$, $1x10^{-5}$, $1x10^{-6}$, and $1x10^{-7}$ M). While menadione did not affect this system, methyl viologen caused a significant decrease in the Mn SOD activities, accompanied by inhibition of mitochondrial processing of precursor Mn SOD.

The ability of Fe SODs to complement the function of Mn SOD has been investigated in microorganisms. Balzan et al. (1995) expressed an *E. coli* Fe SOD gene in

Mn SOD-deficient *S. cerevisiae* both with and without a mitochondrial targeting sequence. Each Fe SOD form was enzymatically-active in the mitochondria and cytosol of yeast cells. However, only the enzyme that was expressed in mitochondria provided protection against oxidative stress, whereas when the Fe SOD was expressed in the cytosol cells suffered from significant growth inhibition even though the enzyme was active, because the Fe SOD enzyme was able to complement deficient Mn SOD enzyme activity in the mitochondrion, Balzan et al. (1995) concluded that although structural differences exist, the functional capacities of Fe and Mn SODs are equivalent. However, physiological conditions in the cytosol may not be optimum for Fe SOD activity. Therefore, subcellular localization of SODs may have a significance in activity.

Significance of location of SODs within the organalle was investigated in *N. tabacum* plants transformed with an *A. thaliana* Fe SOD gene coupled to the chloroplast targeting sequence from peas (Van Camp et al. 1996). Fe SOD expressed in the chloroplast provided protection against methyl viologen-induced ion leakage in the plasmalemma and methyl viologen-induced inactivation of PSI in the chloroplasts (Van Camp et al. 1996). Mn SOD targeted to and expressed in chloroplasts of *N. tabacum* plants provided protection against methyl viologen-induced ion leakage in the plasmalemma; however, it did not provide protection against methyl viologen-induced inactivation of PSII (Slooten et al. 1995). Van Camp et al. (1996) inferred that the foreign Mn SOD was more soluble than Fe SOD and probably is located in the stroma of

the transformed plants. Fe SOD, on the other hand, is less soluble and may have some association with the stromal membranes, most likely the PSI reaction center, providing the means to scavenge O_2^- where they are formed (Van Camp et al.1996).

DCMU treatment did not cause any significant changes either in the activity or in the amount of protein of Mn SOD or Fe SOD_1, but Fe SOD_2 and Fe SOD_3 responded with increased activity. Appearance of these novel SODs probably result from gene activation. Results obtained from the responses of Fe SOD_1, Fe SOD_2, and Fe SOD_3 suggest that responses of SODs to oxidative stress is controlled both at the enzyme and gene levels.

Tobacco Mn SOD responds to methyl viologen and DCMU stress at the mRNA level (Tsang et al. 1991). These data show that $5x10^{-5}$ M methyl viologen caused 30-fold increases in the amount of Mn transcripts. This increase was light dependent. In our experiments, the same methyl viologen concentration ($5x10^{-5}$ M) in caused an increase in Mn SOD enzyme activity accompanied by with a slight increase in the amount of enzyme protein. This correlation between mRNA and protein level and the enzyme activity may indicate that the response of Mn SODs to oxidative stress may be at the gene level, expressed as increases in transcript abundance. However, the increase in the level of protein was very minor. Therefore, we may conclude that similar to Fe SOD there is no correlation among the increases in transcript abundance, protein levels and enzyme activities of Mn SOD caused by oxidative stress.

3.3. Effects of Oxidative Stress on Cu-Zn SOD Enzyme and Protein:

In contrast to the activity of Mn and Fe SODs, no significant change in the amount of Cu-Zn SOD proteins or enzyme activity was observed in methyl viologen- or DCMU-treated plants (Figure 21). Even though methyl viologen is a chloroplast-localized stress, chloroplastic Cu-Zn SOD did not respond to the imposed stress. This result raises the question of why there are two isoforms of SODs--Fe and Cu-Zn SODs--in the chloroplast and if there is a distinction between the roles of Fe and Cu-Zn SODs in the chloroplast.

Kurepa et al. (1997) investigated the specific functions of chloroplastic Cu-Zn SOD and Fe SOD in chloroplasts of *Nicotiana tabacum*. Two-month-old plants were treated with $25x10^{-6}$, $0.5x10^{-6}$, $2.5x10^{-5}$, and $5x10^{-5}$ M methyl viologen. A decrease in the amount of Fe and chloroplastic Cu-Zn SOD transcripts was observed. When the concentration of methyl viologen was increased, the amount of transcript decreased for Fe and Cu-Zn SODs.

Similarly in peas, a decrease in the amount of chloroplastic Cu-Zn SOD mRNA level was reported after UV-B treatment (Strid, 1994). In *A. thaliana*, we did not observe a change either in the amount of total Cu-Zn SOD activity or in the amount of chloroplastic and cytosolic Cu-Zn SOD protein in response to oxidative stress. This may be a result of inactivation by H_2O_2, which is the end product of the dismutation reaction catalyzed by SODs. As a result of increased SOD activity, concentration of H_2O_2 in the

chloroplast increases and this may cause the inactivation of Cu-Zn SOD enzyme. If this is the case, then Fe SOD may be a more effective protectant against methyl viologen-mediated oxidative stress. Our findings--an increase in the amount of Fe SOD activity and the appearance of newly formed Fe SODs, combined with the results gathered from the responses of Cu-Zn SODs--might suggest that Fe SOD is the better methyl viologen protectant in the plant chloroplast. Chloroplast is a prokaryotic organelle, therefore prokaryotic enzyme Fe SOD may have adapted better to the physiological conditions in this organelle.

Mammalian extracellular SOD (EC-SOD) is a glycoprotein located in the interstitial matrix of tissues and the glycocalyx of cell surfaces, anchored to heparan sulfate proteoglycans secreted by a few distinct cell types. Carlsson et al. (1995) created null mutant mice for EC SOD. Up to 14 month age, these mutant mice developed normally and were healthy and did not show any abnormalities in other SOD isozymes or other antioxidant enzymes, but when exposed to high O_2 these mice showed a significant decrease in survival time. This suggests that under normal physiological conditions, other antioxidant systems may substitute for the loss of EC-SOD, but under oxidative stress conditions other SODs cannot provide adequate protection. Behavior of plant SODs after depleting one of the SOD isoforms has not been addressed. Therefore, investigating the effects of Fe SOD and Cu-Zn SOD separately may help to determine why there is a need for two different SODs in the same cell compartment.

Microcompartmentalization of Cu-Zn SOD enzyme in the chloroplasts has been investigated using immuno-gold labeled antibodies (Ogawa et al. 1995). Most (73 %) of immunogold particles were found within 5 nm from the surface of the stromal faces of the thylakoid membranes, where PSI is located. In the thylakoidal system, there is also a thylakoid-bound ascorbate peroxidase as a part of thylakoid scavenging system indicating that H_2O_2 formed as a result of SOD activity is also scavenged at the site where it is formed. There is also a stromal scavenging system in the stroma for the removal of H_2O_2. This may indicate that different SOD isoenzymes may function in different microcompartments of the chloroplast. While Cu-Zn SOD is membrane-associated, Fe SOD may be the soluble stromal SOD form and these two isoforms may have different roles in the chloroplast.

3.4. Effect of Light on Oxidative Stress Responses

Effects of light and methyl viologen on SOD activities were also measured in $5x10^{-5}$ M methyl viologen-treated *A. thaliana*. Methyl viologen-mediated changes in the activities of Mn SOD and Fe SOD_1 were found to be light independent (Figure 22). Appearance of novel Fe SOD_2 and Fe SOD_3 activities were observed in plants that were kept in either light or in the dark after the treatments. Tsang et al. (1991) showed that when tobacco plants are treated with $5x10^{-5}$ M methyl viologen, transcripts of Mn and Fe SOD_1 increase in light, but are unaffected in the dark. Methyl viologen causes oxidative stress at the site of PSI by causing the transfer of electrons to O_2 instead of ferredoxin in a

chain reaction in a light-dependent reaction. Therefore methyl viologen treatment causes light-dependent changes. In addition, the amount of transcript is about 30 fold higher in the plants that are kept in light, compared to those kept in the dark. Although no increase in Mn and Fe SOD transcript levels was reported by Tsang et al. (1991), we observed an increase in the activity of Mn SOD enzyme in the light. This suggests that increase may be a result of a post-translational control mechanism rather than being result of gene activation. Responses of Fe SOD_2 and Fe SOD_3 at mRNA level are yet to be examined.

4. Comparison of the Fe, Mn, and Cu-Zn SOD Sequences

When the sequences of the known plant SODs are compared, differences among Mn and Fe SODs and chloroplastic and cytosolic Cu-Zn SODs were found. Seventeen available Cu-Zn SOD sequences were aligned in order to compare the relationship of Cu-Zn SODs to one another (Figure 33). Chloroplastic plant Cu-Zn SODs have 77% similarity to one another and 61% similarity to cytosolic Cu-Zn SODs. Cytosolic Cu-Zn SODs have 85% similarity to one another. The similarity between chloroplastic and cytosolic Cu-Zn SODs is considerably lower compared to the similarity between chloroplastic to the other chloroplastic Cu-Zn SODs and cytosolic ones to the other cytosolic Cu-Zn SODs (Figure 24). This indicates that the separation of these two genes took place very early in the evolutionary stage. Theoretically the origin of chloroplastic SOD resulted from gene duplication of the cytosolic isoform (Bordo et al. 1994). The high similarity between these two proteins supports this theory. The ligand regions for

both cytosolic and chloroplastic Cu-Zn SODs are identical. These are His-44, His-46, His-61, and His-118 for Cu^{++}, the functional atom, and His-61, His-69, His-78, and Asp-81 for Zn^{++}, the structural atom. These patterns are conserved in all plant Cu-Zn SODs (Bordo et al. 1994).

When the Cu-Zn SOD sequences were compared with Mn and Fe SODs, about 10% similarity between Cu-Zn SODs and Mn and Fe SODs was observed (Figure 25). This indicates that Fe and Mn SODs are highly divergent from Cu-Zn SODs. However, Mn and Fe SODs have a higher similarity to each other. There is about 35% similarity between plant Fe and Mn SODs, whereas 65% similarity exists among plant Fe SODs themselves, and 77% similarity among plant Mn SODs (Figure 26 A). This shows that, although plant Fe and Mn SODs are highly similar to one another, these two enzymes are not products of the same genes. The residues at the ligand region of Mn SOD are His-26, His-81, His-179, and Asp-175. These aminoacids are identical for all plant Mn SODs as well as the bacterial enzymes. There is a high similarity between prokaryotic and plant Fe SODs, although the plant Fe SODs have a higher similarity to one another than to any of the prokaryotic Fe SODs. The similarity between plant and bacterial Fe SODs supports the endosymbiotic origin of plant Fe SODs. Although there is a high similarity between Fe and Mn SODs and the metal ligand regions of the two enzymes are identical, our DNA blot results show that there is no cross hybridization between Fe and Mn SODs in *A. thaliana* either at high or at low stringency conditions (J. Donahue and R.

Alscher, unpublished data). This indicates that the sequences of these two genes are diverged significantly from one another during evolution.

One class of prokaryotic SODs can use both Fe and Mn as the metal ligand according to the availability of the metal and are therefore classified as Fe/Mn SODs. When these sequences were aligned with the plant Fe and Mn SODs, it was observed that some of the Fe/Mn SODs have a higher similarity to plant Fe SODs, whereas others are more similar to plant Mn SODs. Indicating that the separation of Fe and Mn SODs may be through the evolution of different Fe/Mn SOD enzymes. Some of these enzymes, but not all, have a tryptophan residue at position 80, which provides the resistance to H_2O_2 in Mn SOD. Fe/Mn SODs that have this residue are likely the ones that gave raise to Mn SOD in evolution. The metal ligand regions for Fe and Mn SODs are identical in these enzymes as it is in all prokaryotic and plant Mn and Fe SODs.

All these data support the theory that Fe and Mn SODs are the ancestral forms and that these enzymes are closely related to one another. On the other hand data suggest that Cu-Zn SODs are not related to Fe and Mn SODs. The differences in the sequences as well as the metal ligands of the SODs suggest that Cu-Zn SODs did not evolve as a result of a simple gene duplication from Mn and Fe SODs. When the secondary structure of three different kind of SODs were compared, again high similarity between Mn and Fe SODs was observed, whereas Cu-Zn SOD is distinctly different both from Fe and Mn SODs (Figure 30-32).

In order to further investigate the evolutionary relationship among different classes of SODs, the three dimensional structure of *A. thaliana* Fe SOD protein was modeled using bacterial Fe SODs as a template. The resulting structure showed that plant Fe SODs are highly similar in structure to the bacterial Fe SODs as well as bacterial and eukaryotic Mn SODs. The active site of the protein is still formed from four positively-charged amino acids forming a funnel to attract the negatively-charged O_2^- anion to the active site of the molecule. No significant differences were observed between the structures of the Mn SODs and Fe SODs, leaving the question of why there was a need for such a change in the metal atom used as the prosthetic group in these SODs.

It is clear that the residues at and around the active site region are quite important for the proper function of SODs since the electrical guidance for the dismutation of O_2^- comes from these residues. Therefore this is the most conserved region of the enzyme. When the electrical charge on the active site region of the enzyme was changed by mutating the amino acids, an effect on the activity of the enzyme was observed (Getzoff et al. 1992; Zhou et al. 1997). An effect on catalytic efficiency was observed only if a positive charge was added around the active site (Zhou et al. 1997). In another report, Getzoff et al. (1992) showed that changing the positive charge of the enzyme alone is insufficient, since it may disrupt the structural integrity of the active-site. The position and the integrity of the active site are the main elements in the structure of SOD proteins.

The active site of modeled Fe SOD is similar to that of known Fe and Mn SODs, indicating that the modeled SOD has the characteristics of the Fe-Mn SOD family.

It has been concluded from crystallographic studies that the folds of Fe SODs and Cu-Zn SODs are unrelated (Stallings, et al. 1984). Other than a few exceptions, Fe SODs are dimeric proteins. Although Cu-Zn SODs also have a dimeric structure, Fe and Cu-Zn SODs dimerize differently as a result of folding differences. When the backbone positions of modeled Fe SOD and Mn SODs are compared, striking similarity between two molecules are obvious. The secondary structures of these molecules also are similar in that the positions of the helices and β-turns, as well as the strands are very similar.

5. Summary: Responses of *A. thaliana* Fe and Mn SODs to oxidative stress

In addition to the structural similarities, Fe and Mn SODs act similarly when exposed to oxidative stress caused by methyl viologen. This result may be because:

1. Although superoxide generated in a particular compartment can not cross membranes and cause direct damage to other compartments of the cell, the product of its dismutation can subsequently signal other compartments of the cell and trigger an activation mechanism for gene and/or enzyme activation.

2. Ancestral SODs--Mn and Fe SODs-- respond to chloroplast-located stress similarly with an increase in enzyme activity. It is not known whether this is mediated through gene activation.

3. Site of action for methyl viologen is not exclusively in the chloroplast.

4. All three SODs respond to stress caused by methyl viologen with an increased transcript abundance (Tsang et al. 1991). However, the post-translational activation is controlled differently for prokaryotic and eukaryotic originated SODs.

5. Comparison of primary, secondary, and tertiary structures of Fe, Mn and Cu-Zn SODs shows that Fe and Mn SODs are structrually homologous whereas Cu-Zn SOD is structurally unrelated to Mn and Fe SODs

Chapter V

Bibliography

Adam, A., Farkas, T., Somlyai, G., Hevesi, M., and Kiraly, Z. (1989) Consequence of O_2^- generation during a bacterially induced hypersensitive reaction in tobacco: deterioration of membrane lipids. Physiol. Mol. Plant. Pathol. 34:13-26.

Alscher, R. G and Hess, J. L. (eds.) (1993) Antioxidants in Higher Plants. CRC Press, Bocca Raton, FL.

Andrews, R. K., Blakeley, R. L. and Zerner, B. (1988) Nickel in proteins and enzymes. In: Sigel, H., (ed.) Metal Ions in Biological Systems vol. 23, pp. 165-284, Marcel Dekker, New York.

Asada, K. (1992) Ascorbate peroxidase--a hydrogen peroxide-scavenging enzyme in plants. Physiol. Plant. 85:235-241.

Asada, K. (1994) Production and action of active oxygen species in photosynthetic tissues. In: Foyer and Mullineaux, Causes of oxidative stress and amelioration of defense systems in plants pp. 78-99 CRC Press, Bocca Raton, FL.

Asada, K. and Kiso, K. (1973) Initiation of aerobic oxidation of sulfite by illuminated spinach chloroplasts. Eur. J. Biochem. 33:253-257.

Asada, K. and Takahashi, M. (1987) Production and scavenging of active oxygen in photosynthesis. In: Kyle, D. J. Osmond, C. B., and Arntzen, C. J., (eds.) Photoinhibition, Elsevier Science Publishers B. V., pp.227-287.

Asada, K., Takahashi, M., Tanaka, K., and Nagate, M. (1974) Assay and inhibitors of spinach superoxide dismutase. Agric. Biol. Chem. 38:471-473.

Asada, K., Urano., M, and Takahashi, M. (1973) Subcellular localization of superoxide dismutase in spinach leaves and preparation and properties of crystalline spinach superoxide dismutase. Eur. J. Biochem. 36:257-266.

Baldensperger, J. B., (1978) An iron containing superoxide dismutase from the chemo lithotrophic *Thiobacillus denitrificans* rt strain. Arch. Microbiol. 119:237-244.

Balzan, R., Bannister,W. H., and Hunter, G. (1995) *Escherichia coli* iron superoxide dismutase targeted to the mitochondria of yeast cells protects the cells against oxidative stress. Proc. Natl. Acad. Sci. USA 92:4219-4223

Bannister, W. H., Bannister, J. V., Barra, D., Bond, J., and Bossa, F. (1991) Evolutionary aspects of superoxide dismutase: The copper/zinc enzyme. Free Radical Res. Comms. 12-13:349-361.

Bannister, J. V. and Parker, M. W. (1985) The presence of copper/zinc superoxide dismutase in the bacteruim *Photobacterium leiognathi*. A likely case of gene transfer

from eukaryotes to prokaryotes. Proc. Natl. Acad. Sci. USA 82:149-152.

Barro, D., Schinina, M. E., Bossa, F., Puger. K., and Durosay, P. (1990) A tetrameric iron superoxide dismutase from the eucaryote *Tetrahymena pyridornis.* J. Biol. Chem. 265:17680-17687.

Baum, J. A., Chandlee, J. M., and Scandalios, J. G. (1983) Purification and partial characterization of a genetically defined superoxide dismutase (SOD-1) associated with maize chloroplasts. Plant Physiol. 73:31-35.

Beaman, N. L,. Scates, S. M., Moring, S. E., Deem, R., and Misra, H. P. (1983) Purification and properties of a unique superoxide dismutase from *Nocardia asteroised.* J. Biol. Chem., 258:91-96.

Bolwell, G. P. (1996) The origin of the oxidative burst in plants. Biochem. Soc. Trans. 24:438-442.

Bordo, D., Djinovic, K., and Bolognesi, M. (1994) Conserved patterns in the Cu-Zn superoxide dismutase family. J. Mol. Biol. 238:366-386.

Bowler, C., Alliotte, T., De Loose, M., Van Montagu, M., and Inze, D. (1989) The induction of manganese superoxide dismutase in response to stress in *Nicotiana plumbaginifolia*. EMBO J., 8:31-38.

Bowler, C., Slooten, L., Vandenbranden, S., De Rycke, R., Botterman, J., Sybesma, C., Van Montagu, M., and Inze, D. (1991) Manganese superoxide dismutase can reduce cellular damage mediated by oxygen radicals in transgenic plants. EMBO J., 10:1723-1732.

Bowler, C., Van Camp. W., Van Montague. M., and Inze, D. (1994) Superoxide dismutase in plants. Crit. Rev. Plant Sci. 13:199-218.

Bradford, M. M. (1976) A rapid and sensitive method for the quantitation of microgram quantities of protein utilizing the principle of protein-dye binding. Anal. Biochem. 72:248-254.

Bridges, S. and Salin, M. L. (1981) Distribution of iron-containing superoxide dismutase in vascular plants. Plant Physiol. 68:275-278.

Brisson, L. F., Tenhaken, R., and Lamb, C. (1994) Function of oxidative cross-linking of cell wall structural proteins in plant disease resistance. Plant Cell 6:1703-1712.

Bueno, P., Varela, J., Gimenez-Gallego, G., and del Rio, L. A. (1995) Peroxisomal copper, zinc superoxide dismutase. Plant Physiol. 108:1151-1160.

Burdon, R.H., O'Kane, D., Fadzillah, N., Gill, V., Boyd, P. A., and Finch, R. R. (1996)

Oxidative stress and responses in *Arabisopsis thaliana* and *Oryza sativa* subjected to chilling and salinity stress. Biochem. Soc. Trans. 24:469-472.

Cadenas, E. (1989) Biochemistry of oxygen toxicity. Annu. Rev. Biochem. 58:79-110.

Carlsson, L. M., Jonsson, J., Edlund, T., and Marklund, S. L. (1995) Mice lacking extracellular superoxide dismutase are more sensitive to hyperoxia. Proc. Natl. Acad. Sci. USA 92:6264-6268.

Chen, G. X. and Asada, K. (1989) Ascorbate peroxidase in tea leaves: Occurrence of two isozymes and their differences in enzymatic and molecular properties. Plant Cell Physiol. 30:987-998.

Clare, D. A., Rabinowitch, H. D., and Fridovich, I. (1984) Superoxide dismutase and chilling injury in *Chlorella elliposidea*. Arch. Biochem. Biophys. 231:158-163.

Crowell, D. N. and Amasino, R. M. (1991) Induction of specific mRNAs in cultured soybean cells during cytokinin or auxin starvation. Plant Physiol. 95:711-715

Cudd, A. and Fridovich, I. (1982) Electrostatic Interactions in the Reaction Mechanism of Bovine Erythrocyte Superoxide Dismutase. J. Biol. Chem. 257:11443-11447.

del Rio, L. A., Lyon, D. S., Olah, I., Glick, B., and Salin, M. L. (1983) Immunocytochemical evidence for a peroxisomal locallization of manganese superoxide dismutase in leaf protoplasts from a higher plant. Planta 158:216-224.

del Rio, L. A., Pastori, G. P., Palma, J. M., Sandalio, L. M., Corpas, F. J., Jimenez, A., Lopez-Huertas, E., and Hernandez, A. J. (1998) The activated oxygen role of peroxisomes in senescence. Plant. Physiol. 116:1195-2000.

del Rio, L. A., Sandalio, L. M., Palma, J. M., Bueno, P., and Corpas, F. J. (1992) Metabolism of oxygen radicals in peroxisomed and cellular implications. Free Rad. Biol. Med. 13:557-580.

Dhaunsi, G. S., Gulati, S., Singh, A. K., Orak, J. K, Asayama, K., and Singh, I. (1992) Demonstration of Cu-Zn superoxide dismutase in rat liver peroxisomes: biochemical and immunochemical evidence. J. Biol. Chem. 267:6870-6873.

Dixon, R. A., Harrison, M. J., and Lamb, C. J. (1994) Early events in the activation of plant defense responses. Ann. Rev. of Phytopathol. 32:479-501

Dodge, A., (1994) Herbicide action and effects on detoxification processes. *in* Foyer, C. H. and Mullinaux. P. M., (eds)(1994) Stress and Amelioration of Defense Systems in Plants. CRC, Boca Raton, FL, pp. 219-236.

Donahue, J., Okpodu, C. M, Cramer, C. L., Grabau, E. A., and Alscher, R. G. (1997)

Responses of Antioxidants to Paraquat in Pea Leaves. Plant Physiol. 113:249-257.

Doulis, A., Donahue, J. L., and Alscher, R. G. (1998) Differential responses to paraquat-induced oxidative injury in a pea (*Pisum sativum*) protoplast system. Physiol. Plant. 102:461-471.

Droillard, M. J. and Paulin, A. (1990) Isozymes of superoxide dismutase in mitochondria and peroxisomes isolated from petals of carnation (*Dianthus caryophyllus*) during senescence. Plant Physiol. 94:1187-1192.

Elstner, E. F. (1991) Mechanism of oxygen activation in different compartments of plant cells. In: Pell, E. J. and Steffen, K. L., (ed.) Active Oxygen/Oxidative Stress and Plant Metabolism, pp. 13-25 American Society of Plant Physiologists, Rockville, MD ISBN 0-943088-22-4.

Elstner, E. F. and Osswald, W. (1994) Mechanism of oxygen activation during plant stress. Proc. Royal. Soc. Edin. Section B 102:131-154.

Fadzilla, N. M., Finch, R. F., and Burdon, R. H. (1997) Salinity, oxidative stress and antioxidant responses in shoot cultures of rice. J. Exp. Bot. 48:325-331.

Foster, J. G. and Edwards, G. E. (1980) Localization of superoxide dismutase in leaves of C3 and C4 plants. Plant Cell Physiol. 21:895-906.

Foyer, C. H. and Halliwell, B. (1976) The presence of glutathione and glutathione reductase in chlorplast a proposed role in ascorbic acid metabolism. Planta 133:21-25.

Foyer, C. H. and Mullineaux, (eds.) (1994) Causes of oxidative stress and amelioration of defense systems in plants. CRC Press, Bocca Raton, FL.

Fridovich, I. (1986) Superoxide dismutases. *in*: Meister A. (eds) Advances In: Enzymology, vol 58, John Wiley and Sons, New York, pp 61-97.

Fridovich, I. (1989) Superoxide dismutases: An adaptation to a pragmatic gas. J. Biol. Chem. 264:7761-7764.

Fridovich, I. (1995) Superoxide radical and superoxide dismutases. Annu. Rev. Biochem. 64:97-112.

Getzoff, E. D., Cabelli, D. E., Fisher, C. L., Parge, H. E., Viezzoli, M. S., Banci, L., and Hallewell, R. A. (1992) Faster superoxide dismutase mutants designed by enhancing electrostatic guidance. Nature 358:347-351.

Gilham, D. J. and Dodge, A. D. (1987) Chloroplast superoxide and hydrogen peroxide scavenging sustems from opea leaves: Seasonal variation. Plant Sci. 50:105-109.

Groom, Q. J., Torres, M. A. Fordham-Skelton, A. P., Hammond-Kossack, K. E., Robinson, N. J., and Jones, J. D. G. (1996) *rboh*A, a rice homology of the mammalian *gp*91*phox* respiratory burst oxidase gene. Plant J.10:515-522.

Halliwell, B. (1987) Oxidative damage, lipid peroxidation and antioxidant protection in chloroplasts. Chem. Phys. Lipids 44, 327-340.

Hammond-Kossack, K. E. and Jones, J. D. G. (1996) Resistance gene-dependent plant defence responses. Plant Cell 8:1773-1791.

Hayakawa, T., Kanematsu, S., and Asada, K. (1985) Purification and characterization of thylakoid-bound Mn-superoxide dismutase in spinach chloroplasts. Planta 166:111-116.

Herbert, S. K., Samson, G., and Fork, D. C. (1992) Characterization of damage to photosystems I and II in a cyanobacterium lacking detectable iron superoxide dismutase activity. Proc.Natl. Acad. Sci. USA 89:8716-8720

Hernandez, J. A., Corpaz, F. J., Gomez, M., del Rio, L. A., and Sevilla, F. (1993) Salt-induced oxidative stress mediated by activated oxygen species in per leaf mitochondria. Physiol. Plant. 89:103-110.

Hernandez, J. A., Olmos, E., Corpaz, F. J., Sevilla, F., and del Rio, L. A. (1995) Salt-induced oxidative stress in chloroplasts of pea plants. Plant Sci. 105:151-167.

Hodgson, E. K. and Fridovich, I. (1973) Reversal of the superoxide dismutase reaction. Biochem. Biophys. Res. Commun. 54:279-274.

Huang, A. H. C., Trelease, R. N., and Moore, T. S. (1983) Plant Peroxisomes. Academic Press, New York, NY.

Iturbe-Ormaetxe, I., Escuredo, P. R., Arrese-Igor, C., and Becana, M. (1998) Oxidative damage in pea plants exposed to water deficit or paraquat. Plant Physiol. 116:173-181.

Jackson, C., Dench, J., Moore, A. L., Halliwell, B., Foyer, C. H., and Hal., D. O. (1978) Subcellular localisation and identification of superoxide dismutase in the leaves of higher plants. Eur. J. Biochem. 91:339-344.

Kanematsu, S. and Asada, K., (1978) Superoxide dismutase from an anaerobic photosynthetic bacterium *Chromatium vinosum*. Arch. Biochem. Biophys. 185:473-482.

Kanematsu, S. and Asada, K. (1979) Ferric and manganic superoxide dismutases in *Euglena gracilis*. Arch. Biochem. Biophy. 195:535-545.

Kanematsu, S. and Asada, K. (1990) Characteristic amino acid sequences of chloroplast and cytosol isozymes of Cu-Zn superoxide dismutase in spinach, rice and horsetail. Plant Cell Physiol 31:99-112.

Kangasjarvi, I., Talvinen, J., Utriainen, M., and Karjalainen, R. (1994) Plant defense systems induced by ozone. Plant Cell Environ. 17:783-794.

Kenyon, W. H. and Duke, S. D. (1985) Effects of acifluorfen on endogenous antioxidants and protective enzymes in cucumber. Plant Physiol. 79:862-866.

Kim, E. J., Kim, H. P., Hah, Y. C., and Roe, J. H. (1996) Differential expression of superoxide dismutases containing Ni and Fe/Zn in *Streptomyces coelicolor.* Eur. J. Biochem. 241:178-185.

Kirby, T. W., Lancaster, J. R. Jr. and Fridovich, I. (1981) Isolation and characterization of the iron-containing superoxide dismutases of *Methanobacterium bryantii*. Arch. Biochem. Biophys. 210:140-148.

Kliebenstein, D., Monde, R. A., and Last, R. L. (1998) Superoxide Dismutase in Arabidopsis: An Eclectic Enzyme Family with Disparate Regulation and Protein Localization. Plant Physiol. 118:637-650.

Kono, Y. and Fridovich, I. (1983) Inhibition and reactivation of manganase catalase implications for valence changes at the active site manganase J. Biol. Chem, 258:13646-13648.

Kuo, C.F., Mashino, T., and Fridovich, I. (1987) α-β-dihydroyisovalerate dehydratase a superoxide sensitive enzyme J. Biol. Chem. 262:4724-4727.

Kurepa, J., Herouart, D., Van Montagu, M., and Inze, D. (1997) Differential Experession of Cu-Zn- and Fe-Superoxide Dismutase Genes of Tobacco during Development, Oxidative Stress, and Hormonal Treatments. Plant Cell Physiol. 38:463-470.

Kwiatowski, J. and Kaniuga, Z. (1986) Isolation and characterization of cytosolic and chloroplastic isozymes of Cu-Zn superoxide dismutase from tomato leaves and their relationships to other Cu-Zn superoxide dismutases. Biochim. Biophys. Acta 874:99-115.

Laemmli, U. K. (1970) Cleavage of the structural proteins during the assembly of the head of the bacteriophage T4. Nature 227:680-685.

Leunissen, J. A. M. and de Jong, W. W. (1986) Copper/zinc superoxide dismutase: How likely is gene transfer from ponyfish to *Photobacter leiognathi* ? J. Mol. Evol. 23:250-258.

Lopez-Huertas, E., Sandalio, L. M., and del Rio, L. A. (1996) Superoxide generation in plant peroxisomal membranes: Characterization of redox proteins involved. Biochem. Soc. Trans. 24:195S.

Madamanchi, N. R., Anderson, J. V., Alscher, R. G., and Cramer, C. L., (1992) Purification of multiple forms of glutathione reductase from pea (*Pisum sativum* L.) seedlings and enzyme levels in ozone-fumigated pea leaves. Plant Physiol. 100:132-145.

Madamanchi, N. R. and Alscher, R. G. (1991) Metabolic bases for differences in sensitivity of two pea cultivars to sulfur dioxide. Plant Physiol. 97:88-93.

Madamanchi, N. R., Donahue, J. L., Cramer, C., Alscher, R. G., and Pederson, K. (1994) Differential response of Cu,Zn superoxide dismutases in two pea cultivars during short-term exposure to sulfur dioxide. Plant Mol. Biol. 26:95-103.

Marino, M., Galvano, M., Cambria, A., Polticelli, F., and Desideri, A. (1995) Modeling the three-dimensional structure and the electrostatic potential field of two Cu,Zn superoxide dismutase variants from tomato leaves. Protein Eng. 8:551-556.

Martin, J. P. and Fridovich, I. (1981) Evidence for a natural gene transfer from the ponyfish to its bioluminescent bacterial symbiont *Photobacter leiognathi*: The close relationship between bacteriocuprein and the copper-zinc superoxide dismutase of teleost fishes. J. Biol. Chem., 256:6080-6089.

McCord, J. M. and Fridovich, I. (1969) Superoxide dismutase: An enzymatic function for erythrocuprein (Hemocuprein). J. Biol. Chem. 22:6049-6055.

Mehler, A. H. (1951) Studies on reactivities of illuminated chloroplast. I. Mechanism of the reduction of oxygen, and other Hill reagents. Arch. Biochem. Biophys. 33:65.

Melhorn, A. H. (1990) Ethylene-promoted ascorbate peroxidase activity protects plants against hydrogen peroxide peroxide, ozone and methyl viologen. Plant Cell Environ. 13:971-976.

Mittler, R. and Zilinskas, B. A. (1991) Purification and characterization of pea cytosolic ascorbate peroxidase. Plant Physiol. 97:962-968.

Mittler, R. and Zilinskas, B. A. (1992) Molecular cloning and characterization of a gene encoding pea cytosolic ascorbate peroxidase. J. Biol. Chem. 267:21802-21807.

Mittler, R. and Zilinskas, B. A. (1993) Regulation of pea cytosolic ascorbate peroxidase and other antioxidant enzymes during the progressions of drought stress and following recovery from drought. Plant J. 5:397-405.

Miyake, C., Michihata, F., and Asada, K. (1991) Scavenging of hydrogen peroxide in

prokaryotic and eukaryotic algae: Acquisition of ascorbate peroxidase during the evolution of cyanobacteria. Plant Cell Physiol. 32:33-43.

Nakano,Y. and Asada,K. (1980) Spinach chloroplast scavenge hydrogen peroxide on illumination. Plant Cell Physiol. 21:1295-1307.

Nohl, G., Jordan, N., and Hegner, D. (1981) Identification of free hydroxyl radicals in respiring rat heart mitochondria by spin trapping with the nitrone DMPO. FEBS Lett. 123:241-44.

Ogawa, K., Kanematsu, S., and Asada, K. (1996) Intra- and extra-cellular localization of "cytosolic" Cu-Zn-superoxide dismutase in spinach leaf and hypocotyl. Plant Cell Physiol. 37:790-799.

Ogawa, K., Kanematsu, S., and Asada, K. (1997) Generation of superoxide anion and localization of CuZn-superoxide dismutase in the vascular tissue of spinach hypocotyls: Their association with lignification. Plant Cell Physiol. 38:1118-1126.

Ogawa, K., Kanematsu, S., Takabe, K., and Asada, K. (1995) Attachment of Cu-Zn-superoxide dismutase to thylakoid membranes at the site of superoxide generation (PSI) in spinach chloroplasts: Detection by immuno-gold labeling after rapid freezing and substitution method. Plant Cell Physiol. 36:565-573.

Okada, S., Kanematsu, S., and Asada, K. (1979) Intracellular distribution of manganese and ferric superoxide dismutases in blue-green algae. FEBS Letters 103:106-110.

Okajima, T., and Yamazaki, I. (1972) Myelo peroxidase EC-1.11.1.7 of the leukocyte of normal blood part 5 spectral conversion of myelo-peroxidase EC-1.11.1.7 to a cytochrome oxidase like derivative. Biochim. Biophys. ACTA 284:355-359.

Ormrod, D. P., Landry, L. G., and Conklin, P. L. (1995) Short term UV-B radiation and ozone exposure effects on aromatic secondary metabolitye accumulation and shoot growth of flavonoid-deficient Arabidopsis mutants. Physiol. Plant. 93:602-610.

Palma, J.M., Sandalio, L.M., and del Rio, L. A., (1986) Manganese superoxide dismutase and higher plant chloroplasts: A reappraisal of a controversial cellular localization J. Plant Physiol. 125:427:439.

Pan, S. M. and Yau, Y. Y. (1992) Characterization of superoxide dismutase in Arabidopsis. Plant Cell 37:58-66.

Peng, M. and Kuc, J. (1992) Peroxidase-generated hydrogen peroxide as a source of antifungal activity in vitro and on tobacco leaf disks. Phytopathology 82:696-699.

Perl, A., Perl-Treves, R., Galili, S., Aviv, D., Shalgi, E., Malkin, S., and Galun, E. (1993)

Enhanced oxidative-stress defense in transgenic potato expressing tomato Cu,Zn superoxide dismutases. Theor. Appl. Genet. 85:568-576.

Pearlman, D. A., Case, D. A., Caldwell, J. W., Ross, W. S., Cheatham, T. E., DeBolt, S., Ferguson, D., Seibel, G., and Kollman, P. (1995) AMBER, a package of computer programs for applying molecular mechanics, normal mode analysis, molecular dynamics and free energy calculations to simulate the structural and energetic properties of molecules. Comput. Phys. Commun. 91, 1-41.

Puger, K. and Michelson, A. M. (1974) Iron containing superoxide dismutase from luminous bacteria. Biochimie 56:1255-1267.

Quartacci, N. F. and Navari-Izzo, F. (1992) Water stress and free-radical mediated changes in sunflower seedlings. J.Plant Physiol. 139:621-625.

Reddy, C. D. and Venkaiah, B. (1982) Studies on isoenzymes of superoxide dismutase from mung bean (*Vigna radiate*) seedlings. J. Plant Physiol. 116:279-284.

Rubinstein, B. and Luster, D. G. (1993) Plasma membrane redox activity: Components and role in plant porocesses. Annu. Rev. Plant Physiol.-Plant Mol. Biol. 44:131-155.

Sali, A. and Blundell, T. L. (1993) Comparative protein modelling by satisfaction of spatial restraints. J. Mol. Biol. 234:779-815

Salin, M. L. (1988) Plant Superoxide Dismutases: A means of coping with oxygen radicals. Curr. Top. Plant Biochem. Physiol. 7:188-200.

Salin, M. L. and Bridges, S. M. (1980) Localization of superoxide dismutase in chloroplasts from *Brassica campestris*. Z Pflanzenphysiol 99:37-47.

Salin, M. L. (1988) Toxic oxygen species and protective systems of the chloroplast. Physiol. Plant 72:681-689.

Sambrook, J., Fritsch, E. F., and Maniatis, T. (1989) Molecular Cloning: A Laboratory Manual. Second Edition, Cold Spring Harbor Laboratory Press, New York, NY.

Sandalio, L. M. and del Rio, L. A. (1987) Localization of superoxide dismutase in glyoxysomes from *Citrullus vulgaris*: Functional implications in cellular metabolism. J. Plant Physiol. 127:395-409.

Sandalio, L. M., Jose, M., and del Rio L. A. (1987) Localization of manganese superoxide dismutase in peroxisomes isolated from *Pisum sativum* L. Plant Science. 51:1-8.

Searcy, K. B. and Searcy, D. G., (1981) Superoxide dismutase from the Archaebacterium *Thermoplasma acidophilum*. Biochim. Biophys. Acta 680:39-46.

Sharma, Y. K., Hinojos, C. M., and Mehdy, M. C. (1992) cDNA cloning, structure, and expression of a novel pathogenesis-related protein in bean. Mol. Plant. Microbe. Interact. 5:89-95.

Slooten, L., Capiau, K., Van Camp, W., Van Montagu, M., Subesma, C. and Inze, D. (1995) Factors affecting the enhancement of oxidative stress tolerance in transgenic tobacco overexpressing manganese superoxide dismutase in the chloroplasts. Plant Physiol. 107:737-750.

Smirnoff, N. and Colombe, S. V. (1988) Drought influences the activity of the enzymes of the chloroplast hydrogen peroxidase scavenging system. J. Exp. Bot. 39:1097-1108.

Smith, M. W. and Doolittle, R. F. (1992) A comparison of of evolutionary rates of the two major kinds of superoxide dismutases. J. Mol. Evol. 34:175-184.

Snijder, A. J., Wastie, R. L., Glidewell, S. M. and Goodman, B. A. (1996) Free radicals and other paramagnetic ions in interactions between fungal pathogens and potato tubers. Biochem. Soc. Trans. 24:442-446.

Stallings, W. C., Pattridge, K. A., Strong, R. K., and Ludwig, M. L. (1984) Manganese and iron superoxide dismutases are structural homologs. J. Biol. Chem. 259:10695-10699.

Steinman, H. M. (1982) Copper-zinc superoxide diemutase from *Caulobacter crescentus* CB15. A novel bacteriocuprein form of the enzyme. J. Biol. Chem. 257:10283-10293.

Steinman, H. M. (1985) Bacteriocuprein superoxide dismutases in pseudomonads. J. Bacteriol. 162:1255-1260.

Strid, A., Chow, W. S., and Anderson, J. M. (1994) UV-B damage and protection at the molecular level in planst. Photosynthesis Research 39:475-489.

Takahashi, M. and Asada, K. (1988) Superoxide production in aprotic interior of chloroplast thylakoids. Arch. Biochem. Biophys. 267:714-722.

Takahashi, M. and Asada, K. (1983) Superoxide anion permeabilty of phospholipid membranes and chloroplast thylakoids Arch. Biochem. Biophys. 226:558-566.

Tanaka, K. Masuda, R., Sugimoto, T., Omasa, K., and Sakaki, T. (1990) Water deficeincy-induced changes in the contents of defensive substances against active oxygen in spinach leaves. Agric. Biol. Chem. 54:2629-2634.

Tanaka, K., Otsubo, T., and Kondo, N. (1982) Participation of hydrogen peroxide in the inactivation of calvin-cycle SH enzymes in SO2-fumigated spinach leaves. Plant. Cell. Physiol. 23:1009-1018.

Tepperman, J. M. and Dunsmuir, P. (1990) Transformed plants with elevated levels of chloroplastic SOD are not more resistant to superoxide toxicity. Plant Mol. Biol. 14:501-511.

Thomas, D. J., Avenson, T. J., Thomas, J. B., and Herbert, S. K. (1998) A cyanobacterium lacking iron superoxide dismutase is sensitized to oxidative stress induced with methyl viologen but is not sensitized to oxidative stress induced with norflurazon. Plant Physiol., 116:1593-1602.

Thomsen, B., Drumm-Herrell, H., and Mohr, H. (1992) Control of the appearance of ascorbate peroxidase (E.C. 1.11.1.11) in mustard seedlings cotyledons by phytochrome and photooxidative treatments. Planta, 186:600-608.

Tsang, E. W. T., Bowler, C., Herouart, D., Van Camp, W., Villarroel, R., Genetello, C., Van Montagu, M., and Inze, D. (1991) Differential regulation of superoxide dismutases in plants exposed to envirionmental stress. Plant Cell, 3:783-792.

Van Camp, W., Bowler, and C., Villarroel, R. (1990) Characterization of iron superoxide dismutase cDNAs from plants obtained by genetic complementation in *Escherichia coli.* Proc. Natl. Acad. Sci. USA 87:9903-9907.

Van Camp, W., Capiau, K., Van Montague, M. V., Inze, D., and Slooten, L. (1996) Enhancement of oxidative stress tolerance in transgenic tobacco plants oveproducing Fe-Superoxide dismutase in chloroplasts. Plant. Physiol. 112:1703-1714.

Van Camp W., Willekens H., and Bowler C., (1994) Elevated levels of superoxide dismutase protect transgenic plants against ozone damage. Bio/Technology 12:165-168.

Van den Bosch, H. (1992) Biochemistry of peroxisomes. Annu. Rev. Biochem. 61:157-197.

Wellburn, A. R. and Wellburn, F. A. M. (1996) Gaseous pollutants and plant defense mechanisms, Biochem. Soc. Trans. 24:461-464.

Wright, G., Reichhenbecher, V., Green, T., Wright, G. L., and Wang, S. (1997) Paraquat inhibits the processing of human manganese-dependent superoxide dismutase by SF-9 insect cell mitochondria. Exp. Cell Res. 234:78-84.

Yost, F. J., Jr. and Fridovich, I. (1973) An iron containing superoxide dismutase from *E.coli*. J.Biol. Chem. 248:4905-4908.

Youn, H. D., Kim, E. J., Roe, J. H., Hah, Y. C., and Kang, S. O. (1996) A novel nickel-containing superoxide dismutase from *Streptomyces* spp., Biochem. J. 318:889-89.

Zhang, K., Chance, B., and Reddy, K. S. (1991) Structural differences in solution and

crystalline forms of met-myoglobin. Biochemistry 30:9116-9120

Zhou, H. X., Wong, K. Y., and Vijakumar, M. (1997) Design of fast enzymes by optimizing interaction potential in active site. Proc. Natl. Acad. Sci. USA 94:12372-12377.

Zhu, D. and Scandalios, J. G. (1993) Maize mitochondrial manganese superoxide dismutases are encoded by a differentially expressed multigene family. Proc. Natl. Acad. Sci. USA 90:9310-9314.